Altered rice nutritional quality resulting from environmental change: An investigation into the implications of temperature, phenology, and flooding on rice metal and metalloid accumulation

Yasmine Farhat

A dissertation
submitted in partial fulfillment of the
requirements for the degree of

Doctor of Philosophy

University of Washington
2022

Reading Committee:
Rebecca Neumann, Chair
Soo-Hyung Kim
Gordon Holtgrieve

Program Authorized to Offer Degree:
Civil and Environmental Engineering

University of Washington

Abstract

Altered rice nutritional quality resulting from environmental change: An investigation into the implications of temperature, phenology, and flooding on rice metal and metalloid accumulation

Yasmine Farhat

Chair of Supervisory Committee:

Rebecca Neumann

Department of Civil and Environmental Engineering

Rice (*Oryza sativa*) is one of the world's most important food crops, serving as a key dietary staple to over half of the world's population. Rice is especially important in many low-income countries, where micronutrient deficiencies are often widespread and there is less access to alternative nutrient dense foods. At the same time, rice is also a main dietary source of arsenic, a toxin and carcinogen. These underlying dietary burdens may be exasperated by alerted climatic and hydrologic factors which influence soil chemistry and plant ecophysiology. In this study, I investigate how elevated temperature impacts rice arsenic uptake and how seasonal flooding influences mineral dynamics in the Tonle Sap floodplain of Cambodia.

In Chapter 2, we established four temperature treatments, increasing 2.5°C between treatments, in climate-controlled growth chambers where we grew potted rice plants (*Oryza sativa* cv. M206). We observed that arsenic concentrations in porewater, root iron plaque, and plant tissue increased in response to elevated temperature. There was a positive linear relationship between temperature and rice grain arsenic. Rice plants grown at higher temperatures had more adsorbed arsenic per unit of iron plaque (measured as [As]/[Fe]),

indicating temperature may impact arsenic sorption to root plaque. We present evidence that increased soil mobilization of arsenic was the driving factor responsible for increased arsenic uptake into rice grain. Our soils had low soil arsenic concentrations and our findings indicated that elevated temperatures may increase dietary arsenic exposure in rice systems that were previously considered low risk.

In Chapter 3, we expand on the previous chapter by delving into the impact of timing of temperature exposure during specific developmental windows. We grew potted rice plants of the same variety in temperature-controlled growth chambers with different temperature regimes: (1) baseline temperature, (2) elevated temperature, (3) baseline temperature with a heat spike in vegetative stage (4) baseline temperature with a heat spike in the ripening stage. We observed that heat spikes in the ripening stage greatly increased arsenic mobilization from soil to porewater, but heat spikes in the vegetative stage did not. Plants which experienced a vegetative heat spike had increased arsenic concentrations in plant tissue immediately following the heat spike, but the magnitude of this increase was small and did not persist to maturity. Plants which experienced a heat spike during the ripening stage had a significant increase in arsenic concentrations in various plant tissues which persisted to maturity. We present several likely explanations for the discrepancy between the two timepoints, including differences in microbial mobilization, plant biomass, and root development. Our research shows that heat spikes later in the rice growing season present a larger threat for dietary arsenic exposure from rice.

In Chapter 4, I widen the scope of my work to also include mineral nutrients, specifically zinc and iron, as well as toxic arsenic. In this two-year field study, we investigated the movement of these metals (+ metalloid) in the Tonle Sap floodplain, an important area for rice cultivation in Cambodia. We collected surface soil, flood sediment, and dry-season plant

tissue from 12 rice fields along a flooding gradient in the Steung Saen Municipality of Kampong Thom Province. We found that sites with greater flooding had higher concentrations of total metals but a lower fraction of plant available metals. Flood sediment had consistently greater concentrations of all three metals, indicating that flood sediment may act as a natural source of both nutrients and toxins. Concentrations of these elements were variable in rice tissue, though we found seasonal trends in zinc concentrations. Finally, we found relatively high concentrations of arsenic in rice grains given that Kampong Thom is often overlooked in studies on rice arsenic in Cambodia. These observations as well as additional in-depth studies are needed to understand how rice agriculture and rice nutritional quality might change with the anticipated alterations in flooding due to dam construction.

Acknowledgements

Firstly, I would like to thank my advisor, Rebecca Neumann, without whose guidance and mentorship none of this would be possible. You taught me to strive to be a scientist in service to humanity, to ask questions which might provide insights to solve global challenges. You modelled both strength and compassion in these stormy years of anxiety and upheaval. Thank you for always treating me as your scientific peer, giving me the freedom to explore places and ideas, and standing with me through the ups and downs of science.

I would also like to thank all the members of the Neumann Lab with whom I have had the pleasure of working. Thanks to Lara Pracht for answering emails long after she should, to Nick Waldo for sharing a U-Haul full of soil, to Pam Barrett for organizing everything/everyone, and to Robin Ruhm for bringing a little magic to the lab. A very deep sincere thanks to Samantha Fung, Joel Eklof, and Rachel Strickman who provided me so much laughter, commiseration, and support throughout the pandemic. I honestly can't list everything you guys have done over the years, so I'll just leave it at thank you. I also had the pleasure of working with UW's Plant Ecophysiology lab run by Soo-Hyung Kim. Thanks to Hyungmin "Tony" Rho for being my rice plant guru and to Man Marcaida III for being my travel buddy. I owe a special thanks to J Sean Yeung for helping me fix instruments with no money and letting me cut to the front of the line for your help, truly your patience is saint-like. My research was also supported by many UW student researchers who helped with the un-glamours but vital parts of science: Alex Ratcliff, Catherine Ikeda, Colin Kolbus, Evan Lester, Maggie Honig, Mikaela Balkind, Teresa Wang.

The work I accomplished in Chapter 4 was made possible by my collaborations with many amazing people in Cambodia. Principally, I would like to thank E-Nieng Muth, one of the most competent, organized, and generous women with whom I have worked. Thanks for always having my back, from having that datapoint I forgot to write down to picking me up from the side of the road after I wiped out on my moto bike. I can't wait to see the scientist you become. I would also like to thank Dr. Lyda Hok from the Royal University of Agriculture and Chou Chethyrith of the Cambodian Rice Crop Department. Additionally, I would like to thank the 20+ farmers who gave me their rice, time, and patience.

Thanks to all the friends who helped me think about things besides research: Jakob Sumearll, Angie Mouki, Alex Butcher, Dylan Moir, Alison Stagner, Shirley Leung and more.

One of my greatest joys since moving to Seattle has been rediscovering swimming, a sport I've loved since I was 10 years old. I met so many great people swimming in Seattle who became some of my closest friends here. Thanks to David Bell, Anna Neufeld, Jospeh Bowley, Amanda Winans, and Elizabeth Thompson for the hours together in the water.

A very genuine thanks to my cat, Nelson, who can't read this but has given me more hours of companionship during my education than anyone else. One time I cried over how much I love you, my furry little desk mate. Thanks for weathering all our moves these last 10 years.

I dedicate this dissertation primarily to my family. My grandma and Aunt Nett have been my second parents since I moved back to the US and have given me so much love and support. My sister, Hela, and my brother, Omar, have been my best friends my entire life and understand me more than anyone else. Everything I do in my career is thanks to my awe-inspirating parents. Thank you to my mom, Jennifer Farhat, who taught me to work with unending passion and dedication. You showed me how to grow continuously and live adventurously. I love you. And to my dad, Ali Farhat, who taught me to fight for a cause and love courageously. For teaching me what it means to be from a land, a people, a faith, and a family.

بحبك يا بابا

Lastly, I dedicate this dissertation to my partner, Andy Rashid. Thank you for holding me during the bad times and celebrating the victories. For supporting me when I let life slip out from under me and finding joy with me everywhere we go. From the tedious to the adventurous, in every corner of the world, I'm yours.

This publication is based upon work supported by the University of Washington Innovation Award, a travel grant from the US Asia Rice Foundation, a grant from the National Science Foundation (1740042), and the National Science Foundation Graduate Research Fellowship (1762114). Any opinion, findings, and conclusions or recommendations expressed in this material are those of the authors and do not necessarily reflect the views of funders, including the National Science Foundation.

Table of Contents

List of Figures

List of Tables

1. Chapter 1: Introduction

1.1. Background

1.1.1. Rice and rice cultivation

Rice (*Oryza sativa*) is one of the world's most important food crops, serving as a key dietary staple to over half the world's population. It accounts for 35-75% of daily caloric intake for 3 billion people (Fageria, 2014). It is cultivated on every continent besides Antarctic and on 10.5% of global cropland (Food and Agriculture Organization, 2020). Rice cultivation looks different around the world; from the more mechanized systems in the United States where rice seeding is done by airplane, to the small-scale farmer in the Philippines who weeds their field by hand. The widespread cultivation of rice means it has significant genetic diversity (Yan et al., 2010) and is grown on a huge range of soil types and conditions (Haefele et al., 2014).

Rice is a C-3 plant, for the time being (von Caemmerer et al., 2012). Traditional rice varieties take up to 6 months to mature, whereas modern high yield varieties can mature in about 3 months. Rice development (i.e., phenology) can be divided into three phases: vegetative, reproductive, and ripening (Fageria, 2014; GRiSP, 2013). The vegetative stage occurs after germination when leaves develop, the stem lengthens and tillers form. Entrance into the reproductive stage occurs when the immature panicle forms within the main stem. The developing panicle then grows and elongates in the leaf sheath and when it eventually emerges and becomes fully visible it is described as heading. Flowering (i.e., anthesis) begins after full heading and marks the transition from the reproductive to the ripening stage. Note that flowering can occur over several days at different points along the panicle. During this final developmental stage, the developing caryopses elongate within the hull and then change from milky to firm.

Rice which is grown under flooded conditions is sometimes referred to as lowland rice. Approximately 75% of the world's total rice supply comes from irrigated lowland rice, which is grown under flooded conditions (Bouman et al., 2007). Another 19% percent comes from rainfed lowland rice which has less consistent access to water but ideally grown under flooded conditions as well (GRiSP, 2013). This flooding is used to help control weeds and tends to improve rice yields. Farmers usually try to maintain 5-10 cm of standing water on their fields during flooding (GRiSP, 2013). The submerged nature of paddy soils (anthropogenic soils used for rice cultivations) creates an anaerobic environment with important geochemical implications.

1.1.2. Rice traditions and a changing world

Rice was first cultivated in China, approximately 10,000 years ago (Gross and Zhao, 2014). The long, rich traditions of growing rice means that many rice dependent communities accumulate knowledge and traditions for growing regional varieties of rice. Many communities have strong cultural ties to their local rice traditions, especially in Asia, which grows ~ 90% of the global rice supply (Food and Agriculture Organization, 2020; GRiSP, 2013). For example, a common phrase in Cambodia meaning "to eat" is "pisa bei," literally translates as "to eat rice." Rice farmers' cultural identity and their sense of heritage and tradition, correlates with farmer land use; where farmers with a strong sense of cultural identity tend to use traditional, low-intensity agricultural practices, (Tekken et al., 2017) which can reinforce both their connection and dependence on their land. However, it may also make them less able to adapt to a changing environment. While the intensification of rice agriculture has increased in many parts of the world, rice is still grown primarily by small land-holding farmers and is an important source of employment to the global resource-poor (GRiSP, 2013).

Despite long-standing traditions and continued reliance on rice by the roughly 144 million global farmers (GRiSP, 2013) the environmental conditions surrounding rice cultivation are changing: Climate change will increase growing temperatures in rice-growing regions around the world (IPCC, 2021). Altered precipitation patterns cause uncertainty in water access for irrigation (Naylor et al., 2007). Man-made interventions, like dam construction, may alter flood patterns and nutrient cycling (Arias et al., 2014). Such rapid change necessitates the question: How might rice production and quality be changed by an altered environment? The importance of this question is especially pronounced for communities which heavily rely on rice in meet their daily caloric needs.

In this dissertation, I primarily focus on two aspects of environmental change: changes in (1) temperature and (2) seasonal flooding:

(1) Many rice-growing locations will have to adapt to increasing temperatures due to climate change, including in Northern California – the modelled location of our temperature experiments. Within the United States, California is the second largest rice producing state and 95% of its rice production is in the Sacramento Valley (University of California, 2022; USDA, 2022). The IPCC predicts that median temperatures in California will increase by 3.3°C by mid-century and 6.1°C by end of century relative to pre-industrial levels (Gutiérrez et al., 2021).

(2) Lowland, flooded rice cultivation requires significant amounts of water, meaning that rice fields are often located near large waterbodies or on floodplains. Even irrigated rice can be supplemented with wet season rainfall and seasonal flooding (GRiSP, 2013). Yet the seasonal hydrology of important water systems around the world is changing due to a boom in dam construction coupled with altered precipitation from climate change (Arias et al., 2014; Timpe

and Kaplan, 2017; Zarfl et al., 2014). Resulting hydrologic changes may cause altered wet season flooding and sediment deposition on fields located near these altered water systems.

In the context of environmental change, much research has focused on food supply by estimating agricultural land availability and crop yield (Arias et al., 2014; Peng et al., 2004; Porter et al., 2014; Wang et al., 2016; Yoshida et al., 2020). However, there is an emerging appreciation that food security must consider not only food supply, but also nutritional quality (DaMatta et al., 2010; Dimkpa et al., 2019; Smith and Myers, 2018). Two important aspects of two food quality are the concentrations of nutrients and toxins which foods contain. Metal (and metalloid) minerals can occupy both categories. While there is overlap between certain elements, each mineral's specific soil mobilization, uptake, and allocation patterns within plants causes them to respond differently to each environmental change (Lynch and St.Clair, 2004; St.Clair and Lynch, 2010). Therefore, we are left with the daunting task of considering each mineral on a case-by-case basis in the context of each environmental change.

1.1.3. Mineral uptake and mineral stress

Mineral stress can be defined as the sub-optimal availably of essential mineral nutrients or excessive/toxic concentrations of minerals (Lynch and St.Clair, 2004). In agricultural systems, soils are the highest repository of metals. Given that rice is grown in flooded systems, minerals which move off of soil solids and into the dissolved phase will become more available to plants (i.e. phyto-available). Desorption and solubilization into porewater is driven by environmental parameters like pH, redox conditions, and temperature (Alloway, 2008; Honma et al., 2016; Simmler et al., 2017). Metals are taken up into the plant by root transporters, the expression of which is influenced by the concentration of said metal (Ishimaru et al., 2005; Ma et al., 2008), before they then travel through rice vasculature. Toxic contaminants can highjack the uptake

pathways of useful minerals, such as arsenic with silicon and cadmium with zinc (Clemens and Ma, 2016). The external environment influences plant growth and development (ex. total biomass, root-to-shoot ratio, duration of ripening, etc.) that may also influence metal uptake and allocation within the plant (DaMatta et al., 2010).

Of special note is arsenic (As), a metalloid heavily discussed in all chapters of my dissertation. Arsenic is a potent carcinogen and toxin frequently found in rice paddy environments. Rice is the major dietary source of arsenic and can induce genotoxic effects in humans at levels as low as 200 ng g^{-1} (Banerjee et al., 2013). Arsenic phyto-availability is intimately linked to another metal: iron (Fe). When soils are anoxic, solid-phase arsenic is released via reductive dissolution which liberates arsenic from iron (hydr)oxide minerals to which it is bound. This release occurs when solid Fe(III) is reduced to soluble Fe(II), and/or desorption of arsenic when it reduces from As(V) to As(III) (Borch et al., 2010; Cummings et al., 1999; Tufano and Fendorf, 2008; Xue et al., 2020). Therefore, the flooded nature of rice cultivation dramatically increases the bioavailability of both arsenic and iron.

An important mineral nutrient discussed in Chapter 4 is zinc (Zn). Zinc is essential in the human diet for various cellular functions including growth and development. For this reason, children are at especially high risk for dietary zinc deficiency (Roohani et al., 2013). Zinc deficiency is also recognized as one of the most important nutrient deficiencies in rice and can reduce crop yield (Impa and Johnson-Beebout, 2012). Total soil zinc concentration is typically not a useful measurement for determining crop zinc deficiency, as only a very small portion of total zinc is available to plants (Du Laing et al., 2009). The phyto-available fraction of zinc is composed that which is dissolved in the soil solution and which is easily desorbed from soil particles (Alloway, 2008). Zinc deficiency is common is rice systems due to continuous flooding

which shifts pH to a non-optimal level (Alloway, 2008; Johnson-Beebout et al., 2009). There is evidence that increasing plant available zinc can increase rice grain zinc concentrations though their relationship is complex and not strictly linear (Cakmak, 2007; Wissuwa et al., 2007).

1.2. Dissertation Overview

In this dissertation I investigate how rice nutritional quality as it relates to select metal/loid micronutrients and toxins is influenced by changes in temperature and flooding. An understanding of these connections is necessary to predict how rice nutritional quality might change in the future. In my first research chapter, Chapter 2, I investigate in the impact of elevated temperatures on arsenic mobilization, potential mass-flow, and accumulation in rice root plaque and plant tissue. To perform this investigation, I grew potted rice plants (*Oryza sativa* cv. M206) in Californian paddy soil. Plants grew in one of four temperature treatments in climate-controlled growth chambers with a roughly 2.5°C increase between treatments. We found increases in arsenic mobilization, plant transpiration, and tissue accumulation at elevated temperatures. In particular, we identified temperature fueled increases in arsenic mobilization as strong explanatory variable. This experiment was published in *Science of the Total Environment* in 2021.

I expand on this topic in Chapter 3, where I delve into the interaction of rice plant phenology with temperature-driven increases in rice arsenic. The aim of this experiment is to understand is how the timing of temperature stress might impact arsenic accumulation in rice tissue. We compared heat spikes which occurred in the vegetative stage and in the ripening stage to baseline temperatures. We found that heat spikes which occurred in the vegetative stage only caused a very small increase in arsenic mobilization and tissue arsenic content, which became washed out over time. Alternatively, heat spikes in the ripening stage were able to mobilize more

arsenic off soils and increased grain concentration of arsenic, along with other tissues. This manuscript is currently *in prep* and is expected to be submitted for journal peer review in the coming weeks.

In my last experimental chapter, Chapter 4, I investigate the impact of seasonal flooding on several metals in Kampong Thom Province in Cambodia. In this two-year field study, I collected surface soils, flood sediment, and dry-season plant tissue from 12 rice fields along a floodplain gradient. I quantified the total concentrations and the plant available fractions of zinc, iron, and arsenic. I also measured these same metals rice leaf and grain tissue. I found that sites with greater flooding had higher concentrations of total metals but a lower fraction of potentially phyto-available metals. I noted that flood sediment had consistently higher concentrations of available metals than did surface soils. Concentrations of these elements were variable in rice tissue, though we found seasonal trends in zinc concentrations. I have completed all sample collection, laboratory analysis, and an expansive suite of statistical analyses as it related to this experiment. The most current draft of this manuscript is reproduced in Chapter 4.

1.3. References

Alloway BJ. Zinc in Soils and Crop Nutrition. International Zinc Association and International Ferilizer Associaiton, Brussels, Belgium, 2008.

Arias ME, Cochrane TA, Kummu M, Lauri H, Holtgrieve GW, Koponen J, et al. Impacts of hydropower and climate change on drivers of ecological productivity of Southeast Asia's most important wetland. Ecological Modelling 2014; 272: 252-263.

Banerjee M, Banerjee N, Bhattacharjee P, Mondal D, Lythgoe PR, Martinez M, et al. High arsenic in rice is associated with elevated genotoxic effects in humans. Sci Rep 2013; 3: 2195.

Borch T, Kretzschmar R, Kappler A, Cappellen PV, Ginder-Vogel M, Voegelin A, et al. Biogeochemical Redox Processes and their Impact on Contaminant Dynamics. Environ Sci Technol 2010; 44: 15-23.

Bouman B, Lampayan R, Toung T. Water management in irrigated rice: coping with water scarcity: Int. Rice Res. Inst., 2007.

Cakmak I. Enrichment of cereal grains with zinc: Agronomic or genetic biofortification? Plant and Soil 2007; 302: 1-17.

Clemens S, Ma JF. Toxic Heavy Metal and Metalloid Accumulation in Crop Plants and Foods. Annu Rev Plant Biol 2016; 67: 489-512.

Cummings DE, Caccavo F, Fendorf S, Rosenzweig RF. Arsenic Mobilization by the Dissimilatory Fe(III)-Reducing Bacterium Shewanella alga BrY. Environ Sci Technol 1999; 33: 723-729.

DaMatta FM, Grandis A, Arenque BC, Buckeridge MS. Impacts of climate changes on crop physiology and food quality. Food Research International 2010; 43: 1814-1823.

Dimkpa CO, Singh U, Bindraban PS, Elmer WH, Gardea-Torresdey JL, White JC. Zinc oxide nanoparticles alleviate drought-induced alterations in sorghum performance, nutrient acquisition, and grain fortification. Sci Total Environ 2019; 688: 926-934.

Du Laing G, Rinklebe J, Vandecasteele B, Meers E, Tack FM. Trace metal behaviour in estuarine and riverine floodplain soils and sediments: a review. Science of the total environment 2009; 407: 3972-3985.

Fageria NK. Mineral Nutrition of Rice: CRC Press, 2014.

Food and Agriculture Organization. FAOStat. 2019. United Nations, Rome, 2020.

GRiSP. Rice Almanac. Los Baños (Philippines): International Rice Research Institute, 2013.

Gross BL, Zhao Z. Archaeological and genetic insights into the origins of domesticated rice. Proceedings of the National Academy of Sciences 2014; 111: 6190-6197.

Gutiérrez JM, Jones RG, Narisma GT, Alves LM, Amjad M, Gorodetskaya IV, et al. Atlas (Interactive Tool). In: Masson-Delmotte V, Zhai P, Pirani A, Connors SL, Péan C, Berger S, et al., editors. Climate Change 2021: The Physical Science Basis. Contribution of Working Group I to the Sixth Assessment Report of the Intergovernmental Panel on Climate Change. Cambridge University Press, 2021.

Haefele SM, Nelson A, Hijmans RJ. Soil quality and constraints in global rice production. Geoderma 2014; 235-236: 250-259.

Honma T, Ohba H, Kaneko-Kadokura A, Makino T, Nakamura K, Katou H. Optimal Soil Eh, pH, and Water Management for Simultaneously Minimizing Arsenic and Cadmium Concentrations in Rice Grains. Environ Sci Technol 2016; 50: 4178-4185.

Impa S, Johnson-Beebout S. Mitigating zinc deficiency and achieving high grain Zn in rice through integration of soil chemistry and plant physiology research. Plant and Soil 2012; 361: 3-41.

IPCC. Climate Change 2021: The Physical Science Basis. Contribution of Working Group I to the Sixth Assessment Report of the Intergovernmental Panel on Climate Change: Cambridge University Press, 2021.

Ishimaru Y, Suzuki M, Kobayashi T, Takahashi M, Nakanishi H, Mori S, et al. OsZIP4, a novel zinc-regulated zinc transporter in rice. J Exp Bot 2005; 56: 3207-14.

Johnson-Beebout SE, Lauren JG, Duxbury JM. Immobilization of Zinc Fertilizer in Flooded Soils Monitored by Adapted DTPA Soil Test. Communications in Soil Science and Plant Analysis 2009; 40: 1842-1861.

Lynch JP, St.Clair SB. Mineral stress: the missing link in understanding how global climate change will affect plants in real world soils. Field Crops Research 2004; 90: 101-115.

Ma JF, Yamaji N, Mitani N, Xu XY, Su YH, McGrath SP, et al. Transporters of arsenite in rice and their role in arsenic accumulation in rice grain. Proc Natl Acad Sci 2008; 105: 9931-5.

Naylor RL, Battisti DS, Vimont DJ, Falcon WP, Burke MB. Assessing risks of climate variability and climate change for Indonesian rice agriculture. Proc Natl Acad Sci 2007; 104: 7752-7.

Peng S, Huang J, Sheehy JE, Laza RC, Visperas RM, Zhong X, et al. Rice yields decline with higher night temperature from global warming. Proc Natl Acad Sci 2004; 101: 9971-5.

Porter JR, Xie L, Challinor AJ, Cochrane K, Howden SM, Iqbal MM, et al. Food security and food production systems. In: Field CB, Barros VR, Dokken DJ, Mach KJ, Mastrandrea MD, Bilir TE, et al., editors. Climate Change 2014: Impacts, Adaptation, and Vulnerability. Part A: Global and Sectoral Aspects. Contribution of Working Group II to the Fifth Assessment Report of the Intergovernmental Panel of Climate Change. Cambridge University Press, Cambridge, United Kingdom and New York, NY, USA, 2014, pp. 485-533.

Roohani N, Hurrell R, Kelishadi R, Schulin R. Zinc and its importance for human health: An integrative review. Journal of research in medical sciences : the official journal of Isfahan University of Medical Sciences 2013; 18: 144-157.

Simmler M, Bommer J, Frischknecht S, Christl I, Kotsev T, Kretzschmar R. Reductive solubilization of arsenic in a mining-impacted river floodplain: Influence of soil properties and temperature. Environ Pollut 2017; 231: 722-731.

Smith MR, Myers SS. Impact of anthropogenic CO_2 emissions on global human nutrition. Nature Climate Change 2018; 8: 834-839.

St.Clair SB, Lynch JP. The opening of Pandora's Box: climate change impacts on soil fertility and crop nutrition in developing countries. Plant and Soil 2010; 335: 101-115.

Tekken V, Spangenberg JH, Burkhard B, Escalada M, Stoll-Kleemann S, Truong DT, et al. "Things are different now": Farmer perceptions of cultural ecosystem services of traditional rice landscapes in Vietnam and the Philippines. Ecosystem services 2017; 25: 153-166.

Timpe K, Kaplan D. The changing hydrology of a dammed Amazon. Science Advances 2017; 3: e1700611.

Tufano KJ, Fendorf S. Confounding Impacts of Iron Reduction on Arsenic Retention. Environ Sci Technol 2008; 42: 4777-4783.

University of California. About California Rice. In: Resources DoAaN, editor, 2022.

USDA. Rice Yearbook. U.S. rice acreage, production, and yield, 2022.

von Caemmerer S, Quick WP, Furbank RT. The development of C4 rice: current progress and future challenges. science 2012; 336: 1671-1672.

Wang DR, Bunce JA, Tomecek MB, Gealy D, McClung A, McCouch SR, et al. Evidence for divergence of response in Indica, Japonica, and wild rice to high CO_2 x temperature interaction. Glob Chang Biol 2016; 22: 2620-32.

Wissuwa M, Ismail AM, Graham RD. Rice grain zinc concentrations as affected by genotype, native soil-zinc availability, and zinc fertilization. Plant and Soil 2007; 306: 37-48.

Xue S, Jiang X, Wu C, Hartley W, Qian Z, Luo X, et al. Microbial driven iron reduction affects arsenic transformation and transportation in soil-rice system. Environ Pollut 2020; 260.

Yan W, Agrama H, Jia M, Fjellstrom R, McClung A. Geographic Description of Genetic Diversity and Relationships in the USDA Rice World Collection. Crop Science 2010; 50: 2406-2417.

Yoshida Y, Lee HS, Trung BH, Tran H-D, Lall MK, Kakar K, et al. Impacts of mainstream hydropower dams on fisheries and agriculture in lower Mekong Basin. Sustainability 2020; 12: 2408.

Zarfl C, Lumsdon AE, Berlekamp J, Tydecks L, Tockner K. A global boom in hydropower dam construction. Aquatic Sciences 2014; 77: 161-170.

2. Chapter 2: Altered arsenic availability, uptake, and allocation in rice under elevated temperature

In print: Farhat YA, Kim S-H, Seyfferth AL, Zhang L, Neumann RB. Altered arsenic availability, uptake, and allocation in rice under elevated temperature. Sci Total Environ 2021; 763: 143049. https://doi.org/10.1016/j.scitotenv.2020.143049

2.1. Abstract

Climate change is expected to increase growing temperatures in rice cultivating regions worldwide. Recent research demonstrates that elevated temperature can increase arsenic concentrations in rice tissue, exacerbating an existing threat to rice quality and human health. However, the specific temperature-induced changes in the plant-soil system responsible for increased arsenic concentrations remain unclear and such knowledge is necessary to manage human dietary arsenic exposure in a warmer future. To elucidate these changes, we established four temperature treatments in climate-controlled growth chambers and grew rice plants (*Oryza sativa* cv. M206) in pots filled with Californian paddy soil with arsenic concentrations of 7.7 mg/kg. The four chosen temperatures mimicked IPCC forecasting for Northern California, with a roughly 2.5°C increase between treatments (nighttime temperatures ~2°C cooler). We observed that arsenic concentrations in porewater, root iron plaque, and plant tissue increased in response to elevated temperature. There was a positive linear relationship between temperature and rice grain arsenic, almost all of which was present as inorganic As(III). Aboveground allocation patterns were consistent across treatments. We found no upregulation in the gene encoding the OsABCC1 transporter, believed to be important for arsenic sequestration in vacuoles and thereby preventing arsenic transfer to grain. Rice plants grown at higher temperatures had more adsorbed

arsenic per unit of iron plaque (measured as [As]/[Fe]), indicating temperature may impact arsenic sorption to root plaque. We present evidence that increased soil mobilization of arsenic was the driving factor responsible for increased arsenic uptake into rice grain. Transpiration, which can increase arsenic transport to roots, was also heightened with elevated temperature but appeared to play a secondary role. Our system had low soil arsenic concentrations typical for California. Our findings highlight that elevated growing temperatures may increase the risk of dietary arsenic exposure in rice systems that were previously considered low risk.

2.2. Introduction

Rice is a critical staple food for billions of people who consume rice to meet their daily caloric needs and is therefore an important component of global food security. There is an emerging appreciation that food security must consider not only food supply, but also food quality (Britz et al., 2007; DaMatta et al., 2010; Myers et al., 2014; Smith and Myers, 2018). One aspect of crop quality is the concentration of harmful elements like arsenic (As), a potent carcinogen and toxin frequently found in rice paddy environments. Rice is the major dietary source of arsenic to those without contaminated drinking water (Meharg and Zhao, 2012), and can induce genotoxic effects in humans at levels as low as 200 ng g^{-1} (Banerjee et al., 2013). Inorganic forms of arsenic, like As(III) (i.e., arsenite) and As(V) (i.e., arsenate), are considered more toxic to humans than their common organic counter parts (Vahter and Concha, 2001) and therefore most regulatory guidelines are set to limit inorganic arsenic exposure (Codex 2014; FDA 2016; The European Commision, 2015).

Arsenic is highly mobile in rice paddy environments due to its geochemistry and efficient uptake by rice roots. Rice is often cultivated under flooded conditions leading to an anoxic soil environment. When soils are anoxic, solid-phase arsenic is released in a microbially mediated

reductive dissolution pathway that liberates arsenic from iron (hydr)oxide minerals to which it is bound. This release occurs through dissolution of iron (hydr)oxides when Fe(III) is reduced to Fe(II), and/or desorption of arsenic when it reduces from As(V) to As(III) (Borch et al., 2010; Cummings et al., 1999; Tufano and Fendorf, 2008; Xue et al., 2020). Solutes like arsenic travel via mass-flow and diffusion to the rhizosphere, the soil immediately surrounding and influenced by roots (Barber, 1962; Williams et al., 2014). In the rhizosphere inorganic arsenic can be intercepted by an insoluble iron plaque layer coating rice roots, primarily composed of ferrihydrite with smaller amounts of goethite and lepidocrocite (Amaral et al., 2017; Seyfferth et al., 2011; Yamaguchi et al., 2014). Arsenic species which penetrate or bypass iron plaque are taken up by root cellular transporters. As(III) is taken up by silicon transporters Lsi1 and Lsi2 (Ma et al., 2008) and As(V) is taken up by phosphate transporters (Wu et al., 2011). Arsenic concentrates in vegetative tissue within the plant and can eventually migrate toward grain. To reduce arsenic toxicity, a tonoplastic transporter, OsABCC1, shuttles inorganic arsenic into vacuoles (Song et al., 2014). Within these vacuoles, arsenic is bound to phytochelating agents and prevented from interfering with normal cellular function (Clemens and Ma, 2016). *OsABCC1* expression can occur in many different tissue types and expression levels vary based on plant phenology and arsenic exposure level (Song et al., 2014).

Arsenic-relevant components of the plant-soil system are sensitive to temperature and may therefore be altered by climate change, which will increase average growing temperatures in rice growing regions worldwide (IPCC, 2013b). The magnitude of this temperature increase is uncertain, in large part because of unknown human actions to mitigate climate change. Therefore, IPCC predictions simulate various scenarios, called Representative Concentration Pathways (RCPs), which describe warming predictions from moderate to very severe.

Commonly used RCPs are RCP2.6, RCP4.5, RCP6.0 and RCP8.5. During rice growing months in Northern California, an important rice cultivation region within the USA, these four scenarios predict increased average daily temperatures of up to 1.5°C, 3°C , 4°C and 8°C, respectively (IPCC, 2013a).

Increasing temperature can have numerous impacts on plant biology and function (Arai-Sanoh et al., 2010; DaMatta et al., 2010; Dieleman et al., 2012; Hatfield and Prueger, 2015). For example, it is well known that temperature stress can diminish rice spikelet fertility and overall yield (Baker, 2004; Peng et al., 2004; Porter et al., 2014; Prasad et al., 2006). There is evidence that rice yields are more susceptible to heat stress from increased nighttime temperatures than from daytime temperatures (Kanno et al., 2009; Peng et al., 2004). These temperature-induced changes in plant biology will interact with temperature-driven arsenic mobilization (Simmler et al., 2017; Weber et al., 2010), impacting final arsenic concentrations in plant tissue and grains. Two previous studies have demonstrated that elevated temperature mobilizes soil-bound arsenic and can increase rice uptake of arsenic (Muehe et al., 2019; Neumann et al., 2017). These two studies present conflicting data as to whether an increase in temperature can directly impact concentrations of arsenic within edible grain tissue, where Muehe et al. (2019) detected this increase but Neumann et al. (2017) did not.

Here we attempt to build upon these previous studies and understand how future warming will impact the arsenic uptake pathway in rice with specific attention to three potential points for change: mobilization of arsenic from soil, transport of arsenic to roots, and allocation of arsenic within plant tissue. The mobilization rate, or the solubilization rate of arsenic from soil, is microbially meditated and can be heightened at elevated temperature when microbial rates accelerate (MacDonald et al., 1995; Weber et al., 2010). This response therefore increases the

pool of dissolved arsenic (Simmler et al., 2017; Weber et al., 2010). Root uptake of arsenic may be influenced by temperature in two opposing ways. First, increased temperature can induce increased transpiration rates, leading to greater mass-flow and uptake of solutes (Lynch and St.Clair, 2004; McGrath and Lobell, 2013). Second, elevated temperature can increase iron plaque development (Neumann et al., 2017), which could suppress arsenic uptake. Arsenic distribution within the plant is influenced by both biomass gain and biomass allocation (ex. root to shoot ratio). Growth temperature impacts biomass gain in a nonlinear manner, where biomass production and spikelet fertility increase until an optimal temperature and then fall off precipitously (Arnold et al., 2019; Baker, 2004). For *japonica* rice varieties, the optimal growing temperature is around ~28°C and spikelet sterility occurs between 32–36°C (Baker, 2004). Arsenic allocation is also affected by its sequestration into vacuoles by OsABCC1, which prevents grain loading of arsenic (Song et al., 2014). Increased *OsABCC1* expression is induced by elevated arsenic exposure and may therefore help reduce human exposure to edible arsenic.

We hypothesize that in the soil environment, elevated temperature will increase arsenic availability by boosting arsenic mobilization from soil into porewater. We also hypothesize that transport of arsenic to rice roots will increase due to greater mass-flow, but elevated temperature will simultaneously increase root plaque formation and subsequent sorption of arsenic to plaque. We anticipated that arsenic mobilization and transport will outweigh plaque sorption, resulting in increased plant uptake of arsenic with temperature. Within the plant, we hypothesize that additional arsenic uptake will trigger an upregulation of *OsABCC1* expression, preventing a temperature-fueled increase in rice grain arsenic. To investigate these hypotheses, we cultivated potted rice plants using a gradient temperature approach spanning different IPCC scenarios for

rice cultivating months in Northern California. We used unamended soil with a low total arsenic concentration, representative of baseline arsenic content in most rice growing soils of California.

2.3. Methods

2.3.1. Soil and Plant Material

2.3.1.1. Soil: We collected soil from a rice field in Davis, California. Total soil arsenic was 7.7 ± 0.3 mg kg^{-1} (mean ± SD, n = 3) and oxalate extractable arsenic was 73.0 ± 1.8 μg kg^{-1} (n = 3) (Keon et al., 2001; U.S. EPA, 1996). We moistened soil with deionized water, homogenized it with a portable cement mixer, and added 21 ± 1g of moistened soil into 3-gallon pots. Each chamber had 8 pots; 7 for plants and 1 as an unplanted control.

2.3.1.2. Germination: We grew a Californian, medium-grain rice variety, (*Oryza sativa* L. ssp. *japonica* cv. M206). We planted 10 rice seeds into moistened but not flooded soil in each pot designed for plants, and placed pots in experimental chambers to germinate for 16 days. Then we thinned seedlings to 6 per pot to match number of plants that germinated at low temperature. Treatment temperatures are further described in Section 2.2.

2.3.1.3. Plant Care: One week after plant thinning, we flooded pots to 5cm above soil surface and kept pots flooded with twice weekly watering. We irrigated using a 10× dilution of Hoagland solution (Hoagland and Arnon, 1950). We allowed freshly prepared irrigation solution to equilibrate with chamber temperature in a carboy for at least 24 hours before watering to moderate soil temperature. We recorded volume of water added to planted and unplanted pots to estimate volume of water lost by evaporation (water lost from the unplanted pot) and transpiration (planted pot water loss - unplanted pot water loss). Water use efficiency was calculated by dividing mature plant biomass by volume of water transpired.

2.3.2. Growth Chamber Set-up and Temperature Treatments

We cultivated rice in growth chambers (DarkRoom II DR90, 36" × 36" × 72") at four different temperatures: 25.4 / 22.6°C, day/night (low temperature, LT); 27.9 / 25.8°C (medium-low, MLT); 30.5 / 28.9°C (medium-high, MHT) and 32.9 / 31.0°C (high temperature, HT) (**Figure 2.1**). Temperatures were controlled using heaters (Dr Infrared Heater) and fans connected to an environmental controller (model CHHC-4i, Sentinel). Each week we used a random number generator to rearrange pots to help control for any variation in temperature throughout the chamber.

We measured air temperature at leaf level (Smart Sensor, Onset) and soil temperature at 10 cm depth in half of the pots in each treatment (TidbiT, Onset). Average light intensity at leaf level was 290 µmol m^{-2} s^{-1} (PAR Smart Sensor, Onset). Plants grew on a 12-hr light-dark schedule. Additional information about growing conditions is in Appendix 1 in **Table A1.1**.

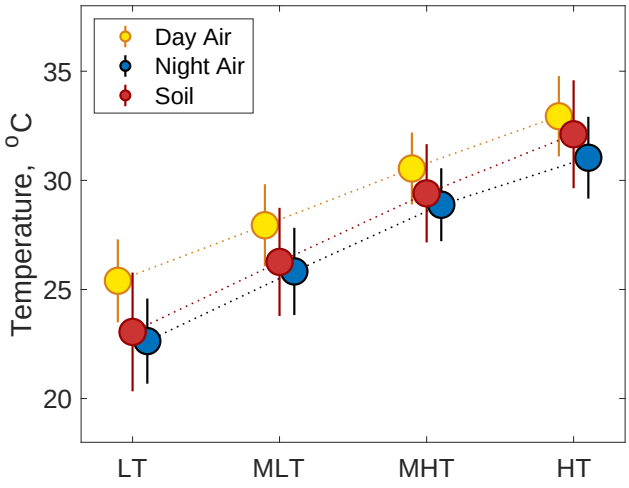

Figure 2.1. *Average temperatures of each treatment group over the course of the experiment with associated standard deviations. Temperature treatments are as follows: Low temperature (LT), Medium Low Temperature (MLT), Medium High Temperature (MHT), and High Temperature (HT). We measured air temperature using RH/Temperature Sensor (Onset) and soil temperature using a TidbiT Temperature Logger (Onset) buried at a 10cm depth in 4 of 8 pots.*

2.3.3. Sample Collection

2.3.3.1. Timing: We defined three time points for sample collection: vegetative growth, flowering, and maturity. Briefly, we collected porewater at all three time points and collected plant and soil samples during the latter two time points (further described in Sections **2.3.2-3**). The vegetative sampling point occurred 38 days after seeding, at the beginning of tillering stage, and was consistent across treatments. We defined flowering and maturity points observationally to adjust for differences in phenology with temperature. The flowering collection point occurred when over 75% of all plants in a given treatment had entered flowering stage. Most treatment groups flowered within the same week, with the exception of LT treatment, which flowered roughly 2 weeks later than other treatments. Maturity was defined for groups LT, MLT, and MHT by completion of grain filling. There was a roughly 2-week separation between full maturity in these three groups (first MLT, then MHT, and last LT). It was difficult to determine a full maturity time point for HT treatment because spikelets remained unfilled likely due to heat stress, even though plants were allowed to mature for longer than other treatments. Therefore, the definition of "maturity" in this treatment was not physiologically based, but rather when the treatment was harvested, which was two and a half weeks after other treatment groups.

2.3.3.2. Porewater Collection: We collected porewater samples at vegetative, flowering, and maturity time points. We installed MicroRhizons (0.15 μm filter, Rhizosphere Research Products) into pot soil 24 hours before the vegetative sampling event and left them in the pots throughout the experiment. We connected MicroRhizons to a 2-way stopcock with an attached needle used to pierce the septum of 12mL glass vials (Exetainer, Labco). During porewater sampling events we collected three samples with vials prepared in the following ways. The first vial cleared the sampler and, because collected solution was discarded, these vials were not

rigorously cleaned. Next, we collected the porewater sample for elemental analysis using an acid washed, foil wrapped, N_2-purged, and evacuated vial. The last sample we collected for electrochemical characterization and carbon content, and therefore the vial was ashed as well as acid washed, foil wrapped, N_2-purged, and evacuated. Each of the three vials was left to collect porewater for between 30 minutes and 1 hour.

We preserved porewater for elemental analysis by acidifying to 2% v/v with trace metal grade HNO_3 immediately after opening anoxic vials. Within two hours of collection, we transferred the sample for electrochemical characterization to an anaerobic glovebox. We removed 2mL of each sample into a sealed vial, which we refrigerated (4°C) for 1-2 days before analysis for dissolved organic and inorganic carbon. We measured pH and conductivity of remaining porewater solution in the glovebox.

2.3.3.3. Destructive Harvest: We performed two destructive harvests at flowering and at maturity to collect plant and soil samples. Harvests occurred 1-2 days after porewater collection. During destructive harvests, we used a 4 × 30cm cylindrical plastic tube (AMS) with a hand pressed firmly on top as a vacuum seal to collect a soil sample within the rooting zone. Immediately after removal, we capped the tube, sealed it with electrical tape, placed it in a gas impermeable liner (ESCAL, Mitsubishi Gas Chemical) with an oxygen scavenging packet (BD GasPak™), and heat-sealed liner. We refrigerated the soil until analysis.

From each pot during both harvests, we removed two plants for physiological measurements then combined them into a composite sample for arsenic analysis, and we removed one plant for expression of *OsABCC1*. We used a random number generator to select plants. We cut the two plants at the soil surface and measured plant height, leaf number, leaf area, and tiller number. Due to high planting density, most plants did not produce tillers.

Following physiological measurements, we partitioned and combined tissues from these two plants into one composite sample that was oven-dried at 60°C (Arao et al., 2009; Li et al., 2009). During the harvest at maturity we also collected root samples from these two plants, carefully removed by hand. After removal, we rinsed roots in Milli-Q water to remove adsorbed soil and allowed roots to air-dry. For the gene-expression plant (further described in Section 2.5), we flash froze tissue in liquid nitrogen and then stored tissue at -80°C until analysis.

2.3.4. Extractions

2.3.4.1. Plant Tissue: We removed root plaque using a modified hot dithionite-citrate-bicarbonate (DCB) extraction (Taylor and Crowder, 1983). We cut large root systems into fragments of 0.5g or smaller (mass known exactly) and performed extractions on all fragments of the root system. Detailed instructions of extraction procedure can be found in supplemental information. After washing, we air-dried root systems again in preparation for digestion.

We analyzed dried roots, stems, leaves, spikelets, mature hulls, and unpolished grains for arsenic content. Rice grains were separated from hulls using a simple rice huller with two rubber rollers moving in opposite directions. We ground each tissue and separated ~300mg of sample for hot HNO_3-H_2O_2 digestion. We then added 3mL of H_2O_2 and 7.5mL of HNO_3. A microwave digester (Anton Parr) heated samples to 190°C and digested them for 30 minutes. Then we decantated and brought extractant volume up to 25 or 50mL volumetrically, based on expected arsenic concentration. Each extraction contained two sample blanks and 2/3^{rds} of runs contained a NIST Standard Reference Material (SRM) 1568b rice flour. Average arsenic recovery from NIST 1568b was 105 ± 12% at 95% confidence limits (n = 32).

We analyzed arsenic speciation in brown rice using a 2% HNO_3 extraction (Maher et al., 2013). Detailed instructions of extraction procedure can be found in supplemental information.

Our extraction also contained a sample of SRM1568b rice flour sample and quantification of our detected arsenic species was within 95% confidence limits certified by supplier.

2.3.4.2. Soil: We air-dried collected soil in an anoxic glovebox until weight was constant. Within the glovebox we finely ground each soil sample. We subjected soil to an abbreviated two-step sequential extraction procedure. We performed extractions on soil samples collected during flowering and at maturity, for at least four pots randomly selected (via number generator) from each treatment at both time points. First, we desorbed weakly adsorbed arsenic with a concentrated phosphate extraction (Keon et al., 2001; U.S. EPA, 1996). In the second step, we removed Fe-associated arsenic using a CBD extraction (Mehra and Jackson, 1958). Detailed instructions can be found in the supplemental methods.

2.3.5. Analytical Methods

2.3.5.1. Elemental analysis and speciation: We used inductively coupled plasma mass spectroscopy (ICP-MS) to quantified total arsenic dissolved in porewater and in soil extractions (PerkinElmer, Elan DRC-e), and arsenic in root extractions and tissue digestions (PerkinElmer, NexION 2000, upgraded model). We analyzed porewater samples using an arsenic standard curve with a yttrium internal standard. In tissue and soil extraction analysis, we used a standard addition of arsenic to each sample to correct for stronger matrix effects. We evaluated iron removal from root plaque during DCB extraction using inductively coupled optical emission spectroscopy (ICP-OES, Perkin-Elmer, Optima 8300). We quantified inorganic As(III), As(V), DMA, and MMA in unpolished grain samples using an HPLC-ICP-MS (Thermo ICS-6000 HPLC coupled to a Thermo TQ). Separations were achieved with a PRP-X100 anion exchange column (Hamilton) with a gradient mobile phase of 3% methanol and 50mM $NaHCO_3$ in 3% methanol according to established methodology (Jackson, 2015).

2.3.5.2. RT-qPCR: We chose to analyze flag leaf and spikelet tissue, based on their high expression during flowering stage (Song et al., 2014). We removed tissue from -80°C freezer and freeze-dried samples for at least 12 hours. We then extracted RNA with RNeasy Plant Mini Kits (Qiagen, Valencia, CA). We used oligo (dT) 12-18 primers (Invitrogen) and M-MLV Reverse Transcriptase (Invitrogen) to produce cDNA. Finally, we preformed quantitative PCR (qPCR) of *OsABCC1* expression normalized to reference gene *HisH3*, using primer sequences published in Song et al. (2014) and SensiFAST™ SYBR® No-ROX Kits.

2.3.6. Statistical Methods

We performed statistical analyses using MATLAB (ver. R2019a). We first analyzed temperature trends using a linear regression model fit to all data, including replicates, and plotted residuals of model output. Based on residual plots and apparent nonlinearity in many trends, we decided most outputs did not meet assumptions of a linear regression model, though there were a few exceptions. Therefore, we performed a one-way ANOVA analysis followed by Tukey HSD post-hoc using $\alpha = 0.05$. Data for ANOVA was $\log_{10}$ transformed to reduce skew and improve normality. Data was graphed in non-transformed space for visual clarity.

2.3.7. Mass Balance Estimate of Arsenic

Recognizing that both increased mobilization of arsenic into porewater and increased transpiration at higher temperatures could be involved in heightened arsenic mass-flow, we performed a simple illustrative mass balance to understand the potential arsenic response to each. Mass-flow (μg) was calculated as dissolved arsenic concentration multiplied by the amount of water transpired:

$$\mathrm{As}_{mass} = \mathrm{W} \times [\mathrm{As}]$$

where, W is the volume of water transpired per plant (L) and [As] is the dissolved arsenic concentration in the unplanted pot (μg L^{-1}). At higher temperatures we expect an increase in both terms relative to LT treatment:

$$As_{mass} = (W_{LT} + \Delta W)([As]_{LT} + \Delta[As])$$

where, W_{LT} is the average volume of water transpired by LT treatment, ΔW is the increased average volume of water transpired by other three treatments relative to LT treatment, $[As]_{LT}$ is the time-averaged concentration of dissolved arsenic in the unplanted pot of LT treatment, and Δ[As] is the increase in time-averaged dissolved arsenic concentrations in other three treatments relative to LT treatment. The equation can be expanded into four terms:

$$As_{mass} = W_{LT}[As]_{LT} + \Delta[As]W_{LT} + \Delta W[As]_{LT} + \Delta W\Delta[As]$$

The first term describes arsenic mass-flow in LT treatment, the second term describes the increase in arsenic mass-flow due solely to the temperature-fueled increase in arsenic mobilization, the third term describes the increase in arsenic mass-flow due solely to the temperature-fueled increase in transpiration, and the final term describes the increase in arsenic mass-flow due to the combined response of arsenic mobilization and transpiration to temperature (i.e. plants pulling more water with more dissolved arsenic toward their root systems at higher temperatures). It is important to note that this mass balance is an illustrative calculation of mass-flow and therefore does not account for diffusion or desorption of arsenic.

2.4. Results

2.4.1. Arsenic Concentrations in Rice Tissue

Arsenic concentrations increased in plant tissue with temperature (**Figure 2.2**). Statistical analysis of grain arsenic contained only 3 treatment conditions (LT, MLT, and MHT) due to unfilled grain in HT that induced spikelet infertility. There was a positive linear relationship

between temperature and arsenic concentration in brown rice grain as well as in stem tissue at maturity (**Figure 2.2A** and **G**). In all other tissues, residuals plots indicated that linearity or normality assumptions did not hold (Appendix 1, **Figure A1.1**).

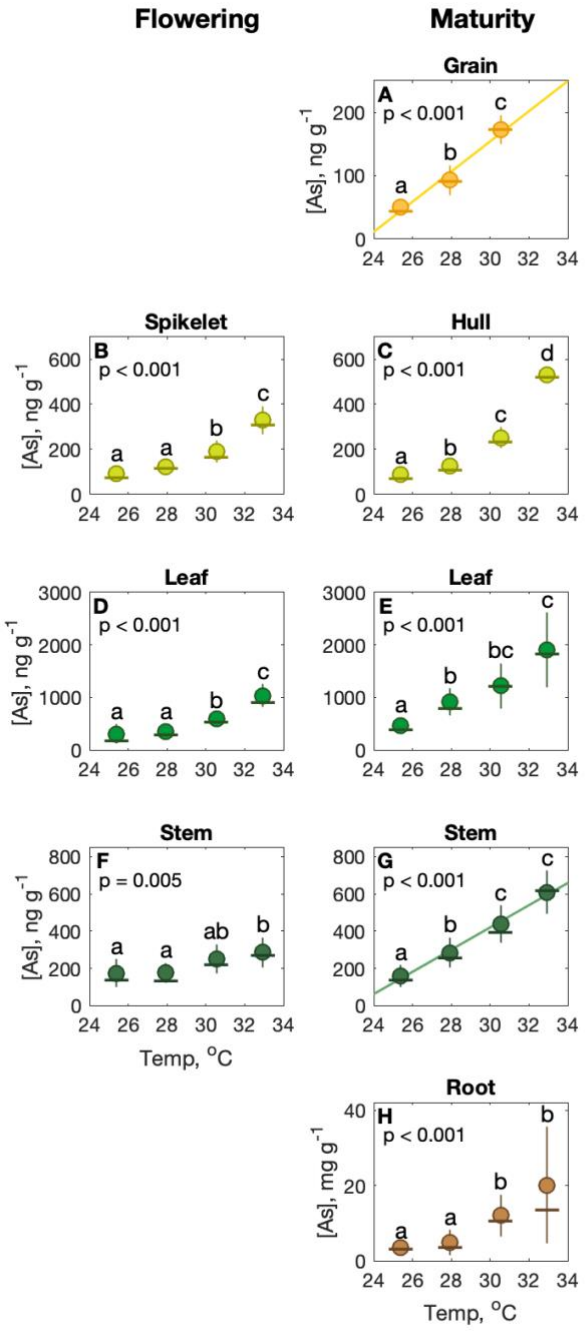

Figure 2.2. *Concentrations of arsenic in plant tissue vs. average daytime temperature during the experiment. Mean concentration depicted with circle, median with dash, and associated interquartile ranges with error bars. Columns represent one of two developmental stages: flowering and maturity. No grain samples were collected from highest temperature treatment (HT) due to severe heat stress which prevented seed set. Trend lines are shown for tissues with a linear arsenic-concentration response to temperature (i.e.,* ***A*** *and* ***G****). ANOVA p-value for* log_{10} *transformed concentrations are shown along with statistical groups, marked with lowercase letters, determined by Tukey-Kramer post hoc at 95% confidence.*

Figure 2.2 shows ANOVA p-values and statistical groups determined by Tukey HSD test ($\alpha = 0.05$) of $\log_{10}$ transformed data. In all tissue types the temperature impact on arsenic concentrations was highly significant ($p < 0.01$), though not uniform across treatment groups or plant development stage. Arsenic response to temperature was weaker in tissue at flowering than in the tissues at maturity. At flowering stage, arsenic concentrations in spikelet, leaf, and stem (**Figures 2.2B, D,** and **F**) were not significantly different between the two coolest temperature treatments (LT and MLT). Arsenic concentrations were increased in spikelet and leaf tissue in the MHT treatment, and in all sampled tissues, arsenic concentrations were highest in the HT treatment.

At maturity stage, the response of arsenic in plant tissue to temperature was more dramatic. In grain and hull tissue, arsenic concentrations were significantly different in each temperature treatment, with concentrations increasing across the treatment groups (**Figure 2.2A** and **C**). In leaf tissue, arsenic concentrations similarly increased with temperature, though there was overlap in concentrations between MLT and MHT treatments, as well as MHT and HT treatments (**Figure 2.2E**). Root tissue, sampled at plant maturity, showed a step response to temperature with arsenic concentrations in the two coolest treatments being significantly different than concentration in the two warmest treatments (**Figure 2.2H**).

Almost all arsenic in grain tissue (96%) was in the arsenite, As(III), form. On average, DMA made up 3% of grain arsenic and MMA was only present above detection limits in four samples. As the vast majority of total arsenic was arsenite, ANOVA and post-hoc results shown in total grain arsenic (**Figure 2.2A**) were mirrored in grain arsenite concentrations (**Figure A1.2A**, $p < 0.001$, $F = 61$). There was no significant effect of temperature on grain DMA

concentration (**Figure A1.2B,** p = 0.054, F = 3.4). Sum of arsenic species was close to total grain arsenic (116 ± 20%, mean and SD).

2.4.2. Arsenic Content and Allocation

We calculated total arsenic content (i.e., accumulation) using partitioned masses of each tissue type multiplied by relevant concentrations. A large portion of arsenic taken up by rice plants resided in roots, which contained, on average, 52% of plant arsenic (**Figure A1.3B**). However, variance in this estimate was large (SD = 20%). **Figure 2.3A** shows average total arsenic content in just above-ground tissue compartments and outputs of Tukey HSD post-hoc (α = 0.05). Temperature increased arsenic content of all above-ground tissue, with statistically significant differences between LT, MHT and HT treatments. Arsenic content of MLT overlapped with that of MHT for all tissue compartments, and with that of LT in stems and hulls.

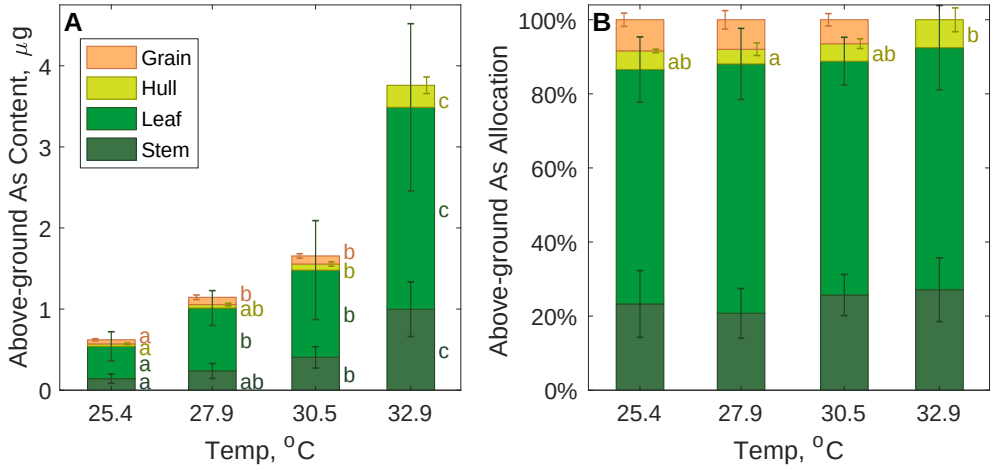

Figure 2.3. *Arsenic content and allocation in mature tissue. (A) Average total arsenic in above-ground tissue types (grain, hull, leaf, and stem) in different temperature treatments, calculated as tissue concentration of arsenic multiplied by tissue mass. Error bars show standard deviation from mean. (**B**) Percentage of total above-ground arsenic present in each tissue compartment. In both graphs, lowercase letters indicate statistical differences for each tissue type based on ANOVA (α = 0.05) performed on* log_{10} *transformed values followed by Tukey-Kramer post hoc test.*

There was a notable jump in total arsenic accumulation between MHT and HT treatments, most of which was located in leaf and stem tissue. This jump was the result of both higher arsenic concentration in these tissues (**Figures 2.2C** and **E**), and an increase in vegetative tissue biomass with temperature (**Figure A1.4A**, $p < 0.001$, $F = 6.2$). Differences in grain arsenic content were not attributable to changes in grain yield as there was no consistent decrease in yield across all treatments). Instead, there was no difference between grain biomass between LT and MLT treatment and only decrease in grain yield in MHT treatment (**Figure A1.4B**).

Even though warmer temperatures increased arsenic accumulation, the distribution of arsenic within above-ground tissue types was similar across temperature treatments (**Figure 2.3B**). On average 24% of above-ground arsenic was allocated to stems, 65% to leaves, and 5% to hulls. Of the three treatments which produced grain, an average of 8% of above-ground arsenic ended up in rice grains. There was no difference in percent arsenic allocated to stems, leaves, or grains across treatments (ANOVA, $p > 0.05$). There was a discernable statistical effect of temperature on arsenic allocated to hull ($p = 0.008$, $F = 5.0$), though the only difference was between HT and MLT.

To further examine potential changes in allocation, we quantified *OsABCC1* expression at flowering. We were unable to detect a consistent temperature trend in *OsABCC1* expression in response to temperature in flag leaves or spikelet (**Figure A1.5**). There was a large degree of variance in RT-qPCR results, especially in flag leaf.

2.4.3. Arsenic in Iron Plaque

Higher temperature was associated with more sequestration of arsenic in iron plaque per gram of root biomass (**Figure 2.4A**, $p < 0.001$, $F = 54$), where the higher two temperature treatments had more arsenic than the lower two temperature treatments. Iron plaque formation was also

impacted by temperature (**Figure 2.4B**, $p < 0.001$, $F = 30$) though the relationship was not monotonic; iron plaque, measured as mass of iron per gram of root biomass, first decreased between LT and MLT and then increased between MLT, MHT and HT treatments. The amount of arsenic sequestered per gram of iron plaque was greater in the two warmer temperature treatments than in the two cooler treatments (**Figure 2.4C**, $p < 0.001$, $F = 56$). The increased ratio of arsenic to iron in warmer treatments indicates that the sorption capacity of iron plaque was greater in these treatments than in the cooler treatments.

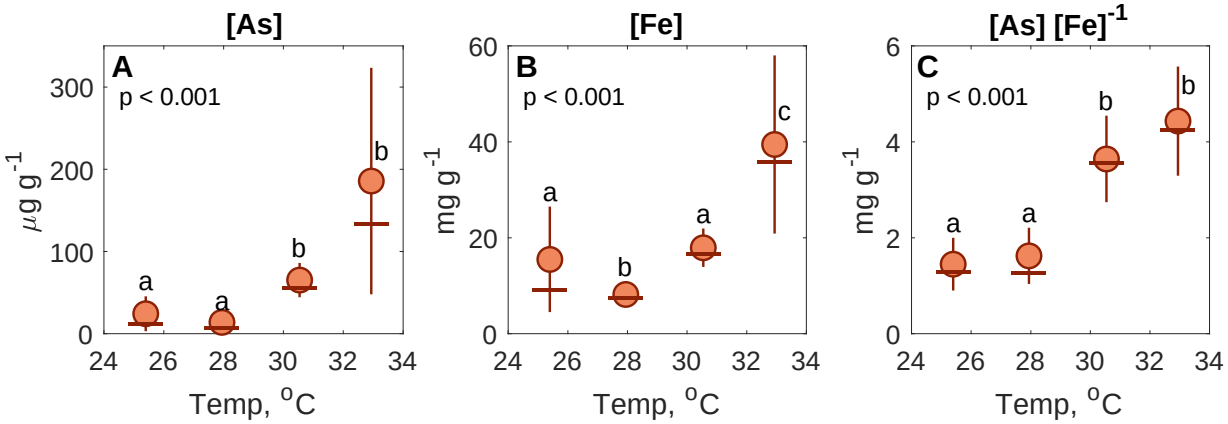

Figure 2.4. *Root plaque removed by hot dithionite-citrate-bicarbonate (DCB) extraction. (**A**) Arsenic, As, and (**B**) iron, Fe, concentrations above are the mass of both chemicals removed by extraction, normalized to root biomass. (**C**) As/Fe ratio is the ratio of arsenic to iron removed by DCB extraction. Means (circles, •) and median (dashes, –) of each value are presented above with associated interquartile ranges (error bars). Statistical differences were determined by ANOVA ($\alpha = 0.05$) on log_{10} transformed values followed by Tukey-Kramer post hoc, as marked by lower case letters.*

2.4.4. Arsenic in Porewater

Porewater concentrations of arsenic in planted pots were impacted by temperature at all three time points (**Figure 2.5**). During the vegetative porewater sampling, dissolved arsenic was elevated only in HT treatment (**Figure 2.5A**, $p < 0.001$, $F = 81$); concentrations were statistically

similar across the other three temperature treatments. At both flowering and maturity stage (**Figure 2.5B** and **C,** $p < 0.001$, $F = 28$ and 28), porewater arsenic concentrations in planted pots were greatest in HT, comparable in MHT and MLT, and lowest in LT. Overall, concentrations of dissolved arsenic within a given temperature treatment were greatest during the flowering stage.

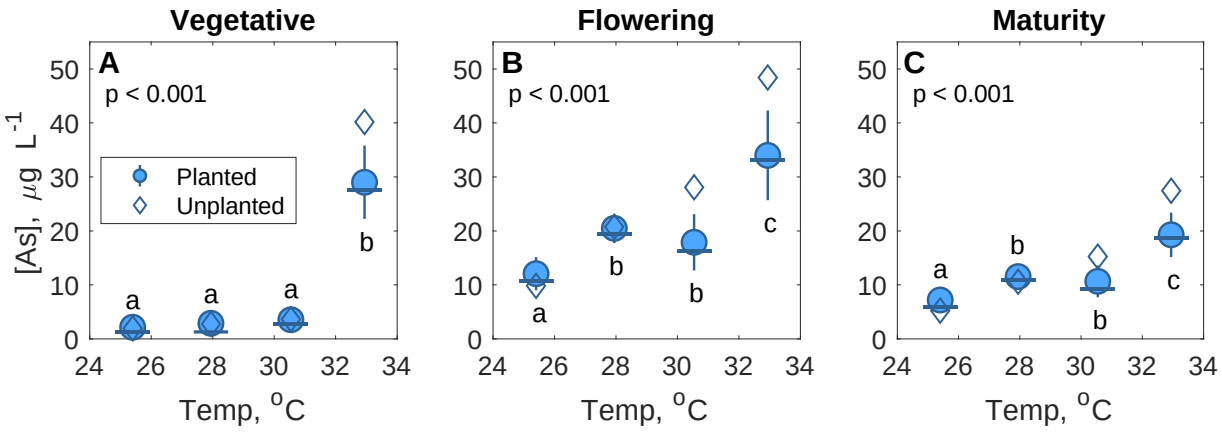

Figure 2.5. *Arsenic concentrations in porewater. Mean (circle, •) and median (dash, –) concentrations of arsenic (As) in eight planted pots with associated interquartile ranges (error bars). The arsenic concentration of the unplanted pot is depicted with a diamond (◊). Statistical differences in dissolved arsenic concentrations in planted pots were determined by ANOVA ($\alpha = 0.05$) on log_{10} transformed values followed by Tukey-Kramer post hoc, as marked by lowercase letters.*

At the vegetative sampling point, dissolved arsenic concentrations of the unplanted pots (n=1 per treatment) fell within interquartile range of planted pots for all treatments except HT, which had higher dissolved arsenic in the unplanted pot. At flowering and maturity time points, dissolved arsenic in the unplanted porewater was above interquartile ranges of planted pots for MHT and HT treatments. Arsenic in porewater of unplanted pots provides a visualization of arsenic concentrations without plant uptake; though we only had one pot per treatment and therefore cannot perform descriptive statistics.

Porewater dissolved iron response to temperature was less consistent. At the vegetative time point dissolved iron in porewater increased with temperature (**Figure A1.6A**, $p = 0.012$, $F = 4.33$); planted pots in the HT treatment had significantly more dissolved iron than in the LT treatment, and dissolved iron in planted pots of the MHT and MLT treatments fell between these two extremes. This trend was not present in planted pots during the other two time points, though it was visible in unplanted pots (**Figure A1.6B** and **C**). At flowering and maturity time points, dissolved iron in unplanted pots was lower than mean and median iron concentrations in planted pots for the two cooler temperature treatments, while in the two warmer temperature treatments dissolved iron in unplanted pots was greater than the mean and median of planted pots.

2.4.5. Arsenic in Soil

There was no clear relationship between temperature and the amount of arsenic removed by either Phosphate (Phos) or CBD extraction (**Figure A1.7A** and **B**). Phosphate extractable arsenic made up 72.3 ± 8% (mean ± SD) of extracted arsenic (arsenic removed by sequential extraction) while CBD extractable arsenic made up 28 ± 8% of extracted arsenic (**Figure A1.7C** and **D**). During the flowering time point, MHT had significantly more arsenic removed by CBD extraction relative to LT treatment during (**Figure A1.7A**), leading to a greater relative share (%) of extracted arsenic being removed in the CBD step (**Figure A1.7C**). However, this effect was not consistent across temperature treatments nor detectable at the harvest at maturity. Average total extracted arsenic (Phos + CBD) was within one SD of total soil arsenic (7.7 ± 0.3 mg kg^{-1}, mean and SD).

2.4.6. Transpiration and Water Use Efficiency

Average daily transpiration, measured as total volume of water transpired by each plant divided by number of days to maturity, and the total transpired volume of water by each plant

increased with temperature (**Figure 6A** and **B**, ANOVA, $p < 0.001$, $F = 32$ and 45). Plants in the warmer two temperature treatments transpired significantly more water and at a faster rate than those in the two cooler treatments. Water Use Efficiency (WUE) decreased with temperature (**Figure 6C**, $p < 0.001$, $F = 18$), where HT WUE was significantly lower than that in the MLT and LT treatments. This difference in WUE was primarily driven by changes in transpiration as we found no significant change in total biomass across temperature treatments groups ($p = 0.33$, $F = 1.2$, **Figure A1.4C**). We note that while total biomass and above-ground biomass did not change across treatments (**Figure A1.4C** and **S4D**), root biomass did experience statistical differences with temperature (**Figure A1.4E**, $p = 0.015$, 4.1). These root biomass variations resulted in a generally decreasing root to shoot ratio with temperature (**Figure A1.4F**, $p = 0.003$, $F = 5.8$); LT had the highest ratio and the two warmest treatments (MHT and HT) had the lowest ratio.

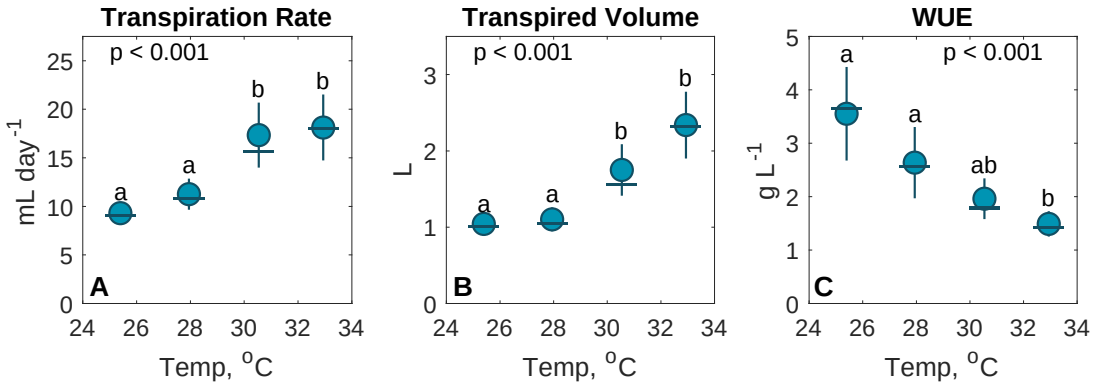

Figure 2.6. *Water relations of each treatment group. Per plant water relations as (**A**) transpiration rate and (**B**) total transpired water volume and (**C**) water use efficiency (WUE), with mean (circle, •), median (dash, –interquartile ranges (error bars). WUE is measured as total biomass normalized by transpiration rate. Statistical differences were determined by ANOVA ($\alpha = 0.05$) on log_{10} transformed values followed by Tukey-Kramer post hoc, as marked by lowercase letters.*

2.4.7. Mass Balance Estimate of Arsenic

Our calculations (**Figure 2.7)** indicate that average arsenic mass-flow can increase with temperature and that this increase was mainly the result of increased arsenic mobilization from soil solids (38-47%), with a lesser contribution from increased transpiration rate (2-15%). The combined effect of increased arsenic mobilization from soil and increased transpiration grew in importance across MLT, MHT and HT treatments, accounting for 3%, 26%, and 47% of arsenic mass-flow, respectively. In **Figure 2.7**, mean observed arsenic accumulation in plants within each treatment is also shown. Accumulated arsenic includes mass of plaque-associated arsenic and mass of arsenic in plant tissues. Calculated arsenic delivery to roots via mass-flow surpassed mean observed arsenic accumulation within plants in the MLT, MHT and HT treatments.

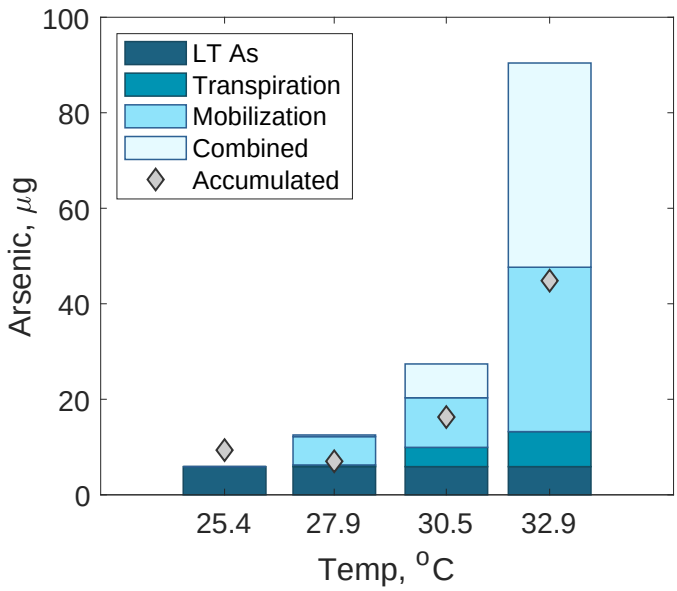

Figure 2.7. *Simple mass balance of expected increase in the mass of arsenic available for uptake or sorption to root plaque relative to low temperature treatment. Arsenic mass is broken up into the amount attributable to increased mobilization of arsenic from soil, increased transpiration, and their combined effect. Diamonds (◊) illustrate mean observed arsenic accumulation per treatment (sum of in-plant and root plaque arsenic).*

2.5. Discussion

This work builds on a growing body of literature what examines arsenic concentrations in rice tissue as a function of temperature (Arao et al., 2018; Muehe et al., 2019; Neumann et al., 2017). In this experiment we sought to gain a more mechanistic understanding of how increasing temperatures impacts key components of the plant-soil system, including mobilization of arsenic from soil, transport of arsenic to rice roots, and allocation of arsenic within plant tissue.

2.5.1. Arsenic Concentrations with Temperature

We detected temperature-increased arsenic concentrations in various plant tissue types (**Figure 2.2**). This finding is consistent with previous research showing that elevated temperature increased arsenic content in straw and leafy tissue (Muehe et al., 2019; Neumann et al., 2017). Most importantly, we observed an increasing trend between temperature and both total grain arsenic and grain inorganic arsenic (**Figure 2.2A**, **Figure A1.2A**), indicating that higher temperatures can increase human exposure to inorganic arsenic. This result is an important finding as previous studies have been inconsistent with regard to the ability of increased temperature to translate into higher arsenic in grain tissue. Neumann et al. (2017) was unable to track elevated temperature to increased arsenic concentration in grain using a Bangladeshi rice variety; however, Muehe et al. (2019) found an increase in grain arsenic under higher temperature conditions using the M206 variety (same variety as used in this study). Additional research is necessary to compare response rates of different rice varieties and different severity levels of arsenic contamination as these findings may inform adaptation strategies.

The system modeled here is a low arsenic system, with soil arsenic concentrations similar to average California paddy soils (Chang et al., 2004). This contamination level may help explain the sensitivity of plant tissue arsenic to temperature within our experiment, because

inorganic arsenic influx exhibits a classic uptake Michaelis–Menten kinetics curve that is more linear at low concentrations but approaching an asymptotic peak at higher concentrations (Abedin et al., 2002). Neumann et al. (2017) used amended soil with a higher arsenic concentration, and uptake rates may have been closer to an asymptotic level with less sensitivity to temperature. Muehe et al. (2019) compared low and amended soil arsenic systems and found that increasing arsenic contamination of soil resulted in greater total arsenic (inorganic + organic) concentrations in rice grain. However, in their study most of the additional arsenic in rice grain was comprised of DMA, which is less toxic to humans but can cause yield declines in rice (Limmer et al., 2018a). The increased DMA may have resulted from arsenic methylating microbes responding to higher arsenic desorption in the amended soils (Dykes et al., 2020, In Press). Therefore, increased soil arsenic contamination does not necessarily lead to additional inorganic arsenic content in grains. Similar to our study, Muehe et al. (2019) found that temperature increased inorganic arsenic in grain in both the low and amended arsenic systems – indicating that temperature is an important factor in determining inorganic arsenic concentrations in grain at various levels of soil contamination.

2.5.2. Mobilization and Soil Sources

Increased microbial respiration occurs at higher temperatures and can therefore lead to heightened solubilization of arsenic (Simmler et al., 2017; Weber et al., 2010). Currently, this process is thought to be driven by increased activity of Fe(III)-reducing microorganisms and consequent reductive dissolution of As-bearing Fe(III) minerals (Weber et al., 2010). Our mass balance calculation highlighted that this temperature-driven mobilization of arsenic was a key component of increasing arsenic delivery to roots and can therefore increase arsenic accumulation in above-ground tissue (**Figure 2.7**).

Our hypothesis that elevated temperature would increase arsenic availability in porewater was proven correct. The unplanted pot in each treatment can act as a proxy for mobilization of arsenic from soil with no arsenic loss to plant uptake; porewater concentrations in the unplanted pots showed an increase with temperature during flowering and maturity stages (**Figure 2.5B** and **C**). Porewater arsenic concentrations in planted pots were not linear, though warmer temperatures did increase dissolved arsenic relative to the LT treatment (**Figure 2.5B** and **C**). In the two high temperature treatments (HT and MHT) the gap between unplanted and planted dissolved arsenic was noticeable during flowering and mature stages. Such a gap likely represents the amount of arsenic lost to plant uptake, indicating that this additional pool of arsenic released at higher temperatures was taken up into plant tissue.

We used phosphate and CBD extractions to simulate arsenic pools accessible by competitive ion desorption and iron reduction, respectively (Keon et al., 2001; Mehra and Jackson, 1958). These two arsenic pools are likely assessable to soil microbes. Arsenic removed by phosphate and CBD extractions showed little change over time and between treatments (**Figure A1.7**). Thus, there was no substantial change to these two pools of microbially accessible arsenic, supporting the claim that increased dissolved arsenic was a stronger predictor of arsenic in tissue than in solid phase arsenic. Given that soil solid phases hold a much larger amount of arsenic than the fraction found in the dissolved phase, it is not surprising that we were unable to detect reductions in arsenic content found in the soil but were able to detect changes in porewater concentrations.

2.5.3. Transport to Roots

Plant uptake of solutes is influenced by their movement of said mineral in soil solution through the transpiration stream (Barber, 1962). It is common knowledge that increasing

temperature increases vapor pressure deficit at leaf surface, increasing transpiration through stomata. We observed both increasing transpiration and decreasing seasonal water use efficiency (WUE; total biomass/water used) (**Figure 2.6**), supporting our second hypothesis of increased arsenic mass-flow to roots. Changes in transpiration can impact uptake of solutes that travel by mass-flow and can therefore impact arsenic uptake and concentration (McGrath and Lobell, 2013; Wan et al., 2015). However, our mass balance calculation indicated increased transpiration was likely not a dominant contributor to increased arsenic uptake (**Figure 2.7**). Transpiration was a significant factor in MHT and HT treatment when paired with increased mobilization, in "the combined effect" term. The importance of this combined effect in MHT and HT treatments is due to increasing difference in both dissolved arsenic and total transpiration relative to LT treatment (i.e. greater Δs).

One shortcoming of our mass balance calculation is that it does not include arsenic transport by diffusion, which can also be an important component of iron and arsenic delivery to roots (Williams et al., 2014). Based on the Wilke–Chang equation (Wilke and Chang, 1955) and parameter values provided in Tanaka et al. (2013) we estimated that the molecular diffusion coefficient would only increase by ~2.5% between LT and HT treatments, while average transpiration rate increased by 95% between LT and HT treatments (**Figure 2.6A**). Therefore, diffusion is likely less sensitive to increased temperature within this thermal range. Whether mass-flow or diffusion is the predominant mechanism of root delivery is ion specific and depends on concentration in the soil solution, soil water flow rate, and rate of root uptake of that specific ion. It is not clear exactly which is the predominant mechanism in the case of As(III) and rice, though the high physiological rates of uptake, such as those observed with arsenic and rice, tends to be associated mass-flow systems (Barber, 1962; Zhao et al., 2009).

Arsenic which travels to the rhizosphere may sorb onto iron plaque coating surrounding rice roots (Chen et al., 2005; Liu et al., 2006; Seyfferth et al., 2011; Yamaguchi et al., 2014). We found that with increasing temperature, there was greater iron plaque formation and that plaque captured more arsenic (**Figure 2.4A** and **B**). As we anticipated in our hypotheses, the increased below-ground storage of arsenic was not sufficient to offset arsenic accumulation observed in above-ground plant tissue. Other work on arsenic and temperature has also shown that temperature can impact root plaque dynamics. Using XRF imaging, Neumann et al. (2017) found that rice plants grown at elevated temperatures had substantially more iron plaque formation and more plaque-associated arsenic. The additional iron plaque formation at higher temperatures may be due to increased iron solubilization with temperature (Weber et al., 2010). Alternatively, Lee et al. (2013) found that arsenic addition lead to increased iron plaque formation on rice roots, though they were not able to elicit the underlying mechanism.

We also found that the $[As]\ [Fe]^{-1}$ ratio increased with temperature (**Figure 2.4C**). We considered various explanations for the relationship between the $[As]\ [Fe]^{-1}$ ratio and temperature. One explanation is that greater arsenic delivery to roots leaded to greater arsenic incorporation in plaque during plaque formation, increasing the [As] numerator more than the [Fe] denominator. Another possible explanation for this phenomenon could be related to changes in plaque minerology and its sorption capacity for arsenic. For instance, temperature can increase root exudation rates (Bokhari and Singh, 1974; Uselman et al., 2000), and root exudates are organic ligands that can both promote the formation of ferrihydrite and prevent aging of ferrihydrite to more ordered iron forms (Cornell, 1987; Violante et al., 2003). Poorly crystalline ferrihydrite is associated with greater plaque arsenic sorption compared with more ordered iron minerals (Seyfferth et al., 2019). In either case, more extensive analysis is needed to understand

the impact of elevated temperature on root plaque formation, sorption capacity, and mineral composition.

The observed average arsenic accumulation in iron plaque and plant tissue was lower than arsenic mass-flow delivery in all treatments besides LT where accumulation was slightly higher than the calculated delivery (**Figure 2.7**). As our mass balance calculation was a fairly simple, it is not surprising that there were discrepancies between calculated and measured values. Some of these differences may be explained mechanistically. The calculated values indicate average arsenic delivered to plant roots via mass-flow. Not all of this potentially delivered arsenic necessarily sorbed to root plaque or was taken up by the plant. While arsenic uptake in rice is a highly efficient process, it is still an active process (Ma et al., 2008; Wu et al., 2011), potentially causing a discrepancy between delivery and accumulation. Other reasons for the measurement-calculation mismatch are methodological. While great care was taken in the removal of roots, tangled root networks and extremely clayey paddy soil meant that some root loss was unavoidable and therefore the true value of accumulated arsenic was likely higher than that reported. Nonetheless, this calculation provides useful insight into the potential magnitude of changes to both mobilization and transpiration, which change simultaneously with temperature.

2.5.4. Arsenic Allocation in Plants

To move towards a more mechanic understanding of arsenic response to temperature requires an analysis of not just ‘how much’ but also ‘where’ arsenic is accumulating within the plant. Arsenic concentrations in tissue decreased in the following order: root > leaf > stem > hull > grain (**Figure 2.2**). In terms of arsenic content this sequence was the same except that grain > hull, due to greater biomass in grain relative to hull (**Figure 2.3A**). The sensitivity of tissue arsenic (i.e., strength of the response) to temperature occurred in a similar sequence, where the

increase in average leaf arsenic at higher temperatures was greater than the increase in grain arsenic at higher temperatures. This trend was also demonstrated in Neumann et al. (2017) and shows that temperature responses can be tissue specific and that increased grain arsenic is only a small fraction of the increase in total arsenic uptake (**Figure 2.3B**).

The assessment of total arsenic found in above-ground tissue showed that more total arsenic was present in shoot tissue under elevated temperature, even when controlling for plant biomass (**Figure 2.3A**). This result highlights that increased arsenic concentrations shown in **Figure 2.2** were not simply result of reduced plant biomass under heat stress. We saw no change in total above-ground biomass though we did observe an increase in stem and leaf biomass in the HT treatment relative to the other treatments, which may have slightly diluted arsenic in these tissues (**Figure A1.4A**). There was a shift towards less root biomass and decreased root to shoot ratio at higher temperatures (**Figure A1.4E** and **F**), which was previously observed in a Japanese rice cultivar as well (Arai-Sanoh et al., 2010). In our study, reduced root to shoot ratios did not suppress uptake to a sufficient degree to mitigate the effects of increased above-ground arsenic at elevated temperature.

The only tissue where arsenic allocation was affected by temperature was hull tissue, where percent of arsenic allocated was higher in HT relative to MLT (**Figure 2.3B**). The larger average allocation of arsenic to hull in HT treatment was likely related to the absence of rice grain. The HT treatment had a day/night temperature of 32.9/31.0°C. Baker (2004) found a similar temperature threshold for grain production in japonica rice, between 32 – 36°C when plants were grown at a constant heat, or 35/31°C day/night. In contrast, Muehe et al. (2019) did not have sterility issues in their high temperature treatment, which had a markedly higher daytime temperature but much cooler nighttime temperature (38/22°C day/night). We posit that

the heat treatment applied at night in our study conducted with the same rice variety of Muehe et al. (2019) was responsible for inducing spikelet sterility in the HT treatment. Previous research has supported the idea that rice physiological responses are more sensitive to nighttime temperatures (Kanno et al., 2009; Peng et al., 2004). This sensitivity may be relevant to future conditions, as nighttime temperatures are expected to increase more than daytime temperatures (Alexander et al., 2006; Davy et al., 2017). High DMA exposure can also induce straighthead disease in rice (Limmer et al., 2018b). However, we did not detect a statistically significant increase in grain DMA with temperature and grain DMA concentrations were quite low (**Figure A1.2B**).

Arsenic was allocated in comparable proportions for stems and leaves across treatments (**Figure 2.3B**), indicating that although plants were exposed to notable heat stress, this heat stress did not significantly impact arsenic flow within plant vasculature. This finding is also consistent with our inability to detect an upregulation in *OsABCC1* expression across treatments, disproving our final hypothesis that *OsABCC1* could mitigate arsenic allocation to grain. Song et al. (2014) characterized *OsABCC1* expression in various tissue types, including roots, leaves, nodes and reproductive tissues. In our low arsenic system *OsABCC1* expression may have been too low to detect significant upregulation. In short term experiments with seedlings, Song et al. (2014) was able to induce an upregulation in *OsABCC1* expression in seedlings when exposed to a dramatic 375 $\mu g\ L^{-1}$ shock, though not at a lower level of 37.5 $\mu g\ L^{-1}$, a more similar to porewater concentration in our study. We contend that greater OsABCC1 activity should be viewed as a plant breeding goal rather than as a mitigating factor in the face of future climate change.

2.5.5. Broader Implications

We acknowledge that pot studies in controlled growth chambers cannot capture the full response of field grown plants to future climate conditions which will be variable across daily and inter-annual timescales. Instead, the value of pot studies lies in allowing us to isolate and manipulate a single variable and understand its isolated impact on the rice-soil system. In this experiment we focused on the effect of temperature, one of the major threats of global climate change. Climate change will lead to increased average temperatures during rice cultivation (IPCC, 2013b) and based on our study this increased temperature will pose risks for human inorganic arsenic exposure through rice.

Relevant guidelines to reduce dietary arsenic exposure are [1] a 200 mg kg^{-1} inorganic arsenic limit for polished white rice recommended by the FAO/WHO (Codex Alimentarius Commission, 2014) and [2] a 100 mg kg^{-1} limit for inorganic arsenic limit in all rice used in infant food (FDA, 2016). Average total and inorganic arsenic concentrations in Californian rice are 170 mg kg^{-1} and 130 mg kg^{-1}, respectively (OEHHA, 2017); some of the lowest concentrations in rice grown around the world (Consumer Reports, 2012). The rice system represented in this study was not excessively contaminated and therefore arsenic concentrations of rice grain in the LT treatment were well below these safety standards recommended for infants. Raising the average growth temperature by roughly 5°C increased total and inorganic arsenic levels well beyond the safety standard used for infants – demonstrating that rice systems that have historically been considered of low concern may become less safe in a warmer future.

Our results highlight the importance of temperature driven soil mobilization in exacerbating arsenic contamination of rice. Plant physiological responses to temperature (i.e., biomass or transpiration changes) do not seem to be a dominant controlling factors for arsenic

accumulation at high temperatures. Therefore, strategies to reduced arsenic contamination of rice should focus on reducing arsenic availability, such as through alternate wetting and drying while monitoring other redox-sensitive contaminants (Carrijo et al., 2018; Honma et al., 2016; Limmer et al., 2018a), or by selecting low arsenic accumulating rice varieties (Chi et al., 2018).

2.6. References

Abedin MJ, Feldmann J, Meharg AA. Uptake Kinetics of Arsenic Species in Rice Plants. Plant Physiol 2002; 128: 1120-1128.

Alexander LV, Zhang X, Peterson TC, Caesar J, Gleason B, Klein Tank AMG, et al. Global observed changes in daily climate extremes of temperature and precipitation. Journal of Geophysical Research 2006; 111.

Amaral DC, Lopes G, Guilherme LRG, Seyfferth AL. A New Approach to Sampling Intact Fe Plaque Reveals Si-Induced Changes in Fe Mineral Composition and Shoot As in Rice. Environ Sci Technol 2017; 51: 38-45.

Arai-Sanoh Y, Ishimaru T, Ohsumi A, Kondo M. Effects of Soil Temperature on Growth and Root Function in Rice. Plant Production Science 2010; 13: 235-242.

Arao T, Kawasaki A, Baba K, Mori S, Matsumoto S. Effects of Water Management on Cadmium and Arsenic Accumulation and Dimethylarsinic Acid Concentrations in Japanese Rice. Environ Sci Technol 2009; 43: 9361-9367.

Arao T, Makino T, Kawasaki A, Akahane I, Kiho N. Effect of air temperature after heading of rice on the arsenic concentration of grain. Soil Science and Plant Nutrition 2018; 64: 433-437.

Arnold PA, Kruuk LEB, Nicotra AB. How to analyse plant phenotypic plasticity in response to a changing climate. New Phytol 2019; 222: 1235-1241.

Baker JT. Yield responses of southern US rice cultivars to CO_2 and temperature. Agricultural and Forest Meteorology 2004; 122: 129-137.

Banerjee M, Banerjee N, Bhattacharjee P, Mondal D, Lythgoe PR, Martinez M, et al. High arsenic in rice is associated with elevated genotoxic effects in humans. Sci Rep 2013; 3: 2195.

Barber SA. A Diffusion and Mass-flow Concept of Soil Nutrient Availability. Soil Science 1962; 93: 39-49.

Bokhari UG, Singh JS. Effects of Temperature and Clipping on Growth, Carbohydrate Reserves, and Root Exudation of Western Wheatgrass in Hydroponic Culture. Crop Science 1974; 14: 790-794.

Borch T, Kretzschmar R, Kappler A, Cappellen PV, Ginder-Vogel M, Voegelin A, et al. Biogeochemical Redox Processes and their Impact on Contaminant Dynamics. Environ Sci Technol 2010; 44: 15-23.

Britz SJ, Prasad PVV, Moreau RA, Allen LH, Kremer DF, Boote KJ. Influence of Growth Temperature on the Amounts of Tocopherols, Tocotrienols, and γ-Oryzanol in Brown Rice. Journal of Agricultural and Food Chemistry 2007; 55: 7559-7565.

California's Office of Environmental Health Hazard and Assessment [OEHHA]. Naturally Occurring Concentrations of Listed Chemicals in Unprocessed Foods; Inorganic Arsenic in White and Brown Rice. In: California Environmental Protection Agency, editor. Title 27, California Code of Regulations, 2017.

Carrijo DR, Akbar N, Reis AFB, Li C, Gaudin ACM, Parikh SJ, et al. Impacts of variable soil drying in alternate wetting and drying rice systems on yields, grain arsenic concentration and soil moisture dynamics. Field Crops Research 2018; 222: 101-110.

Chang AC, Page AL, Krage NJ. Role of fertilizer and micronutrient applications on Arsenic, Cadmium, and lead accumulation in California cropland soils. California Department of Food and Agriculture 2004.

Chen Z, Zhu YG, Liu WJ, Meharg AA. Direct evidence showing the effect of root surface iron plaque on arsenite and arsenate uptake into rice (*Oryza sativa*) roots. New Phytol 2005; 165: 91-7.

Chi Y, Li F, Tam NF-y, Liu C, Ouyang Y, Qi X, et al. Variations in grain cadmium and arsenic concentrations and screening for stable low-accumulating rice cultivars from multi-environment trials. Sci Total Environ 2018; 643: 1314-1324.

Clemens S, Ma JF. Toxic Heavy Metal and Metalloid Accumulation in Crop Plants and Foods. Annu Rev Plant Biol 2016; 67: 489-512.

Codex Alimentarius Commission. Report of the Either Session of the Codex Committee on Contaminants in Foods. 37th Session. Joint FAO/WHO Food Standards Programme, Geneva, Switzerland, 2014.

Consumer Reports. Arsenic in your food: Our findings show a real need for federal standards for this toxin, 2012.

Cornell RM. Comparison and classification of the effects of simple ions and molecules upon the transformation of ferrihydrite into more crystalline products. Zeitschrift für Pflanzenernährung und Bodenkunde 1987; 150: 304-307.

Cummings DE, Caccavo F, Fendorf S, Rosenzweig RF. Arsenic Mobilization by the Dissimilatory Fe(III)-Reducing Bacterium Shewanella alga BrY. Environ Sci Technol 1999; 33: 723-729.

DaMatta FM, Grandis A, Arenque BC, Buckeridge MS. Impacts of climate changes on crop physiology and food quality. Food Research International 2010; 43: 1814-1823.

Davy R, Esau I, Chernokulsky A, Outten S, Zilitinkevich S. Diurnal asymmetry to the observed global warming. International Journal of Climatology 2017; 37: 79-93.

Dieleman WI, Vicca S, Dijkstra FA, Hagedorn F, Hovenden MJ, Larsen KS, et al. Simple additive effects are rare: a quantitative review of plant biomass and soil process responses to combined manipulations of CO_2 and temperature. Glob Chang Biol 2012; 18: 2681-93.

Dykes GE, Chari NR, Seyfferth AL. Si-induced DMA desorption is not the driver for enhanced DMA availability after Si addition to flooded soils. Sci Total Environ 2020; 739.

Food and Drug Administration [FDA]. Inorganic Arsenic in Rice Cereals for Infants: Action Level Guidance for Industry - Draft Guidance. In: Services USDoHaH, editor. Center for Food Safety and Applied Nutrition, Rockville, MD, USA, 2016.

Hatfield JL, Prueger JH. Temperature extremes: Effect on plant growth and development. Weather and Climate Extremes 2015; 10: 4-10.

Hoagland DR, Arnon DI. The water-culture method for growing plants without soil. Circular. California Agricultural Experiment Station 1950; 347: 32 pp.

Honma T, Ohba H, Kaneko-Kadokura A, Makino T, Nakamura K, Katou H. Optimal Soil Eh, pH, and Water Management for Simultaneously Minimizing Arsenic and Cadmium Concentrations in Rice Grains. Environ Sci Technol 2016; 50: 4178-4185.

IPCC. Annex I: Atlas of Global and Regional Climate Projections. [van Oldenborgh, G.J., M. Collins, J. Arblaster, J.H. Christensen, J. Marotzke, S.B. Power, M. Rummukainen and T. Zhou (eds.)]. Climate Change 2013: The Physical Science Basis. Contribution of Working Group I to the Fifth Assessment Report of the Intergovernmental Panel on Climate Change. [Stocker, T.F., D. Qin, G.-K. Plattner, M. Tignor, S.K. Allen, J.

Boschung, A. Nauels, Y. Xia, V. Bex and P.M. Midgley (eds.)]. Cambridge University Press, Cambridge, United Kingdom and New York, NY, USA., 2013a.

IPCC. Climate Change 2013: The Physical Science Basis. Contribution of Working Group I to the Fifth Assessment Report of the Intergovernmental Panel on Climate Change. Cambridge, United Kingdom and New York, NY, USA: Cambridge University Press, 2013b.

Jackson B. Fast ion chromatography-ICP-QQQ for arsenic speciation. Journal of analytical atomic spectrometry 2015; 30: 1405-1407.

Kanno K, Mae T, Makino A. High night temperature stimulates photosynthesis, biomass production and growth during the vegetative stage of rice plants. Soil Science and Plant Nutrition 2009; 55: 124-131.

Keon NE, Swartz CH, Brabander DJ, Harvey C, Hemond HF. Validation of an arsenic sequential extraction method for evaluating mobility in sediments. Environ Sci Technol 2001; 35: 2778-84.

Lee C-H, Hsieh Y-C, Lin T-H, Lee D-Y. Iron plaque formation and its effect on arsenic uptake by different genotypes of paddy rice. Plant and Soil 2013; 363: 231-241.

Li RY, Stroud JL, Ma JF, McGrath SP, Zhao FJ. Mitigation of Arsenic Accumulation in Rice with Water Management and Silicon Fertilization. Environ Sci Technol 2009; 43: 3778-3783.

Limmer MA, Mann J, Amaral DC, Vargas R, Seyfferth AL. Silicon-rich amendments in rice paddies: Effects on arsenic uptake and biogeochemistry. Sci Total Environ 2018a; 624: 1360-1368.

Limmer MA, Wise P, Dykes GE, Seyfferth AL. Silicon Decreases Dimethylarsinic Acid Concentration in Rice Grain and Mitigates Straighthead Disorder. Environ Science Technol 2018b; 52: 4809-4816.

Liu WJ, Zhu YG, Hu Y, Williams PN, Gault AG, Meharg AA, et al. Arsenic Sequestration in Iron Plaque, Its Accumulation and Speciation in Mature Rice Plants (*Oryza Sativa L.*). Environ Sci Technol 2006; 40: 5730-5736.

Lynch JP, St.Clair SB. Mineral stress: the missing link in understanding how global climate change will affect plants in real world soils. Field Crops Research 2004; 90: 101-115.

Ma JF, Yamaji N, Mitani N, Xu XY, Su YH, McGrath SP, et al. Transporters of arsenite in rice and their role in arsenic accumulation in rice grain. Proc Natl Acad Sci 2008; 105: 9931-5.

MacDonald NW, Zak DR, Pregitzer KS. Temperature effects on kinetics of microbial respiration and net nitrogen and sulfur mineralization. Soil Science Society of America Journal 1995; 59: 233-240.

Maher W, Foster S, Krikowa F, Donner E, Lombi E. Measurement of Inorganic Arsenic Species in Rice after Nitric Acid Extraction by HPLC-ICPMS: Verification Using XANES. Environ Sci Technol 2013; 47: 5821-5827.

McGrath JM, Lobell DB. Reduction of transpiration and altered nutrient allocation contribute to nutrient decline of crops grown in elevated CO_2 concentrations. Plant Cell Environ 2013; 36: 697-705.

Meharg AA, Zhao F-J. Arsenic & Rice. Dordrecht: Dordrecht: Springer Netherlands, 2012.

Mehra O, Jackson M. Iron Oxide Removal from Soils and Clays by a Dithionite-Citrate System Buffered with Sodium Bicarbonate. Clays and Clay Minerals 1958; 7: 317-327.

Muehe EM, Wang T, Kerl CF, Planer-Friedrich B, Fendorf S. Rice production threatened by coupled stresses of climate and soil arsenic. Nat Commun 2019; 10: 4985.

Myers SS, Zanobetti A, Kloog I, Huybers P, Leakey AD, Bloom AJ, et al. Increasing CO_2 threatens human nutrition. Nature 2014; 510: 139-42.

Neumann RB, Seyfferth AL, Teshera-Levye J, Ellingson J. Soil Warming Increases Arsenic Availability in the Rice Rhizosphere. Agricultural & Environmental Letters 2017; 2.

Peng S, Huang J, Sheehy JE, Laza RC, Visperas RM, Zhong X, et al. Rice yields decline with higher night temperature from global warming. Proc Natl Acad Sci 2004; 101: 9971-5.

Porter JR, Xie L, Challinor AJ, Cochrane K, Howden SM, Iqbal MM, et al. Food security and food production systems. In: Field CB, Barros VR, Dokken DJ, Mach KJ, Mastrandrea MD, Bilir TE, et al., editors. Climate Change 2014: Impacts, Adaptation, and Vulnerability. Part A: Global and Sectoral Aspects. Contribution of Working Group II to the Fifth Assessment Report of the Intergovernmental Panel of Climate Change. Cambridge University Press, Cambridge, United Kingdom and New York, NY, USA, 2014, pp. 485-533.

Prasad PVV, Boote KJ, Allen LH, Sheehy JE, Thomas JMG. Species, ecotype and cultivar differences in spikelet fertility and harvest index of rice in response to high temperature stress. Field Crops Research 2006; 95: 398-411.

Seyfferth AL, Limmer M, Wu W. Si and Water Management Drives Changes in Fe and Mn Pools that Affect As Cycling and Uptake in Rice. Soil Systems 2019; 3.

Seyfferth AL, Webb SM, Andrews JC, Fendorf S. Defining the distribution of arsenic species and plant nutrients in rice (*Oryza sativa L.*) from the root to the grain. Geochimica et Cosmochimica Acta 2011; 75: 6655-6671.

Simmler M, Bommer J, Frischknecht S, Christl I, Kotsev T, Kretzschmar R. Reductive solubilization of arsenic in a mining-impacted river floodplain: Influence of soil properties and temperature. Environ Pollut 2017; 231: 722-731.

Smith MR, Myers SS. Impact of anthropogenic CO_2 emissions on global human nutrition. Nature Climate Change 2018; 8: 834-839.

Song WY, Yamaki T, Yamaji N, Ko D, Jung KH, Fujii-Kashino M, et al. A rice ABC transporter, OsABCC1, reduces arsenic accumulation in the grain. Proc Natl Acad Sci 2014; 111: 15699-704.

Tanaka M, Takahashi Y, Yamaguchi N, Kim K-W, Zheng G, Sakamitsu M. The difference of diffusion coefficients in water for arsenic compounds at various pH and its dominant factors implied by molecular simulations. Geochimica et Cosmochimica Acta 2013; 105: 360-371.

Taylor GJ, Crowder AA. Use of the DCB Technique for Extraction of Hydrous Iron Oxides from Roots of Wetland Plants. American Journal of Botany 1983; 70: 1254-1257.

The European Commision. Commission Regulation (EU) 2015/1006 of 25 June 2015 amending Regulation (EC) No 1881/2006 as regards maximum levels of inorganic arsenic in foodstuffs. Official Journal of the European Union, 2015.

Tufano KJ, Fendorf S. Confounding Impacts of Iron Reduction on Arsenic Retention. Environ Sci Technol 2008; 42: 4777-4783.

U.S. EPA. Method 3050B: Acid Digestion of Sediments, Sludges, and Soils, Washington, DC, 1996.

Uselman SM, Qualls RG, Thomas RB. Effects of increased atmospheric CO_2, temperature, and soil N availability on root exudation of dissolved organic carbon by a N-fixing tree (Robinia pseudoacacia L.). Plant and Soil 2000; 222: 191-202.

Vahter M, Concha G. Role of Metabolism in Arsenic Toxicity. Pharmacology & Toxicology 2001; 89: 1-5.

Violante A, Barberis E, Pigna M, Boero V. Factors Affecting the Formation, Nature, and Properties of Iron Precipitation Products at the Soil–Root Interface. Journal of Plant Nutrition 2003; 26: 1889-1908.

Wan X-m, Lei M, Chen T-b, Yang J-x, Liu H-t, Chen Y. Role of transpiration in arsenic accumulation of hyperaccumulator Pteris vittata L. Environmental Science and Pollution Research 2015; 22: 16631-16639.

Weber F-A, Hofacker AF, Voegelin A, Kretzschmar R. Temperature Dependence and Coupling of Iron and Arsenic Reduction and Release during Flooding of a Contaminated Soil. Environ Sci Technol 2010; 44: 116-122.

Wilke C, Chang P. Correlation of diffusion coefficients in dilute solutions. AIChE journal 1955; 1: 264-270.

Williams PN, Santner J, Larsen M, Lehto NJ, Oburger E, Wenzel W, et al. Localized Flux Maxima of Arsenic, Lead, and Iron around Root Apices in Flooded Lowland Rice. Environ Sci Technol 2014; 48: 8498-8506.

Wu Z, Ren H, McGrath SP, Wu P, Zhao FJ. Investigating the contribution of the phosphate transport pathway to arsenic accumulation in rice. Plant Physiol 2011; 157: 498-508.

Xue S, Jiang X, Wu C, Hartley W, Qian Z, Luo X, et al. Microbial driven iron reduction affects arsenic transformation and transportation in soil-rice system. Environ Pollut 2020; 260.

Yamaguchi N, Ohkura T, Takahashi Y, Maejima Y, Arao T. Arsenic Distribution and Speciation near Rice Roots Influenced by Iron Plaques and Redox Conditions of the Soil Matrix. Environ Sci Technol 2014; 48: 1549-1556.

Zhao FJ, Ma JF, Meharg AA, McGrath SP. Arsenic uptake and metabolism in plants. New Phytol 2009; 181: 777-94.

3. Chapter 3: When does temperature matter? Response of rice arsenic to heat exposure during different developmental stages

In preparation by Farhat YA, Kim S-H, and Neumann RB.

Target Journal: Science of the Total Envi. *Target Submission date: July 1, 2022*

3.1. Abstract

Climate change is expected to increase air temperatures in rice-growing regions worldwide. Several recent studies have demonstrated these elevated temperatures can increase rice concentrations of arsenic, a toxin and carcinogen commonly found in rice. However, the timing of this temperature exposure (i.e. heat spikes during a specific phenological stages), is. In this experiment, we grew potted rice plants in temperature-controlled growth chambers with different temperature regimes: (1) baseline temperature (26°C/22°C, day/night), (2) elevated temperature (30°C/27°C, day/night), (3) baseline temperature with a 20-day heat spike in vegetative stage (4) baseline temperature with a 20-day heat spike in the ripening stage. Heat spikes roughly mimicked the elevated temperature treatment. When we compared heat spikes in the vegetative and ripening stage, we found that a heat spike during the ripening stage mobilized more arsenic from soil into porewater. Plants which experienced a vegetative stage heat spike had increased concentrations of arsenic in vegetative tissue immediately following the heat spike, but the magnitude of this increase was small and did not persist to maturity. Plants which experienced a heat spike during the ripening stage had a significant increase in arsenic concentrations in various plant tissue types which persisted to maturity. We postulate that the differential response between these two time points may be due to (1) lower microbial

development at earlier timepoints which are not able to mobilize as much arsenic and (2) low plant biomass in the vegetative stage which lessens the magnitude of any increased arsenic content, and (3) lower root biomass in treatments exposed to heat in the vegetative stage that might reduce plants' ability to take up arsenic. Overall, our research shows that heat spikes which occur later in the rice growing season present a greater threat for dietary arsenic exposure from rice.

3.2. Introduction

Billions of people depend on rice as a key dietary staple. Yet in recent years several studies have emerged showing that rice plants grown at elevated temperatures accumulate higher concentrations of arsenic (As), a potent toxin and carcinogen (Arao et al., 2018; Dhar et al., 2020; Farhat et al., 2021; Muehe et al., 2019; Neumann et al., 2017). This increase is common to both vegetative and reproductive tissues, including the edible rice grains. Given that climate change is expected to increase temperatures around the world, including in areas important for rice cultivation, temperature-fueled increases in rice grain arsenic presents a looming human health threat.

In our previous work we grew rice plants across a temperature gradient to understand the various ways in which temperature can alter arsenic cycling in the soil-plant system (Farhat et al., 2021). We investigated changes in arsenic availability, mass-flow, association with root plaque, and tissue allocation. Our experiment highlighted the importance of temperature-driven increases in porewater dissolved arsenic, which can enhance arsenic accumulation in rice tissue. Temperature heightens the mobilization of arsenic from soil to porewater by accelerating the rate at which microbes catalyze the solubilization of arsenic (Weber et al., 2010). We also observed that rice roots exposed to higher temperatures had more iron plaque development and sorbed

more arsenic per mass of iron. Finally, we noted that while higher temperatures promoted greater plant arsenic content (i.e., the total mass of arsenic taken up), the allocation of the arsenic within aboveground tissue was quite consistent across temperature treatments.

Often studies on temperature and rice arsenic, including our previous work, expose plants to a consistent temperature regime from germination to maturity (Farhat et al., 2021; Muehe et al., 2019). However, climate change will not only cause a simple increase in average temperature, it will also increase climate variability and extreme weather events that may result in shorter sporadic heat waves (Field et al., 2012). IPCC predictions for our model system in Northern California indicate that temperature anomalies will be more likely later in the rice growing season, ex. August vs. June (Gutiérrez et al., 2021). Understanding how heat spikes intersect with plant development to affect arsenic uptake is important for identifying future climate-linked food vulnerabilities.

Rice phenology can be divided into three phases: vegetative, reproductive, and ripening stages (Fageria, 2014; GRiSP, 2013). The vegetative stage occurs after germination when leaves develop, the stem lengthens, and tillers form. The vegetative stage is also believed to be important for root lengthening and establishment (Palta and Watt, 2009). Entrance into the reproductive stage occurs at panicle initiation, when the immature panicle forms within the main stem, and the panicle grows and elongates until it eventually emerges and becomes fully visible (i.e., heading). Finally, flowering or anthesis begins a day after full heading and marks the transition from reproductive to ripening stage. During this final stage, the developing rice grains elongates within the hull, then changes from milky to firm. Temperature can influence the length of both vegetative and ripening stages, where cooler temperatures tend to lengthen both processes (Fageria, 2014; GRiSP, 2013; Hatfield and Prueger, 2015).

Arsenic concentrations and content (the total arsenic mass taken up) within rice plants change throughout development. Zheng et al. (2011) conducted an extensive analysis of the spatial and temporal distribution of arsenic in rice tissue. They investigated concentrations of total arsenic, organic arsenic (DMA and MMA), and inorganic arsenic, which is considered to be the more toxic form of arsenic. In almost all tissue types, inorganic arsenic was the predominate form of arsenic. They found that in leaves, stems, and husks both the concentration and content of arsenic peaked approximately 2-weeks into the ripening period. Grain concentrations of total and inorganic arsenic remained steady over time and inorganic arsenic content increased thought development. The DMA made up only a small share of arsenic in grains and its concentration decreased over time.

The increase in plant arsenic within the ripening period may be partially explained by the arsenic uptake pathway. In flooded rice fields the most prominent form of arsenic is arsenite (Xu et al., 2008). Arsenite uptake is intimately linked to silicon uptake, as they both use a common set of root uptake transporters, specifically Lsi1 and Lsi2 (Ma et al., 2008). Expression of both *Lsi1* and *Lsi2* peak near or after flowering, indicating that there may be greater potential for arsenic uptake during this stage (Yamaji and Ma, 2007; Yamaji and Ma, 2011). Ma et al. (1989) showed that the reproductive stage is when most plant silicon is taken up, but that in the panicles specifically, most silicon is taken up during the ripening stage (~75%). This timing may be similar for arsenic, though arsenic is not very mobile in plant tissue and is actively prevented from reaching grain tissue by sequestration in plant vacuoles (Clemens and Ma, 2016).

There are a small number of new studies at the intersection of arsenic uptake, phenology, and temperature. Using ten years of stored rice samples, Arao et al. (2018) showed that increased daily mean air temperature during late ripening stage was associated with increased inorganic

arsenic in brown and polished rice. Dhar et al. (2020) experimentally showed that increasing temperatures from a week after heading until full maturity increased concentrations of arsenic in rice grains. Both papers focused specifically on grain arsenic and did not consider arsenic dynamics in other tissue types. There is a greater amount of research discussing the impact of water management on grain arsenic, which is a useful comparison as both flooding and elevated temperature increase dissolved available arsenic. Flooding during the later period of development increased arsenic, both organic and inorganic forms, in rice grains (Arao et al., 2009). Conversely, drying rice fields during heading was more effective at reducing inorganic grain arsenic than drying fields at panicle initiation (Carrijo et al., 2019). Based on these works we would expect that heat spikes later in development would have a larger impact on grain arsenic.

The objective of this experiment was to investigate how temperature-fueled arsenic mobilization interacts with plant phenology. We hypothesized that heat spikes during the ripening stage would have a greater impact on rice arsenic concentrations in tissue and porewater than heat spikes in the vegetative stage. To investigate this hypothesis, we compared rice exposed to elevated temperatures during vegetative or ripening stage to rice grown at baseline temperatures and rice grown at continuously increased temperature. We quantified arsenic concentrations throughout development at various locations in the uptake pathway, including porewater, iron plaque, and multiple plant tissues.

3.3. Methods

3.3.1. Soil and plant preparation

3.3.1.1. Soil: We collected paddy soil from a fallow rice field in Davis California. In our previous work we characterized soil from this field (Farhat et al., 2021). Notably these values

indicate a low arsenic system, with background levels of arsenic similar to much of California (Chang et al., 2004). We packed approximately 20 g of soil into 3-gallon pots and placed these soil packed pots into larger 4-gallon buckets. These larger buckets allowed up to maintain flooded conditions during the experiment.

3.3.1.2. Germination + Transplanting: We selected a fast maturing, Californian, medium-grain rice variety (*Oryza sativa* L. ssp. *japonica* cv. M206) for use in this experiment. To begin germination we wetted seeds with sterilized Hoagland solution (Hoagland and Arnon, 1950) and the following day we transferred seeds into magenta boxes filled with 125mL of autoclaved 2% agar. Seeds germinated for 19-days on benchtop light racks on a 12-hour light-dark cycle at an approximate light intensity of 500μmol m^{-2} s^{-1} and an approximate temperature of 25°C. The germination rate was roughly 80%. Then we transplanted 9-10 germinated seedlings into each soil packed pots. Eighteen days after transplanting we ensured all pots had 8 plants.

3.3.1.3. Irrigation: Prior to transplanting, soils were wetted a 10× dilution of Hoagland solution (Hoagland and Arnon, 1950). We used this dilute Hoagland solution to irrigate pots throughout the experiment. Freshly prepared irrigation solution was left in large carboys to equilibrate with chamber temperature for at least 24-hours before watering to minimize changes in soil temperature. Eighteen-days after transplanting we raised the irrigation solution level to flood pots. We used a line on the external 4-gal bucket to indicate our desired flooding level, approximately 10cm above the soil surface. We watered plants twice a week to maintain constantly flooded conditions and we recorded the volume of water added to estimate the volume of water lost by evaporation (water lost from an unplanted pot) and transpiration (planted pot water loss - unplanted pot water loss).

3.3.2. Experiment Setup

3.3.2.1. Growth chamber setup: We constructed four growth chambers from free standing growth tents (DarkRoom II DR90, 36" × 36" × 72"). The location was naturally cool so to raise chambers' temperature we placed a greenhouse forced air portable heater into each chamber (Dr Infrared Heater). Each chamber also contained two fans to distribute heat. We connected heaters to an environmental controller (model CHHC-4i, Sentinel) which turned heaters on and off at set temperature levels (described below in Treatment Description). Within each chamber, we placed heaters below shelves which held experimental pots. Each week we randomly rearranged pots within the chamber to control for any variation in temperature within each growth chamber. We measured air temperature at leaf level (Smart Sensor, Onset) and soil temperature (TidbiT, Onset). Growth lamps were located roughly 1ft above plant height, and were continuously raised throughout the experiment as plants grew. Average PAR at leaf level was 236μmol m^{-2} s^{-1} (PAR Smart Sensor, Onset). Plants grew on a 12-hour light-dark cycle. Further information about environmental conditions in each chamber can be found in Appendix 2 in **Table A2.1**.

3.3.2.2. Treatment Descriptions: We established four temperature treatments (**Figure 3.1**): continuous heat (CH), no heat (NH), vegetative heat (VH), and ripening heat (RH). The NH treatment acted as the "baseline" condition, similar to temperatures we might expect during the rice growing season in Northern California (Cline et al., 2010). The average temperatures of this treatment were 25.9/ 22.1°C, day/night. Alternatively, plants in the CH treatment grew at continuously elevated temperatures throughout their development (average: 30.1 / 27.2°C, day/night). This level of warming is consistent with IPCC forecasting during rice growing months in the western United States in the next 60 years (Gutiérrez et al., 2021). This level of

warming was also chosen based off our previous experiment, such that we would observe increased arsenic uptake without including spikelet sterility.

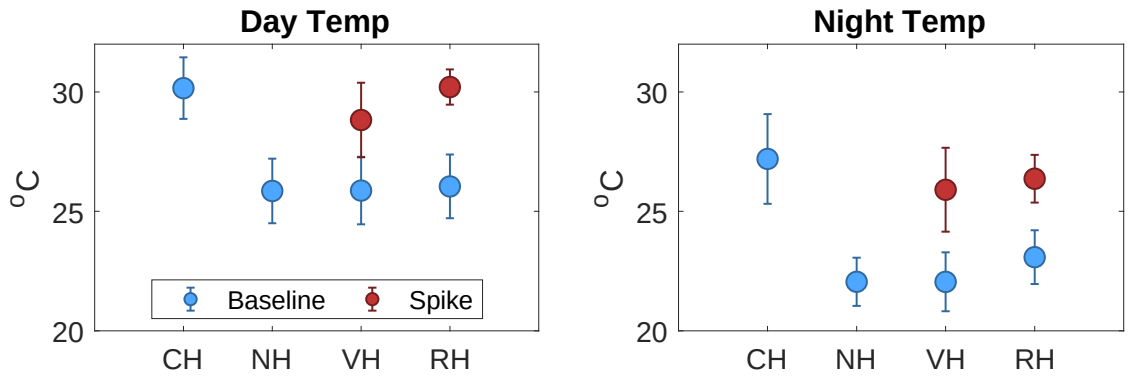

Figure 3.1*. Average temperatures of each treatment group. Error bars are associated standard deviations. Blue circles show average growth temperature under normal experiment conditions. Red circles show the average temperature during the heat spike event for VH and RH treatments respectively.*

During most of their growth, the average day and night temperatures of VH and RH treatments were comparable to the NH treatment (25.9 / 22.0°C and 26.0 / 23.0°C, respectively), but both experienced a 20-day heat spike during their development similar to the growth temperature of the CH treatment. During the vegetative stage, between the 3rd to 6th leaf stage, we increased the average temperature of the VH treatment to 28.9 / 25.9°C, day/night. A week after the RH treatment flowered and we increased the average temperatures to 30.2 / 26.3°C, day/night. We attempted to replicate the temperatures of the CH treatment during the heat spike, and mean spike temperatures were within one standard deviation of CH average temperatures in both day and nighttime temperatures.

3.3.3. Sample collection

3.3.3.1. Porewater: We collected porewater at several timepoints points throughout the experiment based on plant phenology: twice during the vegetative stage, once during the week of

flowering, and at least once more during the ripening stage. These measurements were made based on observed phenology and did not necessarily occur on the same day. **Figure 3.2** further depicts when porewater collections took place and precise dates are in **Table A2.2**. We strategically planned porewater samplings to coincide both with the beginning and end of heat spikes (VH and RH treatments) and at harvests timepoints (all treatments). To collect porewater, we connected MicroRhizons (0.15μm filter, Rhizosphere Research Products) to a 2-way stopcock and a needle. Then the needle pierced the septum of 12mL glass vials (Exetainer, Labco) with a vacuum inside, porewater was transferred into the vial. At the start of sampling, we flushed the system by filling one vial and then degrading that solution. Then we collected 2 samples into 2 acid-washed, foil-wrapped, N_2-purged, and evacuated vials. The second vial was also ashed to use for carbon analysis.

3.3.3.2. Harvests: We preformed three destructive harvests based on rice plant phenology. The first harvest occurred during the vegetative stage, when plants were between the 5^{th} and 6^{th} leave stage. The second harvest occurred the week after at least 50% of plants within that treatment had flowered. Panicles contained a mixture of unfilled spikelets and as well as some very small or chalky grains. The third and final harvest occurred after all plants within those treatments were fully mature, when grains hardened and filled spikelets turned golden brown. During each of the three harvests we used a random number generator to select two plants to remove from each planted pot. We took morphological measurements, including plant height, leaf number, leaf area, and tiller number. Due to high planting density, most plants did not produce tillers. Next, we partitioned each plant into different tissue types and combined the two plants from each pot into one composite sample that was oven dried at 60°C. During the final harvest we also collected the roots of harvested plants by carefully digging out roots by

hand. We briefly rinsed roots in Ultra-pure 18.2 MΩ-cm water, twice. Then we transferred the roots to the laboratory, where we rinsed them thoroughly by placing them in ~30mL of Ultra-pure water and tumbling for 1 hour. After washing, roots air dried on the laboratory benchtop. During the first and third harvest, we also randomly selected one additional plant which we originally intended to use for gene-expression transporters involved in arsenic sequestration. However, based on our earlier experiment (Farhat et al., 2021), we found no change in this gene with temperature and so we did not continue this analysis.

3.3.4. Sample preparation and analysis

3.3.4.1. Porewater: For the two sample vials collected from each pot: we used one vial for metal (arsenic) analysis and the other for both carbon and electrochemical analysis. We preserved the sample used for metal analysis by acidifying to 1% v/v with trace metal grade HNO_3 immediately after opening anoxic vials. Later, we measured dissolved arsenic concentrations using inductively coupled plasma mass spectroscopy (ICP-MS, PerkinElmer, Elan DRC-e) with a yttrium internal standard. We calculated the concentrations by linear regression with a NIST 1640a standard reference material to ensure analytical accuracy.
On the same day as porewater samples were collected, we moved the second vials to an anaerobic glovebox where we decanted 2 mL into a sealed vial. We used the remaining sample volume to measured pH and conductivity. We refrigerated the 2mL sample for 2–3 days then analyzed for dissolved organic and inorganic carbon using a TOC analyzer (Seivers TOC 900) with an HPLC front end (Dionex UltiMate 3000).

3.3.4.2. Root plaque removal: We subjected air dried root samples a modified hot dithionite-citrate-bicarbonate (DCB) extraction (Taylor and Crowder, 1983) to remove Fe-plaque. Our protocol consisted of adding 24mL of 0.3 M sodium citrate and 3mL of 1.0M

$NaHCO_3$ to each fragment and then places samples in a heated water bath to heat to 75-80°C. When samples reached the appropriate temperature, we added 3× 0.6g additions of sodium dithionite 5 minutes apart. We decanted extractant and then rinsed roots twice with 25mL of Ultra-pure 18.2 MΩ-cm water in a tumbler at 60rpm for 30 minutes. The DCB extractant and the two water washes were syringe-filtered (0.2μm, nylon) and acidified extractant to 3% (v/v) using ultra-trace metal grade HNO_3. After washing, we air dried root systems again and digested them with other plant material.

3.3.4.3. Tissue digestions: We partitioned dried rice plants into different tissue types and used a simple rice huller to sperate grains and hulls (BrillEngineering.com). Each tissue type was ground using either a coffee or spice grinder, cleaning with Milli-Q water between samples. To digest plant tissues, we placed ~250mg (mass known exactly) of ground tissue into a Teflon digestion vessel and added 3mL of H_2O_2 and 7.5mL of trace metal grade HNO_3. A microwave digester (Anton Parr) heated the vials to 190°C for 30 minutes. After samples cooled, we decantated and diluted volumetrically to 25mL using Ultra-pure 18.2 MΩ-cm water. To remove silicates, we centrifuged samples (10 min, 4150 rpm) and syringe filtered each solution (0.2μm, polypropylene).

We also used ICP-MS to quantify arsenic concentrations (PerkinElmer, NexION 2000), using standard addition to control for strong matrix effects. Half of the extractions contained a NIST Standard Reference Material (SRM) 1568b rice flour. Average arsenic recovery from NIST 1568b was 99.9% compared to the certified value (n = 20).

3.3.5. Statistics

We performed all statistical analyses using MATLAB (ver. R2019a). Based on residual plots and Anderson-Darling test, we determined that many data sets did not fit normality

assumptions. Therefore, data was $\log_{10}$ transformed to reduce skew and improve normality. We preformed ANOVA with Tukey HSD post hoc to determine statistical differences at individual sampling points. To compare arsenic concentrations before and after heat spikes, we used a paired t-test for the group which experienced the heat spike. In instances where data sets initially appeared more normal, $\log_{10}$ transformation did not change the statistical output and so for simplicity we transformed all datasets. However, we graphed all data in non-transformed space for visual clarity.

3.4. Results

3.4.1. Arsenic Mobilization into Porewater

Porewater concentrations of dissolved arsenic in experimental pots are depicted in **Figure 3.2**. We used a one-way ANOVA of $\log_{10}$ transformed data at each time point with a Tukey Kramer post-hoc to investigate group differences at each time point. We used a paired t-test to compare VH and RH concentrations of arsenic before and after heat spikes, avoiding any comparisons where the number of plants within each pot changed. It is important to note that timepoints were determined on a phenological basis and did not necessarily occur on the same day. For a timeline of collection dates, see Appendix 2 **Table A2.2** and for unplanted pot arsenic concentrations see **Figure A2.1**.

There were statistical differences among treatment groups dissolve arsenic during both the early vegetative and the late vegetative stages (ANOVA, $p = 0.002$ and 0.0001, respectively), though post-doc analysis reveal different multiple comparison statistical groups at the two time points. We observed a small increase in dissolved arsenic in the VH treatment at the end of the heat spike (**Figure 3.2A**). During the early vegetative stage, a day prior to the VH heat spike, the dissolved arsenic concentrations of the VH treatment was significantly lower than the CH

treatment group and similar to the NH treatment group. When we sampled the VH treatment again near the end of its heat spike, dissolved arsenic concentrations of the VH treatment were significantly greater than the NH treatment and no longer significantly different from the CH treatment. But the increase in mean dissolved arsenic of the VH treatment during the heat spike was very small, and the difference between the two timepoints was not significantly different (paired t-test of Early vs. Late Veg, $p = 0.078$). Further, our post-hoc analysis revealed that at the end of the VH heat spike dissolved arsenic concentrations of the VH treatment were not significantly different from the RH treatment, which had yet to be exposed to a heat spike.

Early in the ripening stage, constant elevated temperature continued to increase dissolved arsenic (ANOVA, $p = 0.004$); the CH treatment group had significantly higher dissolved arsenic than other treatment groups. The RH heat spike appeared to have a large impact on dissolved arsenic (**Figure 3.2B**). While RH dissolved arsenic was significantly lower than the CH dissolved arsenic prior to the heat spike, later ripening stage after the heat spike, the were no longer significantly different (ANOVA, $p = 0.695$) and in fact mean dissolved arsenic was quite similar (7.46 and 7.58 $\mu g\ L^{-1}$, RH and CH respectively). Unlike the VH heat spike, post- heat spike dissolved arsenic of the RH treatment was significantly greater than pre-heat spike dissolved arsenic (paired t-test of Early Ripen vs. Late Ripen, $p < 0.001$).

ANOVA results from the mature timepoint continued to show treatment differences in porewater arsenic concentrations ($p = 0.009$, **Figure 3.2**); however, the only significant difference was between the NH and CH treatments. Both VH and RH treatments had intermediate concentrations of arsenic between the NH and CH treatments. Concentrations of dissolved arsenic in the RH treatment decreased from late ripening (just after its heat spike) to full maturity (paired t-test Late Ripen vs. Mature, $p = 0.047$). A comparison of the time points

for the CH treatment showed no significant decrease (paired t-test Late Ripen vs. Mature, p = 0.159).

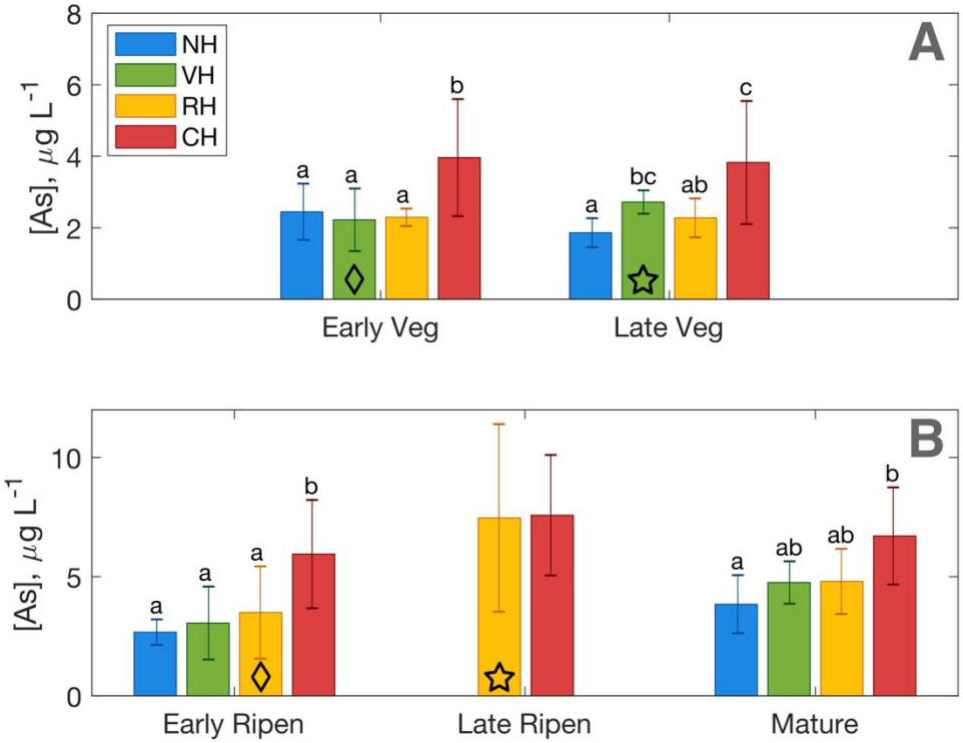

Figure 3.2. *Mean porewater dissolved arsenic concentrations with associated standard deviation in planted pots of each of the four treatments: no heat (NH, blue), vegetative heat (VH, green), ripening heat (RH, yellow), and continuous heat (CH, red). The timepoints depicted are early and late vegetive stage (Early and Late Veg), early and late ripening stage (Early and Late Ripen), and mature. Diamonds (◊) show porewater readings taken just prior to a heat spike and stars (☆) show reading closest to the end of heat spike. Porewater samples were collected based on observed plant phenology and not necessarily on the same day. Statistical analyses were preformed using* log_{10} *transformed data for improved normality. At each time point we performed an ANOVA followed by a Tukey post-hoc, and we performed a paired t-test VH and RH groups before and after their heat spikes.*

3.4.2. Arsenic Concentrations in Rice Tissue

During the late vegetative stage, ANOVA detected treatment difference in the leaves and stems arsenic concentrations (p=0.0268 and p < 0.001, **Figure 3.3A + B**). The VH treatment, which had just completed its heat spike, had higher concentrations of arsenic than the NH treatment and was not significantly different from the CH treatment in both stems and leaves (**Figure 3.3A + B)**. While tissue concentrations in the VH treatment were not significantly different than those in the RH treatment, which had yet to be exposed to a heat spike, both mean and median arsenic concentrations in the VH treatment were greater than in the RH treatment.

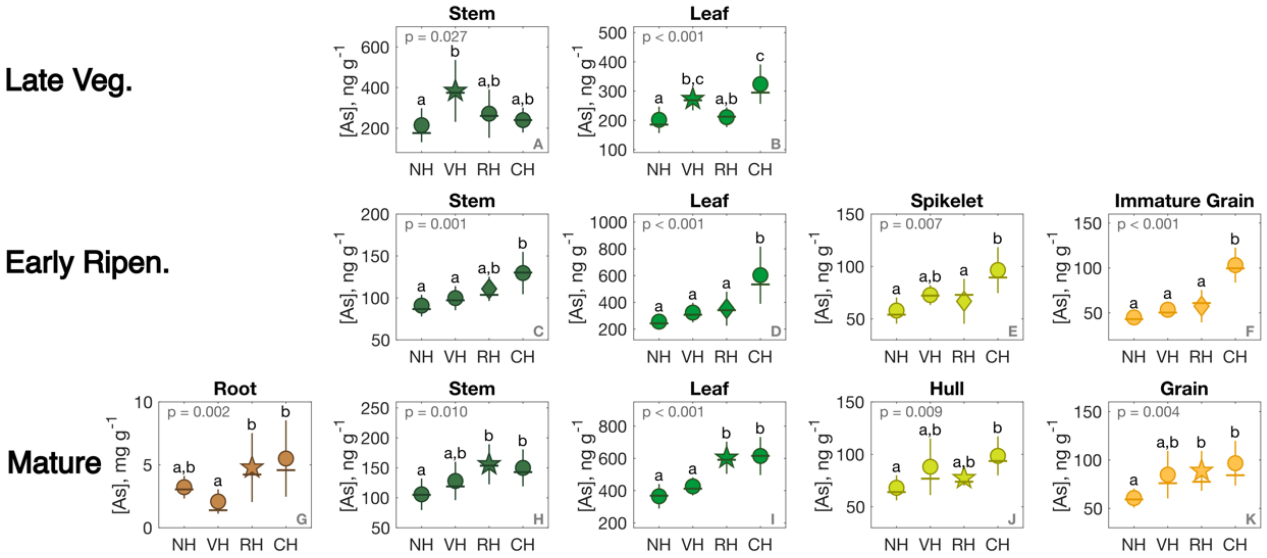

Figure 3.3. *Tissue arsenic concentrations in each of the four treatments. The timepoints depicted are late vegetive stage (Late Veg.), early ripening stage (Early Ripen.), and Mature. Marker indicates mean valued: Default is circle (○), diamonds (◊) show tissue harvested just prior to a heat spike and stars (☆) show reading closest to the end of heat spike. Dash shows median value and error bars are standard deviation. Harvest timing was based on observed plant phenology and groups were not harvested on the same day. Statistical analyses were preformed using* log_{10} *transformed data for improved normality. At each time point and tissue type we performed an ANOVA (p-value shown) followed by a Tukey post-hoc.*

The next harvest timepoint occurred during the early ripening stage, roughly one week after flowering for most plants and prior to the RH heat spike (**Figure 3.3C – F)**. We observed differences in arsenic concentrations between groups in stems, leaves, spikelets, and immature grains ($p < 0.01$ in all tissues). However, the only consistent difference was arsenic concentrations in CH > NH. In the 40-45 days between the first and second destructive harvests, we were no longer able to detect a significant difference between the VH and NH treatment in any of the tissues sampled (**Figure 3.3C – F**). Tissue arsenic concentrations in the VH treatment were significantly lower than the CH treatment in all tissues except spikelets. At this intermediate timepoint the RH treatment was not significantly different from the NH treatment in any tissues sampled and had lower concentrations of arsenic than the CH treatment in leaves, spikelets, and immature grains; validating that treatment conditions of the RH group were sufficiently similar to the NH treatment up to this point to produce similar arsenic concentrations.

Lastly, at the mature time point, we observed treatment differences in the arsenic concentrations in all tissues analyzed (**Figure 3.3G – K,** $p < 0.01$ all). At this final harvest the RH treatment had completed its heat spike and had been allowed to fully ripen for another 15 days. The RH plants' arsenic concentrations in stems, leaves, and grain tissue increased such that they were significantly higher than the NH treatment and comparable to the CH treatment. In the mature rice hulls, the RH treatment was not different from either the NH or the CH treatment. There was high variance in root concentrations of arsenic, and the concentrations in the RH treatment similar to those in the CH and NH treatments, though were greater in the VH treatment.

Concentrations of arsenic in the VH treatment were not significantly different than the NH treatment in any of the five tissue types, though in grain the difference near our statistical threshold of $\alpha = 0.05$ needed to differentiate the two groups (Tukey HSD, $p = 0.055$, **Figure 3.3K)**. Arsenic concentrations in the leaves and roots of the VH treatment were significantly less than in the CH and RH treatment.

3.4.3. Arsenic Content and Allocation

Aboveground arsenic content in each tissue type (arsenic concentration × mass of tissue) and allocation (percent of total aboveground arsenic in each tissue type) are shown in **Figure 3.4**. Tissue biomass data is located in **Figure A2.2**. We analyzed each tissue type at each developmental stage separately by ANOVA ($\alpha = 0.05$) followed by Tukey HSD of $\log_{10}$ values.

During the late vegetative stage, ANOVA demonstrated significant differences in arsenic content in leaves ($p = 0.001$, **Figure 3.4A**), but no difference in stems or total aboveground arsenic, ie. stems + leaves, ($p = 0.056$ and 0.074, respectively). Statistical results for arsenic content in leaves mirrored those of arsenic concentrations at the same timepoint; the VH treatment had significantly more arsenic than the NH treatment and a similar amount as the CH treatment. Again, the increase in arsenic relative to other treatments at that timepoint was small. VH leaf arsenic was not statistically greater than leaf arsenic in the RH treatment, which hadn't yet experienced a heat spike. At this point in the vegetative stage, allocation patterns were similar between the NH, RH, and VH treatments (**Figure 3.4D**); mean arsenic content in the leaves was between 46 – 52% and in the stems mean arsenic content was between 48 – 53%. Only the CH treatment had an altered allocation pattern at this time point, with significantly more arsenic allocated to leaves (mean = 69%) and less to the stems (mean = 31%).

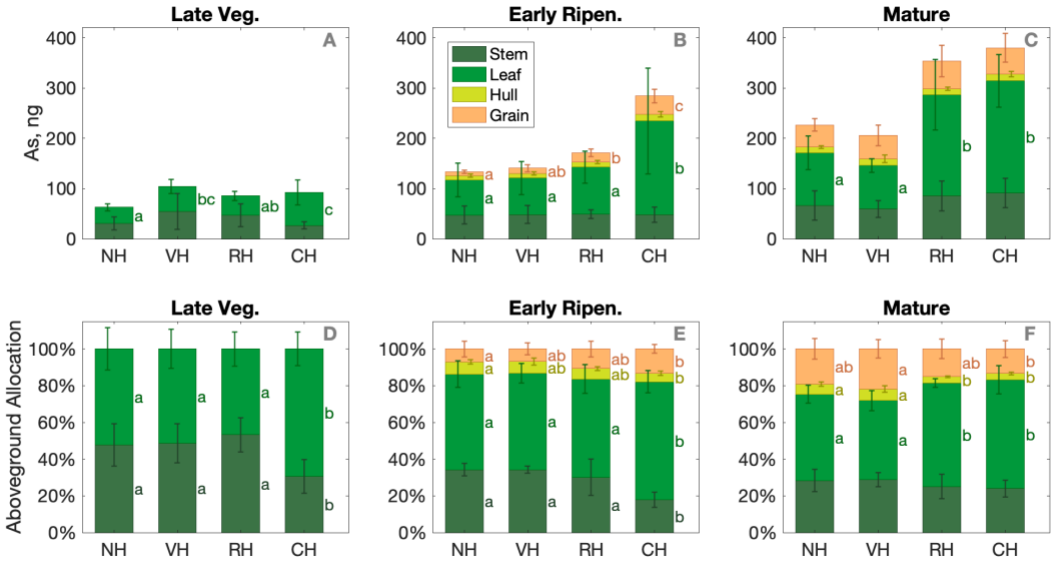

Figure 3.4. *Aboveground arsenic content and allocation at different developmental stages. (A-C) Arsenic content is arsenic concentration × mass of tissue in each tissue type. (D-F) Allocation is percent of aboveground arsenic in found in each tissue type. For each time point and tissue type we performed an ANOVA (p-value shown) followed by a Tukey post-hoc. In instances were p > 0.05, we did not depict lettered groupings to avoid redundancy. Statistical analyses were preformed using* log_{10} *transformed data for improved normality.*

In the early ripening stage, roughly one week after flowering and prior to the RH heat spike, we still observed differences in leaf arsenic content between treatments (ANOVA, $p < 0.001$); the CH treatment had much greater amounts of arsenic in leaves than other treatments (**Figure 3.4B**). As in the previous timepoint, CH plants also had more arsenic allocated to leaves and less to stems. In the immature grains, the CH treatment had the largest arsenic content, followed by the RH, VH and then NH treatments. In the CH treatment, rice plants allocated more arsenic to grains and less to hulls than those in the NH treatment (**Figure 3.4E**).

At the mature timepoint, following the completion of the RH heat spike, we observed differences between treatments in leaf arsenic content as well as total arsenic content (ANOVA, $p < 0.001$, both). In both the RH and CH treatments there was a greater leaf arsenic content and greater allocation of aboveground arsenic to leaves relative to the other two treatments. On average, CH and RH plants allocated 13% more arsenic to leaves than the VH and NH treatments. The high levels of leaf arsenic content led to a difference in total aboveground arsenic (ANOVA, $p < 0.001$), where the RH and CH treatments had substantially greater aboveground arsenic content than the other two treatments. The CH and RH treatment also had lower average allocation of arsenic to grain and hulls than the other two treatments, though for grains the difference was only significant between the CH and VH treatment.

3.4.4. Plant Roots

Temperature impacted root biomass and root to shoot ratio at maturity (ANOVA, $p < 0.001$, both). The RH and the NH treatments had greater root biomass than both the CH and the VH treatments (**Figure 3.5A**). The RH treatment had the highest root to shoot ratio, and the CH treatment had the lowest. The NH and VH treatments had similar intermediate values.

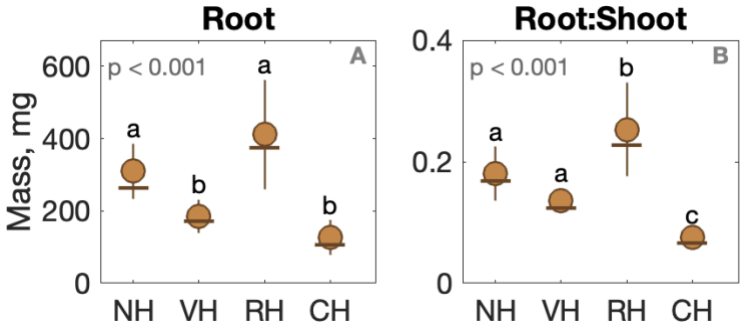

Figure 3.5. *Root biomass and root to shoot ratio of rice plants at maturity. Statistical analyses were preformed using log_{10} transformed data for improved normality. At each time point and tissue type we performed an ANOVA (p-value shown) followed by a Tukey post-hoc.*

Much of the total plant arsenic was in roots and we observed treatment differences in root arsenic content and total arsenic allocation (ANOVA, $p < 0.01$, both). Average root arsenic content was the greatest for the RH treatment though there was substantial variance in the treatment (**Figure 3.6A**). Overall, the RH and NH treatments had the greatest average root arsenic content. The root arsenic content in the RH treatment was significantly greater than in both the VH and CH treatments, whereas the root arsenic content of the NH treatment was only statistically larger than that in the VH treatment. Arsenic content was the lowest in the VH treatment. Allocation patterns were slightly more convoluted (**Figure 3.6B**). On average the NH and RH treatments had greater arsenic allocation to roots than the CH and VH treatments (79% relative increase). The VH and CH treatments had greater average allocation to aboveground tissue than the NH and RH treatments (VH: 38% and CH: 39% increase). Statistically, the RH root arsenic content was only significantly greater than the CH treatment and VH aboveground arsenic was only significantly greater than the RH treatment.

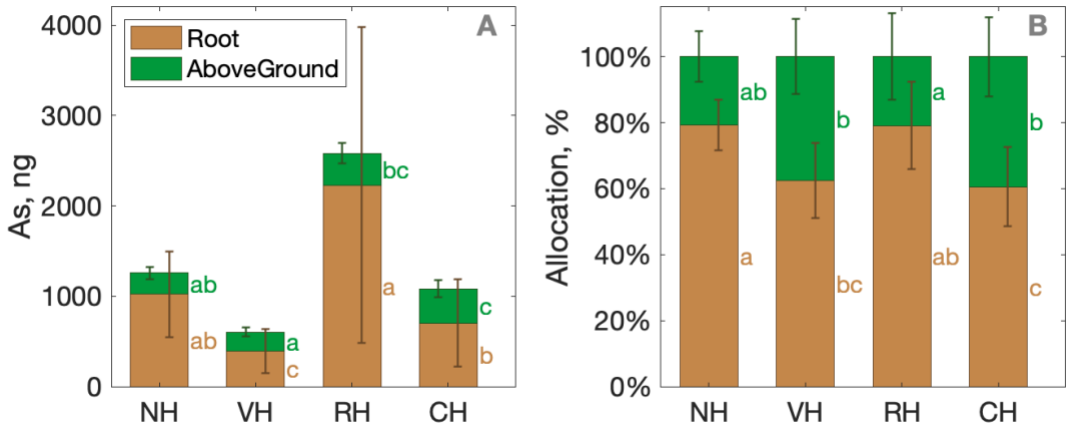

Figure 3.6. *Above and belowground arsenic content and allocation of plants at maturity. (A) Arsenic content is arsenic concentration × mass. Aboveground arsenic is the sum of all arsenic content in aboveground tissues at maturity. (B) Allocation is percent plant arsenic in plant tissue found either above or below ground. Statistical analyses were preformed using log_{10} transformed data for improved*

normality. At each time point and tissue type we performed an ANOVA (p-value shown) followed by a Tukey post-hoc.

3.4.5. Iron Plaque

When normalized by root mass, ANOVA tests revealed differences in iron plaque development (p = 0.004, **Figure 3.7B**) and plaque associated arsenic (p = 0.02 **Figure 3.7A**), as measured by DBC extraction. The CH treatment had both the greatest amount Fe plaque and the greatest amount of plaque-associated As. The NH treatment had the lowest amount of plaque associated arsenic, significantly less than the CH treatment. The other two treatments were intermediates between NH and CH in both plaque arsenic and iron. The VH treatment had the lowest Fe-plaque development, significantly less than the CH treatment. When we normalized plaque associated arsenic by the amount of iron in the plaque, we saw no difference across treatments (ANOVA, p = 0.1, **Figure 3.7C**).

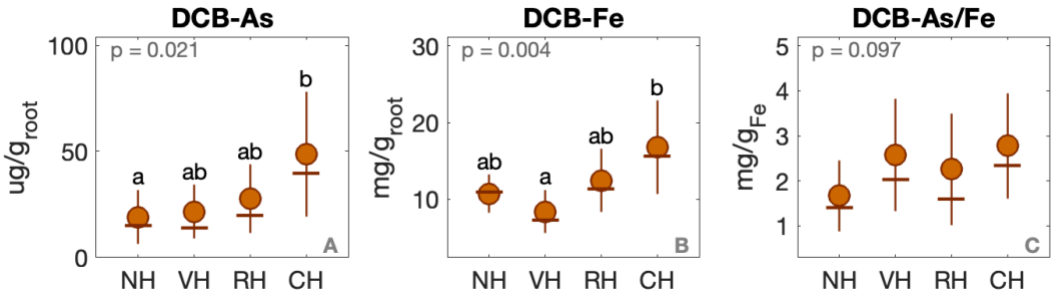

Figure 3.7. *DCB extracted arsenic, iron, and arsenic to iron ratio. Subplots A and B are normalized by root biomass. Subplot C shows extracted arsenic normalized by extracted iron. Statistical analyses were preformed using log_{10} transformed data for improved normality. At each time point and tissue type we performed an ANOVA (p-value shown) followed by a Tukey post-hoc.*

3.5. Discussion

In this work we build on a growing field of knowledge attempting to understand links between increasing temperature and rice arsenic uptake and accumulation, by delving more

deeply into temporal and phenological differences in heat exposure. The integration of timing into our understanding of heat-fueled increases in rice arsenic will allow us to predict when heat exposure may increase rice arsenic most dramatically.

Our study system was a low arsenic system with background levels of available arsenic (Chang et al., 2004) and we did not amend soils with additional arsenic. We also used a lower temperature of heat exposure relative to other experiments on this topic (Dhar et al., 2020; Muehe et al., 2019). Therefore, our study more closely mimics agricultural systems in Northern California, a rice market which is often considered low in arsenic and relatively safe. Even in this conservative system, we were able to detect notable increases in rice plant arsenic. It is possible that larger increases in rice arsenic could occur in high arsenic systems or areas which experience more dramatic increases in heat (FDA, 2013).

3.5.1. Arsenic Mobilization

Porewater concentrations of dissolved arsenic responded to both continuous and shorter duration increases in temperature (**Figure 3.2**). A heat spike during the vegetative stage caused only a small increase in dissolved arsenic which did not persist over time, while a heat spike during the ripening stage saw a much larger increase in average dissolved arsenic. Differences in the magnitude of the response at the two different timepoints likely indicate changes in the soil's potential for arsenic mobilization. One possible reason for the difference between these two time points relates to the microbial community, which mediates the mobilization of arsenic (Ahmann et al., 1997; Turpeinen et al., 1999). Microbial biomass tends to increase from tillering to the ripening stage (Lu et al., 2002). A larger microbial community can mobilize more arsenic causing a commonly observed increase in dissolved arsenic throughout the growing season (Turpeinen et al., 1999). So, one might also expect that during the ripening stage, a heat spike is

acting on a larger and more robust microbial community and fueling on a greater rate of arsenic mobilization.

Exuded carbon from rice roots can also be an important variable in arsenic mobilization and root exudation increases over the growing season (Aulakh et al., 2001). Tu et al. (2004) showed that root exudates can increase arsenic mobilization. The increased microbial biomass throughout the growing season is, in part, related to the increasing availability of plant derived carbon (Beare et al., 1995; Lu et al., 2002; Vezzani et al., 2018). Interestingly, we also observed greater root mass in the RH treatment at the end of the experiment relative to the CH and VH treatments, implying a larger ability to exude carbon to feed the microbial community (Beare et al., 1995). This observation supports the idea that the stronger response to temperature in the RH treatment was linked to root exuded carbon and a larger more active microbial community. Further discussion on differences in root biomass between treatments is found in Section 4.3, below. In this study we did not see large differences between planted and unplanted pots in dissolved arsenic (**Figure A2.1**). However, planted pots may still have mobilized more arsenic than unplanted pots, which was taken up plants. Our previous work indicates may substantially lessen porewater dissolved arsenic concentrations (Farhat et al., 2021).

3.5.2. Arsenic in Plant Tissue

The responses of tissue arsenic concentrations to temperature spikes in both treatments were parallel to that in the porewater: the VH treatment had a small and fleeting increase in arsenic in vegetative tissue, and the RH treatment had a larger response resulting in a detectible increase in arsenic in tissue of mature plants. In the later vegetative stage, the concentration of arsenic in stem and leaf tissue of the VH treatment was higher than the NH treatment, but the relative change was small and the difference between these two treatments diminished over time.

Alternatively, the RH treatment had a much more notable increase in arsenic concentrations following its temperature spike in grains, leaves, stems, and roots. The fact that trends in both treatments mirrored those of porewater arsenic, as well as our previous work showing that arsenic mobilization into the porewater can increase arsenic uptake (Farhat et al., 2021), indicates that arsenic mobilization is a key factor in both season-long and shorter term heat induced increases in arsenic uptake.

Whether a short duration heat spike is able increase arsenic in mature tissue depends on the amount of additional arsenic (total mass of arsenic) taken up due to that heat spike. While the concentrations of arsenic in vegetative tissue of the VH treatment appeared notably higher than the NH treatment following the VH heat spike, the actual difference in arsenic content was small (**Figure 3.4A**) due to the low biomass of the plants during the vegetative stage. Therefore, the heat spike was less able to create a detectible change in mature plants. Alternatively, we see that the RH heat spike resulted in a larger increase in total arsenic content (**Figure 3.4C**), such that at maturity total arsenic content in the RH treatment was similar to the CH treatment. The increase in total arsenic of RH plants was driven primarily by an increase in arsenic content in the leaf tissue. The fact that most aboveground arsenic ended up in leaves is consistent with the knowledge that arsenic is relatively immobile within the plant and only a small fraction of what is taken up by roots typically makes its way to the grains (Zheng et al., 2011). The accumulation of arsenic in straw tissue might also present environmental challenges, as straw incorporation into field soil is a common practice between rice growing seasons. Straw incorporation can increase rice grain arsenic in subsequent seasons, though mostly in the form of less toxic organic arsenic species (Ma et al., 2014). These results motivate investigation of high arsenic systems,

where a vegetative heat spike might mobilize enough arsenic into porewater such that arsenic uptake into plant could have a lasting impact on rice tissue arsenic at maturity.

It is notable that average and median grain arsenic concentrations in all treatments were greater than those in the NH treatment, though for the VH treatment it fell just below the threshold for significance (Tukey HSD, $p = 0.055$). This increase in average and median grain arsenic relative to the NH treatment indicates that even short spikes in temperature can increase arsenic concentrations in rice. The fact that the RH treatment was highly significantly different from the NH treatment ($p < 0.001$) while the VH treatment fell just short our α of 0.05, reinforces the idea that heat spikes later in growing season present a greater threat for dietary arsenic exposure. We observed that mean grain arsenic concentrations of plants in the RH treatment were slightly lower than plants in the CH treatment (82 ng g^{-1} vs. 97 ng g^{-1}), but there was not significant difference between these two treatments. Further research may be useful to determine if continuous warming is more detrimental than temporary heat spikes later in the rice growing season.

In the early ripening stage prior to the RH heat spike, we observed greater rice grain arsenic content in the RH treatment than in the NH treatment (**Figure 3.4B**), primarily driven by the greater grain biomass relative to the NH and VH treatments (**Figure A2.2**). Differences in biomass are likely related to slight differences in ripening phenology and match with our informal observations of rice grains at this timepoint after processing; NH and VH plants had more unfilled and very small caryopses. This timepoint was challenging to coordinate logistically as flowering occur over the course of several days at different locations within the panicle. The difference in rice grain arsenic content between treatments was no longer detectable at the mature timepoint (**Figure 3.4C**).

3.5.3. Plant roots

Larger root systems can have greater surface area to absorb nutrients (Wang et al., 2006), and therefore can also absorb more nutrient analogs, like arsenic. Plants in the RH and NH treatments tended to have greater root biomass, whereas plants in the VH and CH treatments had lower average root biomass. Heat exposure can limit root growth and the vegetative stage is believed to be a critical stage for root development, when significant carbon is allocated towards developing roots for water and nutrient acquisition (Nishar et al., 2017; Palta and Watt, 2009). Therefore, heat exposure during the vegetative stages of both the CH and VH treatments may have limited root growth.

The larger root mass of the RH treatment (**Figure 3.5**) coupled with increased mobilization of arsenic following the heat spike (**Figure 3.2**) might help explain the strong response of both arsenic concentrations and arsenic content in mature tissues within this treatment. After the heat spike, arsenic concentrations in most tissues of the RH increased to similar levels as the treatment continuously exposed to heat (**Figure 3.3**). The same was true for aboveground arsenic content (**Figure 3.4**). The large root systems of the RH treatment may have allowed for the rapid uptake of freshly mobilized arsenic. Conversely, the smaller root systems of the VH treatment (**Figure 3.5**) coupled with lower overall mobilization of arsenic (**Figure 3.2**) may have lessened arsenic uptake. While CH treatment plants also had low root biomass (**Figure 3.5**), these plants still retained high arsenic concentration and content because the dissolved arsenic concentrations were high enough throughout the experiment to induce elevated uptake. The opposite is true for plants in the NH treatment, which had high root biomass but low dissolved arsenic during the experiment.

Belowground arsenic represents a much larger pool of arsenic than aboveground arsenic (**Figure 3.6**). Because plants in the RH treatment had both higher average root biomass and high concentrations of arsenic in roots, they had the highest root arsenic content (**Figure 3.6A**). The variance on this estimate was quite high, likely due to the challenge of removing large roots from paddy soil. Relative to arsenic content, the allocation of arsenic to belowground tissue was more consistent (**Figure 3.6B**). Both the RH and the NH treatments had higher arsenic allocated to roots, indicating that larger root systems may be better able to sequester arsenic. For plants in the RH treatment, greater sequestration of arsenic in roots was not sufficient to overcome the other system drivers which caused greater arsenic mobilization, resulting in more arsenic in grains than the NH treatment.

Iron plaque data reaffirmed our previous finding that continuous heat exposure can increase plaque-associated arsenic (Farhat et al., 2021). Both the VH and RH treatments had intermediate iron plaque between the NH and CH treatments. Neither heat spikes significantly increase plaque associated arsenic above that of the NH treatment (**Figure 3.7**). In our previous experiment (Farhat et al., 2021), we found a non-linear relationship between temperature and Fe extracted from plaque – such that only dramatic increases in temperature caused a difference in iron plaque development. Here we did not find a difference between the NH and CH treatments iron plaque, as the temperature difference between the two treatments was less than the +8°C threshold needed in our previous study to detect a significant increase (Farhat et al., 2021). The lowest iron plaque per unit of root was in the VH treatment. Additionally, we did not find any differences in the As/Fe ratio across treatments. The As/Fe relationship to temperature was also non-linear in our previous work and so the lower temperature differences used in this study could have led to the lack of any differences.

3.5.4. Broader Impacts

To our knowledge there are only two other papers which investigate the intersection of heat, rice arsenic, and phenology. Arao et al. (2018) first showed that heat exposure during the two weeks after heading can increase rice grain arsenic using stored rice samples from across multiple years. Later, Dhar et al. (2020) directly demonstrated in a greenhouse setting that increased temperatures from one week after heading until full maturity increased rice grain arsenic. Both papers specifically look at grain arsenic as grain is the primary route of human exposure. However, a more detailed analysis can help inform our understanding of the underlying mechanisms driving this increase in rice arsenic. For example, Arao et al. (2018) only identified one specific time window (the two weeks after heading) when temperature correlated with rice grain arsenic and did not find a correlation with warmer temperatures even one week prior. Our results suggest that either the earlier heat exposures did not mobilize sufficient arsenic from soils to create lasting changes in rice grain arsenic, or that plants had lower biomass decreasing the mass of arsenic stored in tissue (i.e., content). Potentially, some of the earlier temperature exposures may have caused an increase in vegetative tissue arsenic, as we found that most additional arsenic taken up under elevated temperatures ended up in rice roots and leaves, and only a small fraction made its way to rice grains.

Responsible rice farming must consider increased temperatures not just as a threat to yield, but also a threat to rice consumers who may be exposed to higher levels of arsenic. Here we show that even shorter duration exposure to temperature can increase arsenic mobilization and accumulation in plant tissue. Heat spikes later in the season are more determinantal and are more likely to increase rice grain arsenic. Dhar et al. (2020) has identified silicon amendments as an effective climate adaptation strategy to mitigate strategy to reduce temperature fueled arsenic

mobilization during the ripening stage. Additionally drying fields during the ripening stage is a common farmer practice and is known to reduce arsenic in rice grains (Carrijo et al., 2019). Our work suggests these mitigation strategies may be especially important if the correspond with a timing of a heat wave late in the growing season. These tools, as well as the selection low arsenic accumulating varieties (Chi et al., 2018), may help reduce arsenic exposure to rice consumers in a warmer future.

3.6. References

Ahmann D, Krumholz LR, Hemond HF, Lovley DR, Morel FMM. Microbial Mobilization of Arsenic from Sediments of the Aberjona Watershed. Environmental Science & Technology 1997; 31: 2923-2930.

Arao T, Kawasaki A, Baba K, Mori S, Matsumoto S. Effects of Water Management on Cadmium and Arsenic Accumulation and Dimethylarsinic Acid Concentrations in Japanese Rice. Environ Sci Technol 2009; 43: 9361-9367.

Arao T, Makino T, Kawasaki A, Akahane I, Kiho N. Effect of air temperature after heading of rice on the arsenic concentration of grain. Soil Science and Plant Nutrition 2018; 64: 433-437.

Aulakh MS, Wassmann R, Bueno C, Kreuzwieser J, Rennenberg H. Characterization of Root Exudates at Different Growth Stages of Ten Rice (*Oryza sativa L.*) Cultivars. Plant Biology 2001; 3: 139-148.

Beare MH, Coleman DC, Crossley DA, Hendrix PF, Odum EP. A hierarchical approach to evaluating the significance of soil biodiversity to biogeochemical cycling. Plant and Soil 1995; 170: 5-22.

Carrijo DR, Li C, Parikh SJ, Linquist BA. Irrigation management for arsenic mitigation in rice grain: Timing and severity of a single soil drying. Sci Total Environ 2019; 649: 300-307.

Chang AC, Page AL, Krage NJ. Role of fertilizer and micronutrient applications on Arsenic, Cadmium, and lead accumulation in California cropland soils. California Department of Food and Agriculture 2004.

Chi Y, Li F, Tam NF-y, Liu C, Ouyang Y, Qi X, et al. Variations in grain cadmium and arsenic concentrations and screening for stable low-accumulating rice cultivars from multi-environment trials. Sci Total Environ 2018; 643: 1314-1324.

Clemens S, Ma JF. Toxic Heavy Metal and Metalloid Accumulation in Crop Plants and Foods. Annu Rev Plant Biol 2016; 67: 489-512.

Cline G, Neigher A, Bellinder A. Climate of Sacramento, California. National Weather Service, Sacramento California, 2010.

Dhar P, Kobayashi K, Ujiie K, Adachi F, Kasuga J, Akahane I, et al. The Increase in the Arsenic Concentration in Brown Rice Due to High Temperature during the Ripening Period and Its Reduction by Silicate Material Treatment. Agriculture 2020; 10.

Fageria NK. Mineral Nutrition of Rice: CRC Press, 2014.

Farhat YA, Kim SH, Seyfferth AL, Zhang L, Neumann RB. Altered arsenic availability, uptake, and allocation in rice under elevated temperature. Sci Total Environ 2021; 763: 143049.

FDA U. Analytical Results From Inorganic Arsenic in Rice and Rice Products Sampling September 2013. 2013.

Field CB, Barros V, Stocker TF, Dahe Q. Managing the risks of extreme events and disasters to advance climate change adaptation: special report of the intergovernmental panel on climate change: Cambridge University Press, 2012.

GRiSP. Rice Almanac. Los Baños (Philippines): International Rice Research Institute, 2013.

Gutiérrez JM, Jones RG, Narisma GT, Alves LM, Amjad M, Gorodetskaya IV, et al. Atlas (Interactive Tool). In: Masson-Delmotte V, Zhai P, Pirani A, Connors SL, Péan C, Berger S, et al., editors. Climate Change 2021: The Physical Science Basis. Contribution of Working Group I to the Sixth Assessment Report of the Intergovernmental Panel on Climate Change. Cambridge University Press, 2021.

Hatfield JL, Prueger JH. Temperature extremes: Effect on plant growth and development. Weather and Climate Extremes 2015; 10: 4-10.

Hoagland DR, Arnon DI. The water-culture method for growing plants without soil. Circular. California Agricultural Experiment Station 1950; 347: 32 pp.

Lu Y, Watanabe A, Kimura M. Contribution of plant-derived carbon to soil microbial biomass dynamics in a paddy rice microcosm. Biology and Fertility of Soils 2002; 36: 136-142.

Ma JF, Nishimura K, Takahashi E. Effect of silicon on the growth of rice plant at different growth stages. Soil Science and Plant Nutrition 1989; 35: 347-356.

Ma JF, Yamaji N, Mitani N, Xu XY, Su YH, McGrath SP, et al. Transporters of arsenite in rice and their role in arsenic accumulation in rice grain. Proc Natl Acad Sci 2008; 105: 9931-5.

Ma R, Shen J, Wu J, Tang Z, Shen Q, Zhao F-J. Impact of agronomic practices on arsenic accumulation and speciation in rice grain. Environmental Pollution 2014; 194: 217-223.

Muehe EM, Wang T, Kerl CF, Planer-Friedrich B, Fendorf S. Rice production threatened by coupled stresses of climate and soil arsenic. Nat Commun 2019; 10: 4985.

Neumann RB, Seyfferth AL, Teshera-Levye J, Ellingson J. Soil Warming Increases Arsenic Availability in the Rice Rhizosphere. Agricultural & Environmental Letters 2017; 2.

Nishar A, Bader MKF, O'Gorman EJ, Deng J, Breen B, Leuzinger S. Temperature Effects on Biomass and Regeneration of Vegetation in a Geothermal Area. Frontiers in Plant Science 2017; 8.

Palta J, Watt M. Chapter 13 - Vigorous Crop Root Systems: Form and Function for Improving the Capture of Water and Nutrients. In: Sadras V, Calderini D, editors. Crop Physiology. Academic Press, San Diego, 2009, pp. 309-325.

Taylor GJ, Crowder AA. Use of the DCB Technique for Extraction of Hydrous Iron Oxides from Roots of Wetland Plants. American Journal of Botany 1983; 70: 1254-1257.

Tu S, Ma L, Luongo T. Root exudates and arsenic accumulation in arsenic hyperaccumulating Pteris vittata and non-hyperaccumulating Nephrolepis exaltata. Plant and Soil 2004; 258: 9-19.

Turpeinen R, Pantsar-Kallio M, Häggblom M, Kairesalo T. Influence of microbes on the mobilization, toxicity and biomethylation of arsenic in soil. Science of The Total Environment 1999; 236: 173-180.

Vezzani FM, Anderson C, Meenken E, Gillespie R, Peterson M, Beare MH. The importance of plants to development and maintenance of soil structure, microbial communities and ecosystem functions. Soil and Tillage Research 2018; 175: 139-149.

Wang H, Inukai Y, Yamauchi A. Root Development and Nutrient Uptake. Critical Reviews in Plant Sciences 2006; 25: 279-301.

Weber F-A, Hofacker AF, Voegelin A, Kretzschmar R. Temperature Dependence and Coupling of Iron and Arsenic Reduction and Release during Flooding of a Contaminated Soil. Environ Sci Technol 2010; 44: 116-122.

Xu XY, McGrath SP, Meharg AA, Zhao FJ. Growing Rice Aerobically Markedly Decreases Arsenic Accumulation. Environmental Science & Technology 2008; 42: 5574-5579.

Yamaji N, Ma JF. Spatial distribution and temporal variation of the rice silicon transporter Lsi1. Plant Physiol 2007; 143: 1306-13.

Yamaji N, Ma JF. Further characterization of a rice silicon efflux transporter, Lsi2. Soil Science and Plant Nutrition 2011; 57: 259-264.

Zheng MZ, Cai C, Hu Y, Sun GX, Williams PN, Cui HJ, et al. Spatial distribution of arsenic and temporal variation of its concentration in rice. New Phytol 2011; 189: 200-9.

4. Chapter 4: Connections between seasonal flooding and plant mineral nutrition in Kampong Thom, Cambodia

In preparation by Farhat YA, Muth EN, Cheythyrith C, Holtgrieve GW, Kim S-H, Lyda H, and Neumann RB.

4.1. Abstract

Cambodia is heavily reliant on domestic rice agriculture and historically the Tonle Sap floodplain has been an important location for rice cultivation. While Cambodians have a long traditional history of growing rice, the environmental conditions surrounding rice cultivation are changing. For example, rapid dam construction in the Mekong River Basin is expected to alter seasonal flooding patterns in the Tonle Sap. Yet, the underlying impact of seasonal flooding on both soil fertility and rice nutritional quality is complex and often unclear. In this experiment we focus on rice mineral nutrition, as it relates to two metal micronutrients (zinc and iron) and one metalloid toxin (arsenic). All three of these elements represent potentially important components of both rice crop and human nutrition. In this two-year field study, we collected surface soils, flood sediment, and dry-season plant tissue from 12 rice fields along a flooding gradient in the Steung Saen Municipality of Kampong Thom, Cambodia. We found that sites with greater flooding had higher concentrations of total metals but a lower fraction of plant available metals. Flood sediments had higher concentrations of bioavailable forms of all three elements relative to surface soils, indicating that flood sediment can act both as a natural source of nutrients and toxins. Concentrations of these elements were variable in rice tissue, though we found seasonal trends in zinc concentrations. Finally, we found relatively high concentrations of arsenic in rice

grains, given that Kampong Thom is often overlooked in studies on rice arsenic in Cambodia. These observations and further in-depth research are needed to understand how rice agriculture and rice nutritional quality might change with the anticipated alterations in flooding.

4.2. Introduction

Cambodia has a long, rich history of rice production dating back at least 2,000 years, making rice an integral part of the Cambodian diet and culture (Nesbitt, 1997). The Ministry of Agriculture, Forestry, and Fisheries (MAFF) estimates annual per capita rice consumption in Cambodia is roughly 143 kg, over twice the global average (~64 kg) (GRiSP, 2013; Ministry of Agriculture, 2017). Since the 1990s, there has been rapid growth in Cambodian rice production (Food and Agriculture Organization, 2020; Ministry of Agriculture, 2017; United States Department of Agriculture, 2020). This rapid growth coupled with inadequate research through scientific investigation has left many uncertainties in our understanding of farmer management and nutrient dynamics in the Cambodian rice system.

Historically, the Tonle Sap floodplain has been a key region for rice cultivation due to its plentiful access to water (Nesbitt, 1997). Part of the larger Mekong River Basin, the Tonle Sap consists of the permanent lake, the Tonle Sap River, and the surrounding floodplain. During the wet season, monsoon rains throughout the Mekong River Basin causes water to flow through the Tonle Sap River and into the lake. The Tonle Sap fills with water and expands out into the surrounding floodplain, increasing the lake surface area from 3,500km^2 up to 14,500 km^2 (MRC, 2005). When flood waters recede, rice fields at the edges of the floodplain become available for dry season farming. The duration of flooding is governed by a field's proximity to the lake and influences the length of the dry season. With modern, fast maturing varieties farmers can cultivate up to two dry season rice crops, called the early dry and the late dry season crops. These

seasons are also sometimes referred to as late wet and early wet season crops, respectively. While only about a quarter of domestic rice production, dry season rice production is rapidly increasing in Cambodia – increasing 70% between 2007 and 2016 (Ministry of Agriculture, 2017). This dramatic increase is primarily driven by increasing cultivated area (51% increase between 2007 and 2016) and, to a lesser extent, increased yield (13% increase in the same period). The two largest rice producing provinces in the Tonle Sap floodplain are Battambang and Kampong Thom. Of these two provinces, Kampong Thom is more reliant on dry season rice production (Ministry of Agriculture, 2017).

Seasonal flooding on the Tonle Sap floodplain can influence the amount and bioavailability of minerals in the soils of rice-growing fields. Some of these minerals are micronutrients while others can be toxic. In this paper we focus on two primary metal micronutrients, zinc (Zn) and iron (Fe), and one toxin, arsenic (As).

Both zinc and iron are important micronutrients for crops and the humans who consume them. Zinc is essential in the human diet, especially for children, and zinc deficiency is estimated to impact roughly 43% of children in Cambodia (Johnston and Conkle, 2008). Zinc deficiency is also recognized as one of the most important micronutrient deficiencies in rice and can reduce crop yield (Impa and Johnson-Beebout, 2012). Unlike zinc, rice plant iron deficiency is uncommon in flooded paddy systems, though it is sometimes present in excess which can lead to toxic effects in rice (Aung and Masuda, 2020). Human iron deficiency is much more common, and is in fact one of the most prevalent micronutrient deficiencies worldwide, impacting ~16% of the global population (Pasricha et al., 2021). Human dietary deficiencies of both zinc and iron are both associated with diets containing a high percentage of cereal crops, as is the case in

Cambodia, due to their low concentrations in cereals and/or the lower potential for absorption (Bailey et al., 2015; Gharibzahedi and Jafari, 2017; Roohani et al., 2013).

Arsenic is a potent carcinogen and toxin that is frequently found in rice paddy environments. Rice is a major dietary source of arsenic (Meharg and Zhao, 2012), and can induce genotoxic effects in humans at levels as low as 200 ng g^{-1} (Banerjee et al., 2013). Arsenic is also toxic for rice plants and limits their yield (Awasthi et al., 2017; Meharg and Zhao, 2012). Most of the previous research on rice arsenic in Cambodia has focused on provinces further to the south, especially Kendall province (Gilbert et al., 2015; Murphy et al., 2018a; Murphy et al., 2018b; Quicksall et al., 2008; Wang et al., 2013). There, rice crops are irrigated with groundwater which often contains heightened concentrations of arsenic relative to surface water. Yet, in a small survey of arsenic concentrations in rice grains from across Cambodia, the sample with the highest concentrations of arsenic was collected from Kampong Thom province (Seyfferth et al., 2014). The authors only collected a single sample from Kampong Thom, and therefore there is a need for further study in this province.

The connection between flooding and mineral availability can be broadly broken into two categories: (1) chemical changes in the soils from saturation with water and (2) delivery chemicals associated with freshly deposited sediments.

The most notable chemical changes that occur when soils become waterlogged are shifts in pH and changes in redox potential. Zinc is strongly impacted by soil pH. It is most bioavailable in slightly acidic soils, when organic acids in the soil are protonated and cannot bind Zn(II) (Impa and Johnson-Beebout, 2012; Zeng et al., 2011). Prolonged flooding tends to shift soil pH to near neutral, where zinc is relatively unavailable for plant uptake. It is therefore well known that prolonged flooding tends to decrease bioavailable zinc and leads to zinc deficiencies

in paddy soils (Alloway, 2008; Impa and Johnson-Beebout, 2012). The other chemical change in soils is a reduction in redox potentials as oxygen is depleted and soil microorganisms must use less favorable electron acceptors. Two such electron acceptors are solid Fe(III) and As(V), which are reduced to soluble Fe(II) and As(III). Additionally, both arsenic and zinc can be sorbed onto solid Fe(III) minerals in the soil and can be released into solution when Fe(III) is reduced (Cummings et al., 1999; Trivedi et al., 2004; Tufano and Fendorf, 2008; Xue et al., 2020). Prolonged anoxia can also produce sulfides, which form complexes with other metals that reduce their bioavailability (Du Laing et al., 2009; Pan et al., 2016).

Metal availability may also be impacted by flood sediment deposition, which brings in a flush of new chemicals to the floodplain. Sediments can increase the concentrations of a given metal when the concentration of that metal is higher in the sediment than in the soil surface onto which that sediment is deposited. This situation is often the case when water systems are associated with the weathering of rock or mining (Chen et al., 2016; Salomons et al., 1987). Whether these freshly deposited metals are taken up by plants depends on their chemical form once deposited (i.e., their bioavailability to plants or phyto-availability) (Du Laing et al., 2009). Sediments may also bring in secondary chemicals which influence the bioavailability of our primary element of interest. For example, influxes of organic carbon can feed microbial respiration solubilizing both iron and arsenic (Stuckey et al., 2016; Zeng et al., 2011). Alternatively, influxes of sulfate with high concentrations of organic carbon can produce sulfide which lessons metal availability (Du Laing et al., 2009; Quicksall et al., 2008).

A detailed understanding of the various aspects which influence mineral nutrient and toxin delivery and availability in rice fields is necessary given that Tonle Sap and the larger Mekong River Basin is experiencing rapid change. There has been significant dam construction

in the Mekong River Basin with more development planned (MRC, 2011; Open Development Mekong, 2016; Zarfl et al., 2014). Damming is expected to alter seasonal flooding in the Tonle Sap by reducing the duration of flooding at the edges of the floodplain while increasing the extent of the permanent lake (Arias et al., 2014). Altered flood patterns can increase the area available for dry-season rice production, provided there is adequate access to irrigation. Based on our understanding of the connections soil drying and the chemical availability of our three minerals, we expect that a shorter flood would increase bioavailable zinc in the soil and decease available iron and arsenic. These alterations impact rice plant uptake. Additionally, Arias et al. (2014) predicted that damming of can reduce sediment deposition in the Tonle Sap floodplain by 56%. If sediments act as a source of these metals, we would expect reductions in available metal concentrations.

The purpose of this study is to explore relationships between seasonal flooding in the Tonle Sap and uptake of important metal micronutrients and contaminants. To accomplish this goal, we established a two-year study with the help of local farmers in the Kampong Thom province. We collected surface soils, flood sediment, and plant tissue data which we analyzed for arsenic, iron, and zinc. We installed pressure transducers in a subset of fields to help understand farmer management and seasonal flooding patterns.

4.3. Methods

4.3.1. Field Sites and Rice Cropping

Our field sites were located in the Steung Saen Municipality of the Kampong Thom Province. This region is overseen by a community run water management board. In 2018 we met with the water board to discuss our research aims and inquire about farmer willingness to

participate in the study. After our discussions we selected 12 fields in the area, located along a 4.8km stretch along the floodplain (**Figure 4.1A**). The Saen River feeds an irrigation canal which the water board manages, and which farmers pay to access. This canal provides sufficient access to water for farmers to grow dry season rice.

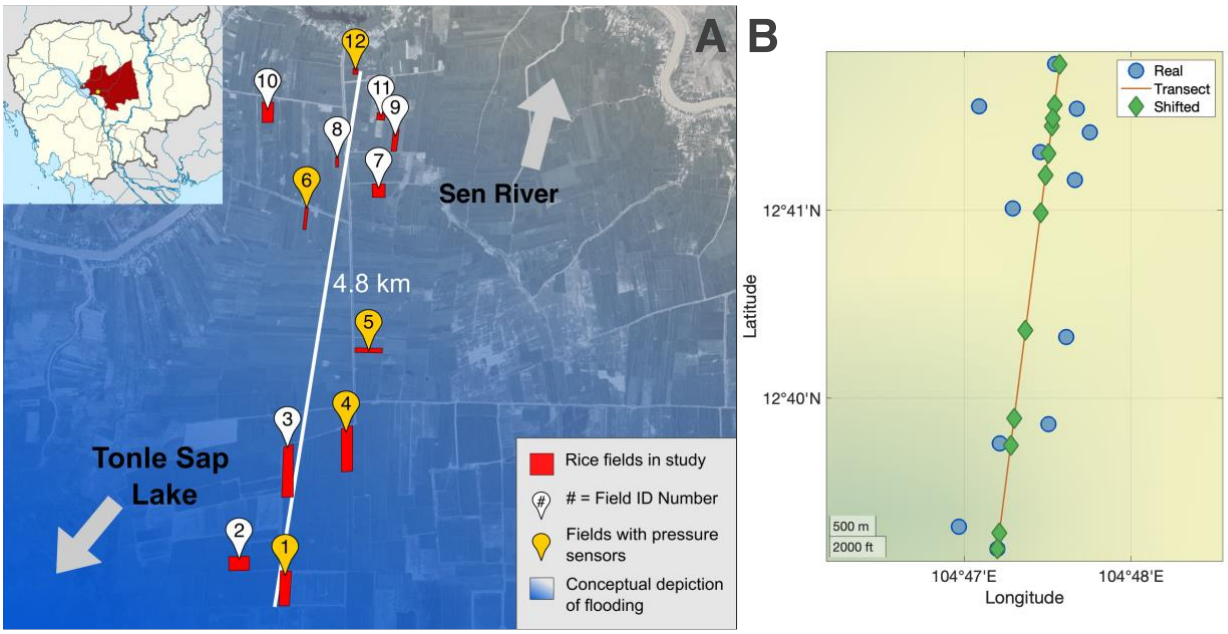

Figure 4.1. *Study fields in the Steung Saen municipality of Kampong Thom. (A) Map showing individual fields. Red squares show total field. Field ID numbers move from furthest South, closer to the lake, to further North, away from the lake. Yellow labels show fields which contained pressure transducers (see section 4.3.5.). Blue shading indicates conceptual depiction of flooding gradient. (B) Transect of experimental fields. Blue circles show GPS coordinates at the center of each study field. We used a simple linear regression of coordinates to create our transect. Fields were then shifted (green diamonds) onto the transect line using the shortest distance between the original field location and the constructed transect line.*

Our study fields were located on a rough transect, starting closer to the lake and travelling North and away from the lake (**Figure 4.1A**). To measure fields relative distance from one

another and we visualized our transect using a regression of the geographic coordinates at the center of each field (**Figure 4.1B)**. Most fields were within 450 meters of the transect line, except for one field which was 800m away. To extrapolate fields onto the transect, we used the shortest distance between each field and our regression line to determine its corresponding latitude and longitude on the transect ("Shifted" fields, **Figure 4.1B**). We then calculated relative distance of each field from the most southern point of the transect by calculating the arc length along the transect and converting it to meters using MATLAB ver. R2019a.

4.3.2. Rice Cropping

Farmers in the Steung Saen Municipality grow two rice crops in the dry season, what we designate the early dry and the late dry season crops. We conducted surveys of the 12 farmers in our study to learn the timing of the two seasons and field management. A conceptual depiction of crop timing based on our surveys is in Appendix 3 (**Figure A3.1**). Briefly, the early dry crop usually planted in November or December and harvested between February and March. The late dry season crop follows, with planting in March or April and harvesting between June and July. There is as substantial variation within Kampong Thom along the floodplain, and it was not uncommon for plants in fields closer to the lake to be in the vegetative stage while plants further up the floodplain were ready to be harvested. Farmers reported that they typically plant along the floodplain gradient, with fields further from the lake planted first and fields closer to the lake planted last. This pattern also causes some overlap between the two dry seasons. There is also interannual variation as farmers must wait for flood waters to begin to recede to start preparing their land for the early dry season crop or wait for sufficient rain to feed the canal system if there is a drought.

4.3.3. Plant Measurements

4.3.3.1. Field Measurements: We collected rice samples from four growing seasons: late dry 2018, early dry 2019, late dry 2019, and early dry 2020. Due to the variation in planting and harvest times, it was not possible to plan sampling trips such that we could collect mature rice plants from all fields. During our days in the field, selected three 0.5m × 0.5m subplots spread throughout the field. In each subplot we noted that developmental stage, counted stems (main stem + all tillers), and collected a sample of young plant tissue. We asked farmers to collect and store mature rice tissue from three different locations within their fields. After the harvest, we returned to collect mature tissue samples from farmers. Due to some miscommunications with farmers, we were only able to collect tissue from 8 out of 12 fields in the late dry season of 2019. Following that miscommunication, we improved our instructions and distributed translated instruction sheets to farmers and were then able to collect mature tissue from all farmers in the final two crop cycles. We returned tissue samples to the Royal University of Agriculture (RUA) in Phnom Penh, where we dried tissue at 105°C for two days. Later, tissue samples were brought back the University of Washington where they were partitioned, weighted, and hulled rice grains.

4.3.3.2. Digestion: We formed composite samples using equal weights (<1% difference) of the field replicates of leaves and grains from each field at each time point (ex. grains from Field 1 in late dry 2018). We ground composite samples into to a powder that we digested to quantify Zn, Fe, and As. Briefly, we placed ~250mg (mass known exactly) into Teflon digestion vessels and added 7.5mL of HNO_3 and 3mL of H_2O_2. A microwave digester (Anton Parr) heated samples to 190°C and held them at that temperature for 30 minutes. We diluted the digestate to 25mL using Ultra DI-Water. Each extraction contained at least one method blank and a NIST Standard Reference Material (SRM) 1568b rice flour. We used inductively coupled plasma mass

spectroscopy (ICP-MS, PerkinElmer, NexION 2000) to quantify zinc and arsenic and grain iron, with a yttrium internal standard and standard addition to correct for strong matrix effects. We used optical emission spectroscopy (ICP-OES, PerkinElmer, Optima 8300) with a yttrium internal standard to measure leaf iron.

4.3.4. Soil Measurements

4.3.4.1. Surface Soil Collection: During our first sampling trip in 2018 we used hand shovels to collect three surface soil samples from the top 15cm in each field and placed the moist soils in clear, waterproof plastic bags. Within one week we measured total metal concentration of the soils in plastic bags using X-Ray Fluorescence (XRF, Innov-X 6000 Alpha Series). After XRF measurements, soils airdried on paper trays in the RUA laboratory.

4.3.4.2. Flood Sediment Collection: We constructed makeshift sediment traps using readily available materials in Kampong Thom. In each field we placed three sediment traps, composed of 1m × 1m plastic tarps laid flat, bricks at the edges to prevent tarps from moving, and bamboo rods to mark the tarp edges above water level. While we had hoped to use sediment traps to estimate sediment deposition, this became challenging due to farmers' need to prepare their fields for planting prior to the fields drying. We carefully removed tarps from any standing water but some sediment loss when the tarps moved through the standing water was evident. We were still able to collect sufficient sediment for chemical analysis. Sediment samples airdried at the RUA campus. We did weight samples to get a rough estimate of sediment deposition, though the variation in sediment weight was high and there was no clear trend in the data.

4.3.4.3. Soil Processing: Surface soils and flood sediments were brought to the University of Washington where they were ground using a soil mill (Thomas Scientific, 3383-L10, Sieve Size 850 μm). Samples from a subset of fields were subjected to chemical

extractions. We selected six fields spread across the transect, five of which later contained pressure transducers during 2019 (see section 4.3.3.4. below). We used surface soils we collected during the late dry season of 2018 and the flood sediment we collected during the following wet season.

4.3.4.4. Chemical Analysis: We performed a modified DTPA extraction to quantify bioavailable zinc (Reed and Martens, 1996). We added 8mL of DTPA extractant (5mM DTPA, 10mM $CaCl_2$, 0.1M TEA, pH = 7.3) to 4g of soil/sediment. The slurry was shaken vigorously for 2 hours at room temperature, then centrifuged for 1 hour at 4150 rpm at 4°C. The supernatant was decanted and syringe filtered (0.2µm, nylon) and acidified with ultra-trace metal nitric acid (2% v/v). We measured zinc concentrations by ICP-MS use a yttrium internal standard and standard additions of zinc to correct for strong matrix effects.

We performed a citrate-bicarbonate-dithionite (CBD) extractions to quantify reducible iron and arsenic (Mehra and Jackson, 1958). In a water bath, we added 8mL of 0.3 M sodium citrate and 1mL of 1.0 M $NaHCO_3$ to 1g of soil or sediment. Solution temperature increased to 75-80 °C and then we added two additions of 1g of sodium dithionate, 5 min apart. Samples centrifuged for 10min at 4150rpm and 4°C. The solution was then decanted, filtered (0.2µm, nylon), and acidified (2% v/v). We washed soils twice more with 25mL of 0.3 M sodium citrate and tumbled for 20 minutes at 60rpm. Again, samples were centrifuged and the filtered supernatant was acidified. Solutions were analyzed for arsenic via ICP-MS with a standard additions of arsenic and an internal standard. Samples were analyzed for iron via ICP-OES with a yttrium internal standard. Based on a preliminary analysis of eight samples, the final sodium citrate rinse contained only 1-3% of the iron and arsenic. Therefore, we neglected this last rinse from further analysis.

4.3.5. Water Measurements

We installed five pressure transducers in the fields depicted on **Figure 4.1,** each separated by between 1,500 and 900m. Between the 29th of January 2019 and the 1st of April 2020 we used these pressure transduces to measure standing water height at our fields (Rugged Troll 100, In-Situ). A barometric pressure sensor (Rugged BaroTROLL, In-Situ) was placed in a shaded and safe location near rice fields. To install pressure sensors, we constructed small wells near the middle of our chosen field. For each well, we used a 6.2cm diameter plastic tube, with a cap on one end and a plastic connector at the other end (total length ~= 74cm). The tube was placed vertically into the ground so that the capped end faced down and the end with the connector was at soil surface. We constructed a wire cap to attach to the connector and seal the tube on the upward side. A pressure transducer was suspending within the tube by tying it to the wire cap at the lip of the tube using a string of known length. Finally, the wired cap was covered with cotton fabric to prevent the intrusion of soil into the tube. When fields were covered in water, the wells filled with water and sensors measured the pressure of water above the sensor. To calculate the standing water height, we subtracted the barometric pressure from the pressure reading of each pressure transducer. We then converted the difference in pressure to water depth and subtracted the depth that the sensors were suspended below the soil surface. To the best of our ability, pressure transducers stayed in the field as much as possible and we only removed them during land preparation and harvesting to allow farmers plow and harvest without damaging wells or sensors.

4.4. Results

4.4.1. Total Metals in Surface Soils

We measured the soil concentrations of various metals in surface soils collected in the late dry seasons of 2018. In **Figure 4.2** we only depict Zn, Fe, and Co for visual clarity, though we observed a similar trends in Mn and Ti as well. We observed a statistically significant decreasing tread ($\alpha = 0.05$) in all of these metals. In the case of Zn, Fe, and Co, the correlation with transect distance was very strong ($r^2 = 0.79$ or greater) and highly statistically significant ($p<0.001$). Arsenic concentrations were below the XRF limit of detection in all but two fields.

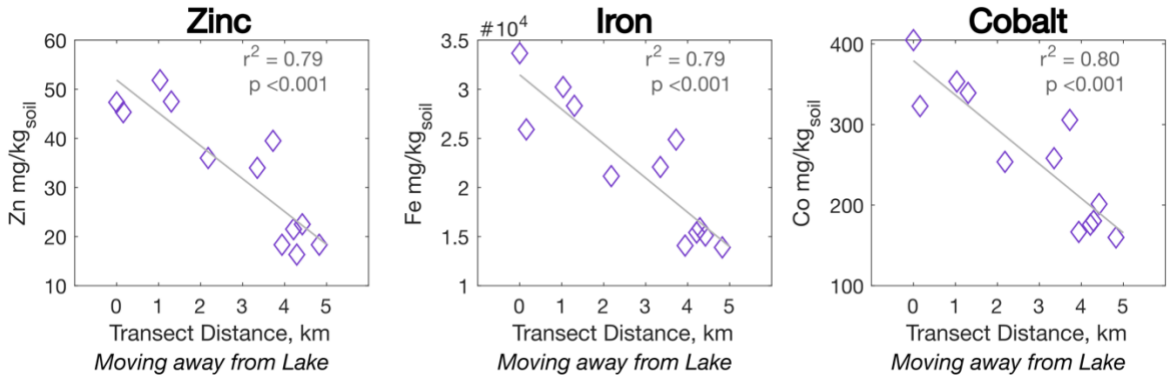

Figure 4.2. *X-Ray Fluorescence (XRF) measurements of selected metals in surface soils collected in the late dry season of 2018 along transect. Results from linear regression also shown with correlation coefficient (r^2) and p-value.*

4.4.2. Available metals in surface soils and flood sediments

Using our two chemical extractions, DTPA and CBD, we compared the extractable metals in the late dry season surface soils of 2018 (i.e., pre-flood) to the flood sediment collected during the 2018 flood. We found that flood sediment contained higher levels of DTPA extractable zinc (t-test, $p = 0.03$, **Figure 4.3**) and higher levels of reducible iron and arsenic ($p = 0.01$ and <0.001, respectively, **Figure 4.3**). While we were not able to get a precise measurement

of flood deposition and variance was high (see section **4.3.4.2.**), median sediment deposition in 2018 was 123 g/m^2 and in 2019 was 457 g/m^2.

There was only a very weak correlation between surface soil concentrations of extractable metals and their transect location (Appendix 3, **Figure A3.2**). Regressions of all three metals across their transect location were not statistically significant at $\alpha = 0.05$. This analysis had a high threshold for statistical significance given our small sample size (n =6).

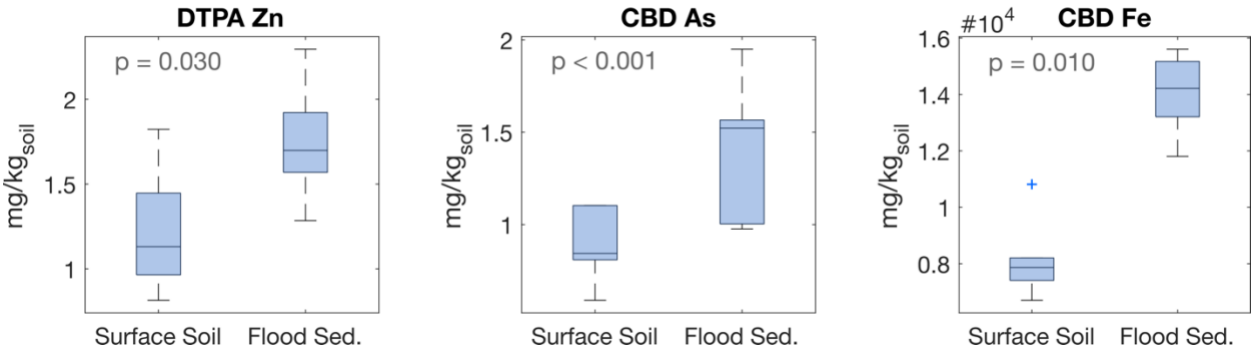

Figure 4.3. *Extractable metals in pre-flood surface soils and flood sediment, collected in 2018. DTPA extraction was used to analyze bioavailable zinc and CBD extractions analyzed reducible iron and arsenic. Results were compared using a two-sample t-test.*

We calculated the fraction of extractable zinc and iron by dividing the extracted metal concentration by the total concentration of that metal. The concentration of extractable zinc was only a small amount of the total zinc concentration, between 2-8% (**Figure 4.4**). The range was more substantial for iron and made up a larger portion of total iron, from 20-80%. When graphed against the transect distance (moving away from the lake), we observed that the data clearly exhibited exponential behavior rather than linear (**Figure 4.4**). Therefore, we $\log_{10}$ transformed the extractable fraction values and fit the transformed values to a linear regression (**Figure 4.4**). The extractable fraction of both zinc and iron increased as fields moved further away from the

lake. These correlations were strong and highly statistically significant (Zn: $r^2 = 0.92$, $p = 0.003$ and Fe: $r^2 = 0.90$, $p = 0.004$). We were unable to perform this analysis for arsenic as it was below XRF detection limits.

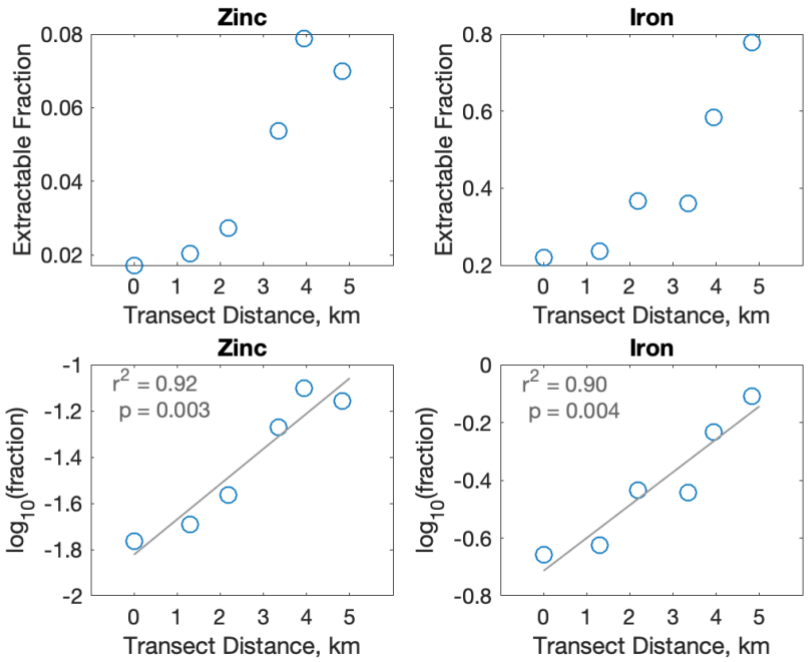

Figure 4.4. *Fraction of total metal removed in chemical extractions of zinc and iron along transect. Zinc was removed by DTPA extraction and iron was removed via CBD extraction. Extracted concentrations (**Figure A3.2**) were normalized by each element's total concentration values determined by XRF. Row 1 shows raw extractable fraction values and row 2 shows the log_{10} formation. Correlation coefficient (r^2) and p-value from regression of log_{10} transformed data are provided.*

4.4.3. Metal concentrations in tissue

We quantified leaf and grain concentrations of our three elements (As, Fe, and Zn) in leaves and grains of rice plants from all four seasons in our study. In **Figure 4.5** we show the concentrations of zinc in mature leaves and grains. Year 1 is the late dry season of 2018 and the early dry season of 2019, and year 2 is the late dry season of 2019 and the early dry season of 2020. We found that leaf concentrations of zinc were significantly lower in the early dry season

of both years relative to the late dry season prior to the flood (two sample t-test, $p < 0.001$). We detected the same trend in year 1 grain tissue, but not in year 2. There were no significant differences in leaf or grain iron concentrations in either year (**Figure A3.3**). There was a small reduction in grain arsenic in early dry season in year 2 (**Figure A3.3**, $p = 0.05$), but not in year 1 grain tissue or in either years' leaf tissue.

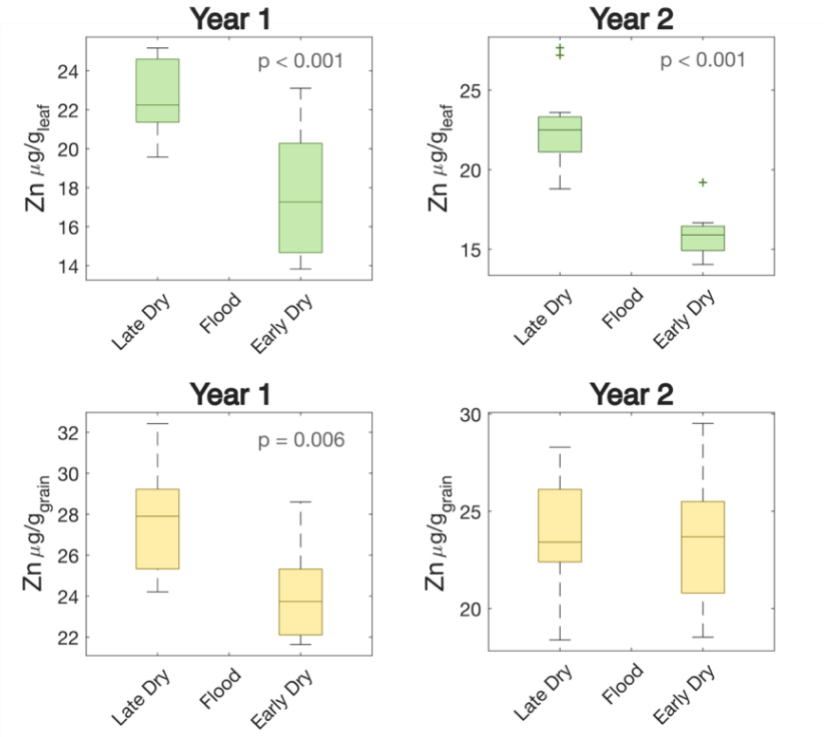

Figure 4.5. *Zinc concentrations in leaf and grain tissue. Year 1 includes the late dry season of 2018 and the early dry season of 2019. Year 2 includes the late dry season of 2019 and the early dry season of 2020. A two-sample t-test was used to compare tissue types before and after the flood and p-values are reported for when significantly different at $\alpha = 0.05$.*

Grain and leaf concentrations of As, Fe, and Zn poorly correlated with transect distances in all four seasons analyzed (**Figure A3.4 and A3.5**). The best correlation for each tissue type was between grain arsenic early dry season of 2019 ($r^2 = 0.54$) and leaf zinc in the late dry

season of 2019 ($r^2 = 0.33$); however, neither were significant at $\alpha = 0.05$ and trends were not consistent between years.

We also compared leaf concentrations of the three metals to their corresponding grain concentration (**Figure 4.6**). To perform this correlation, we used data from all seasons, though one extreme outliner was removed from both iron and arsenic correlations. There was a significant correlation between leaf arsenic and grain arsenic concentrations, though the strength of the correlation was relatively weak ($r^2 = 0.20$, $p = 0.002$). This correlation was primarily driven by trends in the second year of the study (**Figure A3.6,** $r^2 = 0.58$, $p = 0.004$, both seasons). We did not observe similar correlations for iron or zinc (data not shown).

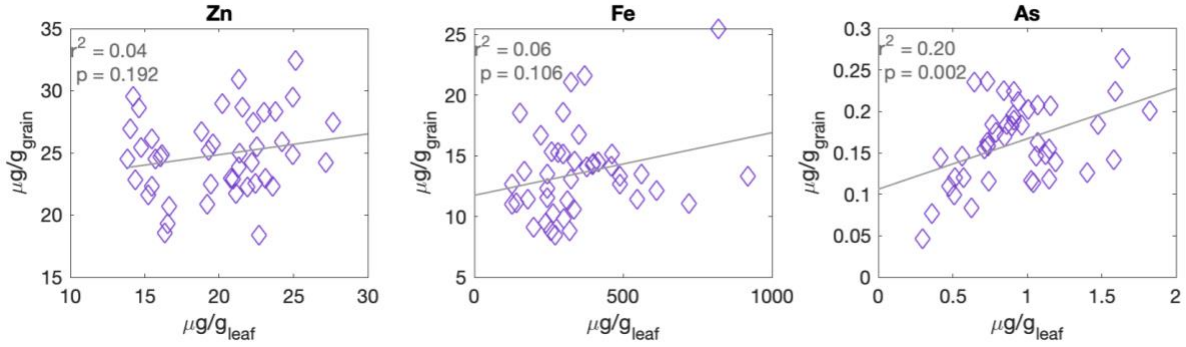

Figure 4.6. *Correlation between leaf and grain concentrations of zinc, iron, and arsenic. Analysis includes samples collected in all four seasons. Correlation coefficient (r^2) and p-value from regression of log_{10} transformed data are provided.*

4.4.4. Connections with flooding depth

Water height above the soil surface between the 29th of January 2019 and the 1st of April 2020 is shown in **Figure 4.7**. Sensors were numbered with the floodplain gradient moving north, i.e., Sensor 1 is in Field 1 and Sensor 5 is in Field 12 as shown in **Figure 4.1A**. Sensors were placed in the field after the early dry season of 2019 had already begun. The fields closer to the lake were still flooded from rice cultivation (Sensors 1 and 2) whereas fields further from the

lake were no longer flooded (Sensors 3-5). Visible in the graphic is the severe drought in dry season of 2019, which lead to power shortages and a government decree for farmers to delay planting until there was rain. The drought caused the 2019 late dry season crop to start unusually late. It appears that this late planting caused was some crossover between the rice crop and the onset of the wet season flood – presenting a challenge to farmers who try to dry their fields before harvesting their rice. There was a dramatic increase in water level during the flood season. Maximum water depths for sensors 1-5 were 107.0cm, 94.6cm, 85.1cm, 79.8cm, and 33.9cm, respectively.

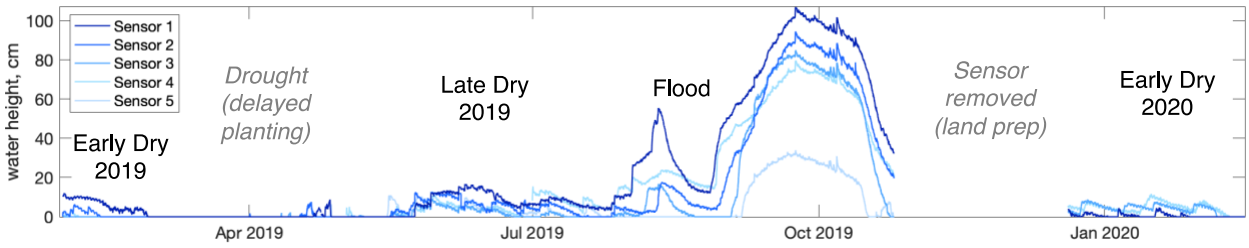

Figure 4.7. *Total water depth above soil surface. Data was collected between the 29th of January 2019 and the 1st of April 2020. Sensors are numbered moving away from the lake. Relative to* ***Figure 4.1A****, Sensor 1 = Field 1, Sensor 2 = Field 4, Sensor 3 = Field 5, Sensor 4 = Field 6, Sensor 5 = Field 12. Water depth indicates standing water level above soil surface.*

Farmers contacted our local team in Phnom Penh and informed them that they needed to start land preparations for the next rice crop in mid-October and we were forced to remove pressure transducers during this time. Unfortunately, several technical errors occurred during the sensor re-deployment in the 2020 early dry season. Sensor 2 was not launched properly and did not collect any readings. Sensor 5 was either corrupted or damaged and data osculated wildly between negative and positive values of unrealistically high magnitude.

We compared the extractable fraction of zinc and iron (**Figure 4.4**) in fields with pressure sensors to the maximum water flood depth in that field. In both zinc and iron there was a significant, negative correlations between maximum flooding depth extractable fraction of metals (**Figure 4.8**). This correlation was especially strong with regards to iron (r^2 = 0.97, p = 0.002). The correlation was less significant for zinc (r^2 = 0.84, p = 0.029). In both cases, correlations were strongly influenced by the lowest water depth reading in Field 12. Correlations between tissue metal concentration and flood water depth were variable. In cases where stronger correlations were observed, these correlations were not repeatable between seasons (ex. grain data in **Figure A3.7**).

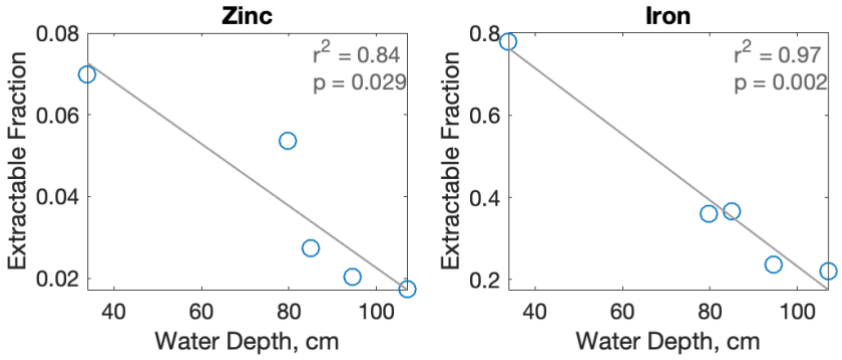

Figure 4.8. *Regression of extractable fraction vs. maximum flooding depth. Extractable ("plant available") zinc was measured by DTPA extraction and iron by CBD extraction. Both values were normalized total concentration of that metal determined by XRF.*

4.5. Discussion

Our work provides novel, in-depth analysis of mineral dynamics on the Tonle Sap floodplain. Mineral nutrients are an often-overlooked component of crop production (Lynch and St.Clair, 2004) and mineral stress can influence human diets; by either suppressing crop yield or changing the concentration of trace elements within their edible tissue. Because of the complex relationship between metal phyto-availability and environmental conditions like seasonal

flooding, the links between soil quality and human nutrition are often unclear. However, the elucidation of these links is even more pressing in developing communities, where resources are limited and local people are highly reliant on a small number of crops. Such is the case in Cambodia.

4.5.1. Flood Sediment

It is noteworthy that the inclusion of flood sediment analyses in our study came from our interviews with local farmers. When asked based on their experience what increased rice yields, three farmers responded that larger or longer floods in the previous wet season increased yield of the following crop. This response highlights the vitality of local knowledge and connections between farmers and the annual hydrologic cycle. Based on those interviews, we hypothesized that flood sediment was loading beneficial nutrients onto rice fields and set up a plan to collect it.

In the scientific literature, nutrient fluxes via flood pulse sedimentation are often assumed to be a key driver of Tonle Sap ecosystem productivity (Kummu et al., 2006; Uk et al., 2018). However, direct analysis of flood sediment nutrient profiles are often missing. Based on our chemical extractions, flood sediments act as a mineral rich source as they have a high concentrations of phyto-available forms of these minerals (**Figure 4.3**). Therefore, sediments may be beneficial to both humans and plants as a zinc source, but also harmful as an arsenic source. The Tonle Sap (lake + floodplain) acts as a net sediment sink, with about 80% of the total influx of sediments remaining in the system after the flood recedes (Kummu et al., 2008). Much of the deposited sediment is suspected to land on the floodplain (Kummu et al., 2008). We suppose this fresh labile influx of metals (and metalloids) has a high probability of contributing to agriculture soils in the floodplain.

Kummu et al. (2008) used a modelling approach to estimated flood deposition throughout the Tonle Sap. While we struggled to quantify flood deposition, our 2018 median value was within range of their estimates of "average year" deposition for the area. Their model showed that sediment deposition on the floodplain typically followed a similar pattern to flooding intensity – where locations closer to the permanent lake had higher sediment deposition and sites further from the lake had less. While we were not able to quantify differences in sediment deposition throughout our transect, we were able document changes in flooding intensity both in differences in maximum water depth and duration of flooding (**Figure 4.7**).

4.5.2. Factors controlling surface soil mineral concentrations

Total metal concentrations in our surface soils strongly correlated with transect locations, where sites closer to the lake had higher concentrations of zinc, iron, and cobalt, among others (**Figure 4.2**). However, the fraction of extractable zinc and iron showed the opposite trend, with sites closer to the lake having a lower fraction of available metals (**Figure 4.4**). The fact that both of these metals responded in a similar way to flooding (though with different magnitudes) indicates that they were both responding to the same driving environmental variable.

An important distinction is that the metal concentrations which we observe associated with soils can represent the remaining metals still associate with those soils following some mobilization which releases them from the soil. Therefore, depletion of the bioavailable fraction of zinc or iron may indicate previous mobilization from soil solids. Prolonged flooding is thought to reduce bioavailable zinc and increased dissolved iron concentrations (Alloway, 2008; Simmler et al., 2017). However, some have observed that there may be a short-term increase in dissolved zinc immediately after flooding (Kelly et al., 2020). One explanation for this short-term increase in dissolved zinc, is that zinc may be associated with iron oxides in these soils

(Impa and Johnson-Beebout, 2012). The onset of flooding triggers the reductive dissolution of Fe(III) oxides and a concurrent solubilization of associated zinc. Soil arsenic is also typically associated with iron minerals and would likely respond in a similar way, though we lack total arsenic concentrations to quantify the extractable fraction of arsenic. Flood sediment may also provide organic carbon which fuels microbial respiration and the reduction of solid Fe(III) in soil. Separate analysis carried out by collaborators at RUA on a small number of samples showed that on average organic carbon concentrations were an order of magnitude higher in flood sediments than in surface soils (Muth et al, *in prep*). They also observed that there was no increase in surface soil organic carbon concentrations pre- and post-flood, indicating that freshly deposit organic carbon from the flood may have been utilized for microbial respiration.

Differences in mobilization do not explain the observed differences in total metals, as the trends run counter to one another. If the transect trend of total metals were governed by mobilization, we would expect sites closer to the lake with more flooding to have lower total iron, not higher. Instead, the positive correlation between transect distance and total metals is more likely due to differences in sedimentation rates. As noted able, sites closer to the lake likely receive greater sediment deposition (Kummu et al., 2008). While some of the bioavailable fraction may be lost following mobilization, another pool of metals is trapped in the soil and likely to persist in soils over time. Higher sediment deposition closer to the lake would increase the size of both the bioavailable and non-available pools of metals. This paradigm suggests that sedimentation may strongly influence the total mass of metals cycling through a given field, whereas the flood status and/or organic carbon delivery influences what fraction of those metals become phyto-available. The available/extractable fraction represents only a small percent of total zinc but can make up a larger percentage of total iron (**Figure 4.4**). Whether or not

mobilized a metal(/lloid) makes its way into the tissue of rice plants depends on if the metal remains in soil porewater or if it is washed off as the flood recedes.

4.5.3. Uptake into plants

The correlations between transect distances and both total metal and bioavailable fraction did not translate well to tissue concentrations of these metals (**Figure A4.3-4**). This finding is not totally surprising as root uptake of these metals is active rather than passive, so it is not only governed by a concentration of that element (Ma et al., 2008; Ramesh et al., 2003; Sakurai et al., 2015). Additionally, as mentioned above, freshly solubilized zinc and iron may move in with surface waters as the flood recedes leave the paddy system, not make their way into plant tissue.

We did find connections between rice crop cycles and zinc concentrations. We found that in mature plant leaves zinc was consistently lower in the early dry season following the flood compared with the late dry season which preceded that flood (**Figure 4.5**). The same trend was observed in one year of grain data (**Figure 4.5**). This finding seems consistent with the knowledge that long term flooding can decrease bioavailable zinc (Impa and Johnson-Beebout, 2012). Typically, farmers in this district prepare their fields while they are still wet, which is why we are forced to remove pressure sensors near the end of the flood (**Figure 4.7**). Therefore, most fields remain flooded from the onset of the flood until farmer dry their fields in preparation for harvest – up to 6 or 7 months. In the future, higher plant zinc with less flooding may end up being a slight benefit, as it is anticipated that flooding duration with decrease on fields at the periphery of the floodplain (Arias et al., 2014). However, this prediction contradicts farmers' assertation that a longer flood actually increases their yield. It is likely that flood sediments also contain useful macronutrients which rice plants need in higher amounts, offsetting the benefits of higher zinc (Muth et al. *in prep*).

We found a correlation between arsenic in rice plant leaves and rice plant grains (**Figure 4.6**). This correlation is consistent with other work in the field (Seyfferth et al., 2014); though not necessarily a given, as rice plants can prevent arsenic allocation to grains causing dissimilar leaf and grain arsenic allocation (Neumann et al., 2017; Song et al., 2014). There was no significant correlation between leaf and grain concentrations of iron and zinc, indicating that their allocation within the plant may be more tightly regulated. The correlation between arsenic in leaf and grain shows that more arsenic uptake by the plant can cause greater concentrations of arsenic in grain. Given that flood sediment seems to act as a source of arsenic onto the fields, there may be concerns about potential arsenic contamination. Grain arsenic concentrations did not correlate well with environmental variables (ex. transect distance, flood water height, pre- vs post-flood, etc.) so soil may already be a larger repository of arsenic than what is being added during the flood. Concerningly, several of our rice samples were above the level for potential arsenic genotoxicity implying that this under studied region of Cambodia warrants further study (Banerjee et al., 2013).

4.5.4. Future implications

The Tonle Sap is often called the "beating heart" of Cambodia, as it rhymical swells and contracts with water every wet season. Our work highlights a second layer of comparison: as oxygen rich blood travels from the lungs through the heart, so too does the Tonle Sap fill with the minerals and sediments dissolved in the flood water. Our work shows that flood sediments are filled with plant available minerals, some nutritious and some toxic. The majority of flood sediment comes from the Mekong River (Kummu et al., 2008), which is currently experiencing significant dam development. Arias et al. (2014) predicted that this damming may reduce flood sediment deposition by 56%, and so we would expect, and overall decrease in sediment

associated mineral deposition as well. This nutrient deposition is a likely reason why several farmers reported that greater flooding during the wet season increases their crop yield.

Dam development will also reduce the duration of flooding at the edges of the floodplain while increased the extent of the permanent lake (Arias et al., 2014). Most rice production is near the periphery of the floodplain, and so we would expect to see more soil drying in the future. Our results show there may be slight benefits to rice zinc concentrations with longer soil drying and less arsenic deposited through flood sediments. However, when taken to an extreme this can be highly detrimental to farmer water management. During 2019, Cambodia faced a severe drought that caused the government to instruct farmers not to plant a second dry season crop until rain arrived. The increasing likelihood of drought from climate change coupled with lower water availability from damming presents a serious threat to dry season rice production in the Tonle Sap in the future.

4.6. Future Works

The ideas in this chapter and their preparation for journal publication would benefit from several additional steps. Firstly, a more in-depth analysis of flood data collected by our pressure sensors would be useful to better understand flooding dynamics in this region. In this chapter, I have used maximum flooding depth as a crude approximation, but as seen in sensor 4 in **Figure 4.7**, maximum depth may not always help to approximate flooding duration. Still, we were able to observe correlations between flooding depth and the extractable fraction of zinc and iron, indicating that flooding characteristics will likely be a valuable addition.

Since surface soil arsenic concentrations were below XRF detection limits, we were unable to examine the relationship between total arsenic and the extractable fraction of arsenic with transect distance. We were only able to theorize that arsenic would behave similarly to the

other metals. Talks are currently under way with the UW Soil Analytics Lab to contract out the digestion of surface soils for total arsenic. The inclusion of this data will help balance our data set and make for a more robust manuscript.

Additionally, inclusion of selected elements of our Cambodian collaborators' plant yield data and soil characterization would also likely provide useful insights into our data and overall soil fertility. The additional soil data set is also in preparation for publication and is referenced as "Muth et al., *in prep*" in the text of this chapter. Her analysis includes surface soils collected during each of our four seasons (late dry 2018 – early dry 2020). Soils were measured for pH, electrical conductivity, available nitrogen, available phosphorous, and organic carbon. She also performed preliminary analyses of these variables on a small subset of flood sediment samples collected during the two wet-season floods in our experiment.

Finally, the successful completion of this project will involve relaying our findings back to local stakeholders, particularly the farmers in Kampong Thom who we worked with. This information delivery will be done in collaboration with our Cambodian partners. We hope to carry out this process will the next year.

4.7. References

Alloway BJ. Zinc in Soils and Crop Nutrition. International Zinc Association and International Ferilizer Associaiton, Brussels, Belgium, 2008.

Arias ME, Cochrane TA, Kummu M, Lauri H, Holtgrieve GW, Koponen J, et al. Impacts of hydropower and climate change on drivers of ecological productivity of Southeast Asia's most important wetland. Ecological Modelling 2014; 272: 252-263.

Aung MS, Masuda H. How Does Rice Defend Against Excess Iron?: Physiological and Molecular Mechanisms. Frontiers in Plant Science 2020; 11.

Awasthi S, Chauhan R, Srivastava S, Tripathi RD. The Journey of Arsenic from Soil to Grain in Rice. Frontiers in Plant Science 2017; 8.

Bailey RL, West Jr KP, Black RE. The Epidemiology of Global Micronutrient Deficiencies. Annals of Nutrition and Metabolism 2015; 66(suppl 2): 22-33.

Banerjee M, Banerjee N, Bhattacharjee P, Mondal D, Lythgoe PR, Martinez M, et al. High arsenic in rice is associated with elevated genotoxic effects in humans. Sci Rep 2013; 3: 2195.

Chen H, Teng Y, Li J, Wu J, Wang J. Source apportionment of trace metals in river sediments: A comparison of three methods. Environmental Pollution 2016; 211: 28-37.

Cummings DE, Caccavo F, Fendorf S, Rosenzweig RF. Arsenic Mobilization by the Dissimilatory Fe(III)-Reducing Bacterium Shewanella alga BrY. Environ Sci Technol 1999; 33: 723-729.

Du Laing G, Rinklebe J, Vandecasteele B, Meers E, Tack FM. Trace metal behaviour in estuarine and riverine floodplain soils and sediments: a review. Science of the total environment 2009; 407: 3972-3985.

Food and Agriculture Organization. FAOStat. 2019. United Nations, Rome, 2020.

Gharibzahedi SMT, Jafari SM. The importance of minerals in human nutrition: Bioavailability, food fortification, processing effects and nanoencapsulation. Trends in Food Science & Technology 2017; 62: 119-132.

Gilbert PJ, Polya DA, Cooke DA. Arsenic hazard in Cambodian rice from a market-based survey with a case study of Preak Russey village, Kandal Province. Environmental geochemistry and health 2015; 37: 757-766.

GRiSP. Rice Almanac. Los Baños (Philippines): International Rice Research Institute, 2013.

Impa S, Johnson-Beebout S. Mitigating zinc deficiency and achieving high grain Zn in rice through integration of soil chemistry and plant physiology research. Plant and Soil 2012; 361: 3-41.

Johnston R, Conkle J. Micronutrient Deficiencies and Interventions in Cambodia: Information for Improved Programming. USAID, 2008.

Kelly TJ, Hamilton E, Watts MJ, Ponting J, Sizmur T. The Effect of Flooding and Drainage Duration on the Release of Trace Elements from Floodplain Soils. Environ Toxicol Chem 2020; 39: 2124-2135.

Kummu M, Penny D, Sarkkula J, Koponen J. Sediment: Curse or Blessing for Tonle Sap Lake? AMBIO: A Journal of the Human Environment 2008; 37: 158-163.

Kummu M, Sarkkula J, Koponen J, Nikula J. Ecosystem Management of the Tonle Sap Lake: An Integrated Modelling Approach. International Journal of Water Resources Development 2006; 22: 497-519.

Lynch JP, St.Clair SB. Mineral stress: the missing link in understanding how global climate change will affect plants in real world soils. Field Crops Research 2004; 90: 101-115.

Ma JF, Yamaji N, Mitani N, Xu XY, Su YH, McGrath SP, et al. Transporters of arsenite in rice and their role in arsenic accumulation in rice grain. Proc Natl Acad Sci 2008; 105: 9931-5.

Meharg AA, Zhao F-J. Arsenic & Rice. Dordrecht: Dordrecht: Springer Netherlands, 2012.

Mehra O, Jackson M. Iron Oxide Removal from Soils and Clays by a Dithionite-Citrate System Buffered with Sodium Bicarbonate. Clays and Clay Minerals 1958; 7: 317-327.

Ministry of Agriculture F, and Fisheries, . MAFF Annual Report 2016-2017. In: MAFF, editor, Phnom Penh, Cambodia, 2017.

MRC. Overview of the hydrology of the Mekong Basin. Mekong River Comission, Vientiane, Laos, 2005.

MRC. Impacts on the Tonle Sap Ecosystem : Assessment of Basin-wide Development Scenarios. Mekong River Commission, Vientiane, Lao, 2011.

Murphy T, Phan K, Yumvihoze E, Irvine K, Wilson K, Lean D, et al. Effects of Arsenic, Iron and Fertilizers in Soil on Rice in Cambodia. J Health Pollut 2018a; 8: 180910.

Murphy T, Phan K, Yumvihoze E, Irvine K, Wilson K, Lean D, et al. Groundwater irrigation and arsenic speciation in rice in Cambodia. Journal of Health and Pollution 2018b; 8.

Nesbitt HJ. Rice production in Cambodia. Manila: International Rice Research Institute, 1997.

Neumann RB, Seyfferth AL, Teshera-Levye J, Ellingson J. Soil Warming Increases Arsenic Availability in the Rice Rhizosphere. Agricultural & Environmental Letters 2017; 2.

Open Development Mekong. Greater Mekong Subregion hydropower dams. 2020. Open Development Initiative, 2016.

Pan Y, Bonten LTC, Koopmans GF, Song J, Luo Y, Temminghoff EJM, et al. Solubility of trace metals in two contaminated paddy soils exposed to alternating flooding and drainage. Geoderma 2016; 261: 59-69.

Pasricha S-R, Tye-Din J, Muckenthaler MU, Swinkels DW. Iron deficiency. The Lancet 2021; 397: 233-248.

Quicksall AN, Bostick BC, Sampson ML. Linking organic matter deposition and iron mineral transformations to groundwater arsenic levels in the Mekong delta, Cambodia. Applied Geochemistry 2008; 23: 3088-3098.

Ramesh SA, Shin R, Eide DJ, Schachtman DP. Differential Metal Selectivity and Gene Expression of Two Zinc Transporters from Rice. Plant Physiology 2003; 133: 126-134.

Reed S, Martens D. Copper and zinc. Methods of Soil Analysis: Part 3 Chemical Methods 1996; 5: 703-722.

Roohani N, Hurrell R, Kelishadi R, Schulin R. Zinc and its importance for human health: An integrative review. Journal of research in medical sciences : the official journal of Isfahan University of Medical Sciences 2013; 18: 144-157.

Sakurai G, Satake A, Yamaji N, Mitani-Ueno N, Yokozawa M, Feugier FG, et al. In silico simulation modeling reveals the importance of the Casparian strip for efficient silicon uptake in rice roots. Plant Cell Physiol 2015; 56: 631-9.

Salomons W, De Rooij N, Kerdijk H, Bril J. Sediments as a source for contaminants? Hydrobiologia 1987; 149: 13-30.

Seyfferth AL, McCurdy S, Schaefer MV, Fendorf S. Arsenic Concentrations in Paddy Soil and Rice and Health Implications for Major Rice-Growing Regions of Cambodia. Environmental Science & Technology 2014; 48: 4699-4706.

Simmler M, Bommer J, Frischknecht S, Christl I, Kotsev T, Kretzschmar R. Reductive solubilization of arsenic in a mining-impacted river floodplain: Influence of soil properties and temperature. Environ Pollut 2017; 231: 722-731.

Song WY, Yamaki T, Yamaji N, Ko D, Jung KH, Fujii-Kashino M, et al. A rice ABC transporter, OsABCC1, reduces arsenic accumulation in the grain. Proc Natl Acad Sci 2014; 111: 15699-704.

Stuckey Jason W, Schaefer Michael V, Kocar Benjamin D, Benner Shawn G, Fendorf S. Arsenic release metabolically limited to permanently water-saturated soil in Mekong Delta. Nature Geoscience 2016; 9: 70-76.

Trivedi P, Dyer JA, Sparks DL, Pandya K. Mechanistic and thermodynamic interpretations of zinc sorption onto ferrihydrite. Journal of Colloid and Interface Science 2004; 270: 77-85.

Tufano KJ, Fendorf S. Confounding Impacts of Iron Reduction on Arsenic Retention. Environ Sci Technol 2008; 42: 4777-4783.

Uk S, Yoshimura C, Siev S, Try S, Yang H, Oeurng C, et al. Tonle Sap Lake: Current status and important research directions for environmental management. Lakes & Reservoirs: Science, Policy and Management for Sustainable Use 2018; 23: 177-189.

United States Department of Agriculture. Production, Supply and Distribution Online. 2019, 2020.

Wang H-S, Sthiannopkao S, Chen Z-J, Man Y-B, Du J, Xing G-H, et al. Arsenic concentration in rice, fish, meat and vegetables in Cambodia: a preliminary risk assessment. Environmental geochemistry and health 2013; 35: 745-755.

Xue S, Jiang X, Wu C, Hartley W, Qian Z, Luo X, et al. Microbial driven iron reduction affects arsenic transformation and transportation in soil-rice system. Environ Pollut 2020; 260.

Zarfl C, Lumsdon AE, Berlekamp J, Tydecks L, Tockner K. A global boom in hydropower dam construction. Aquatic Sciences 2014; 77: 161-170.

Zeng F, Ali S, Zhang H, Ouyang Y, Qiu B, Wu F, et al. The influence of pH and organic matter content in paddy soil on heavy metal availability and their uptake by rice plants. Environmental Pollution 2011; 159: 84-91.

5. Chapter 5: Conclusions

5.1. Major Findings and Implications

Rice is an important dietary source to billions of people, especially in many low-income countries (GRiSP, 2013). Many of these same communities suffer from underlying micronutrient deficiencies and have access to few alternative nutrient dense foods (Ritchie and Roser, 2017). Communities which are heavily reliant on rice may also be exposed to heightened levels of arsenic since rice accumulates much more arsenic than other cereal crops (Williams et al., 2007). These underlying dietary burdens may be exasperated in the future by altered environmental conditions. During my PhD, I worked to link rice mineral nutrition quality to key environmental changes, namely temperature and flooding.

Climate change represents a serious threat to multiple facets of global food security. One such threat is through increased growing temperatures, which can increase rice grain arsenic. I explore this problem in depth in Chapters 2 and 3 of this work. In Chapter 2, we observed an increasing trend between temperature and both total grain arsenic and grain inorganic arsenic, in our rice plants (**Figure 2.2A**, **Figure A1.2A** in Appendix 1). This result was an important finding as previous studies had been inconsistent with regard to the ability of increased temperature to translate into higher arsenic in grain tissue. Neumann et al. (2017) was unable to track elevated temperature to increased arsenic concentration in grain using a Bangladeshi rice variety; however, Muehe et al. (2019) found an increase in grain arsenic under higher temperature conditions using the M206 variety (same variety as used in our experiments). Additional research comparing different rice cultivars may be useful to further explore this discrepancy or identify climate-smart low arsenic rice.

Our work highlights that higher temperatures can increase human exposure to inorganic arsenic. Relevant guidelines related to dietary arsenic exposure are [1] a 200 mg kg^{-1} inorganic arsenic limit for polished white rice recommended by the FAO/WHO (Codex Alimentarius Commission, 2014) and [2] a 100 mg kg^{-1} limit for inorganic arsenic limit in all rice used in infant food (FDA, 2016). Our experimental set up is modelled after lower arsenic systems in Northern California. Still, in Chapter 2 we show that raising the average growth temperature by roughly 5°C increased total and inorganic arsenic levels well beyond the safety standard used for infants – demonstrating that rice systems that have historically been considered of low concern may become less safe in a warmer future.

In Chapter 3, I delve deeper into the intersection between rice arsenic and temperature exposure, investigating specific phenological stages of plant development. We found that rice grain arsenic concentrations were significantly higher in plants which had been exposed to a heat spike during the ripening stage compared with plants in a control, no heat spike treatment. Mean and median rice grain arsenic concentrations were higher in plants exposed to a vegetative heat spike compared with plants which did not experience a heat spike, but the difference between these two groups was not statistically significant. We used lower temperature gradient in Chapter 3 relative to Chapter 2, and our soils contained relatively low, background concentrations of arsenic (Chang et al., 2004). Therefore, all grain arsenic concentrations were below WHO and FDA dietary limits. Other research which used higher arsenic soils and post-heading heat exposure observed an increase in rice grain arsenic concentrations to a much higher extent (Dhar et al., 2020). Their results show that that native soil arsenic concentration is still an important factor in determining the magnitude of temperature-fueled mobilization. Yet, even in a low

arsenic systems we were able to double the average concentration of rice arsenic with a 20-day heat spike of 4°C during the ripening period.

Several studies examining temperature-induced increases in rice arsenic limit their analysis to rice reproductive tissues (Arao et al., 2018; Dhar et al., 2020; Muehe et al., 2019), rather than delving deeper into the driving causes of that increase. In both Chapters 2 and 3, I take a more mechanistic approach to understand this problem, in hopes of providing useful information for future mitigation. In both experiments mobilization of arsenic from soils into porewater was an important explanatory variable. Our mass balance calculation in Chapter 1 highlighted that this temperature-driven mobilization of arsenic was a key component of increasing arsenic delivery to roots and can therefore increase arsenic accumulation in above-ground tissue (**Figure 2.7**). Temperature driven increases in transpiration were merely a secondary factor, only becoming important when viewed alongside mobilization in what we termed the "combined effect" (more water with more dissolved arsenic). In Chapter 3 we also observed a relationship between mobilization and arsenic accumulation. Plants which experienced a vegetative stage heat spike had increased concentrations of arsenic in both porewater and in vegetative tissue immediately following the heat spike, but the magnitude of both increases were small and did not persist over time. Alternatively, plants which experienced a heat spike during the ripening stage had a larger increase in arsenic in porewater and various plant tissue types. The paralleled trends between transpiration and tissue concentrations reaffirms the connection between these two variables.

Another mechanistic explanation we investigate is total arsenic content and allocation. Prior to our experiment in Chapter 2, it was unclear whether increases in tissue arsenic were driven by temperature stressing causing reductions in plant biomass producing a "bio-

concentrating" effect. In Chapter 2, total arsenic content (concentration × biomass) in aboveground tissue was greater under elevated temperature, indicating that there was actually an increase in the actual mass of arsenic being taken up (**Figure 2.3A**). This result highlights that increased arsenic concentrations shown were not simply result of reduced plant biomass under heat stress. In Chapter 3, we also observed differences in arsenic content which helped to explain why there was a larger rice arsenic response in plants with a heat spike in the ripening stage than in plants which had a heat spike in the vegetative stage. Plants which experienced a heat spike in the vegetative stage did have a detectible increase in arsenic concentrations relative to plants which did not experience a heat spike, however the actual increase in arsenic content was small due to the low biomass of the plants during the vegetative stage (**Figure 3.4A**). Therefore, it was less able to create a detectible change in mature plants which accumulate much higher arsenic content throughout their development. Alternatively, plants which experienced a heat spike during the ripening stage had a large increase in total arsenic (**Figure 3.4C**). The high total arsenic content shows that the actual mass of arsenic which made its way into plant tissue was much larger and therefore able to create a greater and more lasting response.

Interestingly, we saw different results regarding the impact of temperature on arsenic allocation. In Chapter 2 there was no differences in aboveground arsenic allocation between temperature treatments. However, in Chapter 3 there were multiple differences in allocation between treatment groups, even in the treatment which was exposed to continuously elevated temperature similar to Chapter 2. It seems that there is still room for more study in this space. The interactions between temperature and arsenic allocation have important implications for breeding climate smart, low-arsenic rice. The cellar transporter which sequesters arsenic in vacuoles, thereby preventing its loading into rice grain, has already been identified in rice (Song

et al., 2014). Increasing cellular production of this transporter may help preventing the additional mass of arsenic taken up at elevated temperatures from reaching grains that are destined for human consumption.

In Chapter 4, I widen the scope of my work to also include mineral nutrients, specifically zinc and iron. I also move my investigations into a real-world context, rather than controlled growth chamber setting. Total metal concentrations in our surface soils strongly correlated with transect locations, where sites closer to the lake had higher concentrations of zinc, iron, and cobalt, among others (**Figure 4.2**). However, the fraction of extractable zinc and iron showed the opposite trend, with sites closer to the lake having a lower fraction of available metals (**Figure 4.4**). The fact that both of these metals responded in a similar way to flooding (though with different magnitudes) indicates that they were both responding to the same driving environmental variable. It is reasonable that the their mirrored response may be due to release of zinc associated with iron minerals when solid Fe(III) is solubilized during flooding.

Mineral bioavailability is complex and often challenging to predict due to the myriad of soil and climatic factors involved (Fageria, 2014). Efforts to predict the bioavailable of different nutrients in floodplains have had mixed success because of the competing processes involved. For example, anaerobic conditions can cause both the reductive dissolution of redox sensitive mineral oxides and the formation of solid metal sulfides (Du Laing et al., 2009). For this reason, the strong relationships we observed between the fraction of extractable zinc and iron and both transect distance and max flooding depth is an exciting and, to my knowledge, novel finding (**Figure 4.4** and **4.8**). These relationships along with rapid, simple XRF measures of total metal concentration, might to be used to help estimate the concentration of bioavailable metals on seasonally flooded lands.

Many of the Cambodian farmers who participated in our study are reliant on their rice crops in two distinct ways: economically and nutritionally. Farmers are influenced by the soil nutrition of their fields as it related to yield and their income. Additionally, several of the farmers we surveyed also report saving some of their rice for their family to eat throughout the year. Seasonal flooding and sediment deposition may be an important factor to both yield and nutrition. We found that flood sediment might act as a natural fertilizer as it is high in mineral micronutrients, (**Figure 4.3**) possibly explaining why farmers observed that large seasonal floods increased the yield of the subsequent rice crop. However, flood sediment might also act as a source of arsenic on rice fields as well (**Figure 4.3**), increasing their dietary exposure to arsenic. Additionally, we found that the first dry season rice crop (early dry) had lower levels of leaf and sometimes grain tissue zinc (**Figure 4.5**). Given that zinc deficiency is widespread in Cambodia (Anderson et al., 2008), farmers may consider saving their second dry season crop as well as incorporating the zinc rich foods to which they have access (ex. fish, eggs, seeds, etc.).

The Mekong River, which feeds into the Tonle Sap during the wet season, has seen a rapid increase in dam development (Open Development Mekong, 2016; Zarfl et al., 2014). This development will reduce the duration of flooding at the edges of the floodplain and reduce flood sediment influxes (Arias et al., 2014). Most rice production is near the periphery of the floodplain, and so we would expect to see more soil drying in the future along with less wet season sediment deposition. Our results show there may be slight benefits to rice zinc concentrations with longer soil drying and less arsenic deposited through flood sediments. However, there may also be less delivery of macro- and micronutrients on fields. Anecdotally, farmers reported that larger or longer floods in the previous wet season increased yield of the following rice crop. These large floods will likely diminish, and farmer yields may suffer. When

taken to an extreme less flooding can be highly detrimental to farmer water management, disrupt planting cycles, or even halt rice production. The lower water availability from damming coupled with the increasing frequencies of drought due to climate change, present a serious threat to dry season rice production in the Tonle Sap in the future.

5.2. References

Anderson VP, Jack S, Monchy D, Hem N, Hok P, Bailey KB, et al. Co-existing micronutrient deficiencies among stunted Cambodian infants and toddlers. Asia Pacific journal of clinical nutrition 2008; 17.

Arao T, Makino T, Kawasaki A, Akahane I, Kiho N. Effect of air temperature after heading of rice on the arsenic concentration of grain. Soil Science and Plant Nutrition 2018; 64: 433-437.

Arias ME, Cochrane TA, Kummu M, Lauri H, Holtgrieve GW, Koponen J, et al. Impacts of hydropower and climate change on drivers of ecological productivity of Southeast Asia's most important wetland. Ecological Modelling 2014; 272: 252-263.

Chang AC, Page AL, Krage NJ. Role of fertilizer and micronutrient applications on Arsenic, Cadmium, and lead accumulation in California cropland soils. California Department of Food and Agriculture 2004.

Codex Alimentarius Commission. Report of the Either Session of the Codex Committee on Contaminants in Foods. 37th Session. Joint FAO/WHO Food Standards Programme, Geneva, Switzerland, 2014.

Dhar P, Kobayashi K, Ujiie K, Adachi F, Kasuga J, Akahane I, et al. The Increase in the Arsenic Concentration in Brown Rice Due to High Temperature during the Ripening Period and Its Reduction by Silicate Material Treatment. Agriculture 2020; 10.

Du Laing G, Rinklebe J, Vandecasteele B, Meers E, Tack FM. Trace metal behaviour in estuarine and riverine floodplain soils and sediments: a review. Science of the total environment 2009; 407: 3972-3985.

Fageria NK. Mineral Nutrition of Rice: CRC Press, 2014.

Food and Drug Administration [FDA]. Inorganic Arsenic in Rice Cereals for Infants: Action Level Guidance for Industry - Draft Guidance. In: Services USDoHaH, editor. Center for Food Safety and Applied Nutrition, Rockville, MD, USA, 2016.

GRiSP. Rice Almanac. Los Baños (Philippines): International Rice Research Institute, 2013.

Muehe EM, Wang T, Kerl CF, Planer-Friedrich B, Fendorf S. Rice production threatened by coupled stresses of climate and soil arsenic. Nat Commun 2019; 10: 4985.

Neumann RB, Seyfferth AL, Teshera-Levye J, Ellingson J. Soil Warming Increases Arsenic Availability in the Rice Rhizosphere. Agricultural & Environmental Letters 2017; 2.

Open Development Mekong. Greater Mekong Subregion hydropower dams. 2020. Open Development Initiative, 2016.

Ritchie H, Roser M. Micronutrient deficiency. Our World in data 2017.

Song WY, Yamaki T, Yamaji N, Ko D, Jung KH, Fujii-Kashino M, et al. A rice ABC transporter, OsABCC1, reduces arsenic accumulation in the grain. Proc Natl Acad Sci 2014; 111: 15699-704.

Williams PN, Villada A, Deacon C, Raab A, Figuerola J, Green AJ, et al. Greatly Enhanced Arsenic Shoot Assimilation in Rice Leads to Elevated Grain Levels Compared to Wheat and Barley. Environmental Science & Technology 2007; 41: 6854-6859.

Zarfl C, Lumsdon AE, Berlekamp J, Tydecks L, Tockner K. A global boom in hydropower dam construction. Aquatic Sciences 2014; 77: 161-170.

A1. Appendix 1: Chapter 2 Supplement

A1.1. Supplemental Methods

A1.1.1. Root DCB Extraction

In a water bath, we added 24 mL of 0.3 M sodium citrate and 3 mL of 1.0 M $NaHCO_3$ to each fragment and allowed solution temperature to rise to 75-80 °C. Then we added three 0.6 g additions of sodium dithionite, 5 minutes apart. We decanted, syringe-filtered (0.2 μm) and acidified extractant to 2% (v/v) with ultra-trace metal grade HNO_3. Finally, we rinsed roots twice with 25 mL of Milli-Q water in a tumbler at 60 rpm for 50 min. We decanted, filtered, and acidified washes to 2% (v/v) with ultra-trace metal grade HNO_3.

A1.1.2. Arsenic Speciation Extraction

We added 10 mL of 2% HNO_3 to ~200 mg (mass known exactly) of ground brown rice samples. Using a microwave digester (Anton Parr), we heated solution at 95 °C for 10 min to remove stable arsenic species. We syringe-filtered (0.2 μm) samples and diluted them 1:1 with Milli-Q water before running on HPLC-ICP-MS.

A1.1.3. Soil Sequential Extractions

Phosphate Extraction: We rinsed ~0.25 g of ground soil (mass known exactly) with 25 mL of 1M $NaH_2PO_4^-$ at pH ~5 and tumbled for 16 h at 60 rpm. We then centrifuged samples at 4500 rpm for 45 min, syringe-filtered (0.2 μm) and acidified samples to 2% HNO_3 (v/v). We repeated $NaH_2PO_4^-$ extraction again and then performed a Milli-Q rinse step for 30 min, which we then centrifuged, filtered, and acidified. We found adding a very small amount of salt to the Milli-Q rinse solution greatly assisted in filtration and helped to settle colloidal material which formed in water wash step. We switched to a 10 mM MgCl wash and did not detect a directional change in arsenic content removed during either sequential extraction step.

CBD Extraction: In a water bath, we added 0.5 mL of 1.0 M $NaHCO_3$ and 4 mL of 0.3 M sodium citrate to soil samples. Solution temperature increased to 75-80 °C and then we added two additions of 0.5 g of sodium dithionate, 5 min apart. As in the previous step, we centrifuged, decanted, filtered, and acidified extractant. Lastly, we rinsed soils twice with 25 mL of Milli-Q water or 10 mM MgCl.

A1.2. Supplemental Table

Table A1.1. *Growth conditions of each temperature treatment. Values in the table are time integrated averages with associated standard deviation. We measured air temperature and relative humidity using RH/Temperature Sensor (Onset) and soil temperature using a TidbiT Temperature Logger (Onset) buried at a 10cm depth in 4 of 8 pots. We measured photosynthetically active radiation, PAR, using Photosynthetic Light Smart Sensors (Onset), placed flag leaf level.*

	Night Temp, °C	**Day Temp,** °C	**Soil Temp,** °C	**Relative Humidity,** %	**PAR,** μmol m^{-2} s^{-1}
Low Temp (LT)	22.6 ± 2.0	25.4 ± 1.9	23.1 ± 2.7	84 ± 14	291 ± 46
Medium Low Temp (MLT)	25.8 ± 2.0	27.9 ± 1.9	26.3 ± 2.5	85 ± 7	269 ± 43
Medium High Temp (MHT)	28.9 ± 1.8	30.5 ± 1.7	29.4 ± 2.3	85 ± 6	296 ± 45
High Temp (HT)	31.0 ± 1.9	32.9 ± 1.8	32.1 ± 2.5	84 ± 6	307 ± 65

A1.3. Supplemental Figures

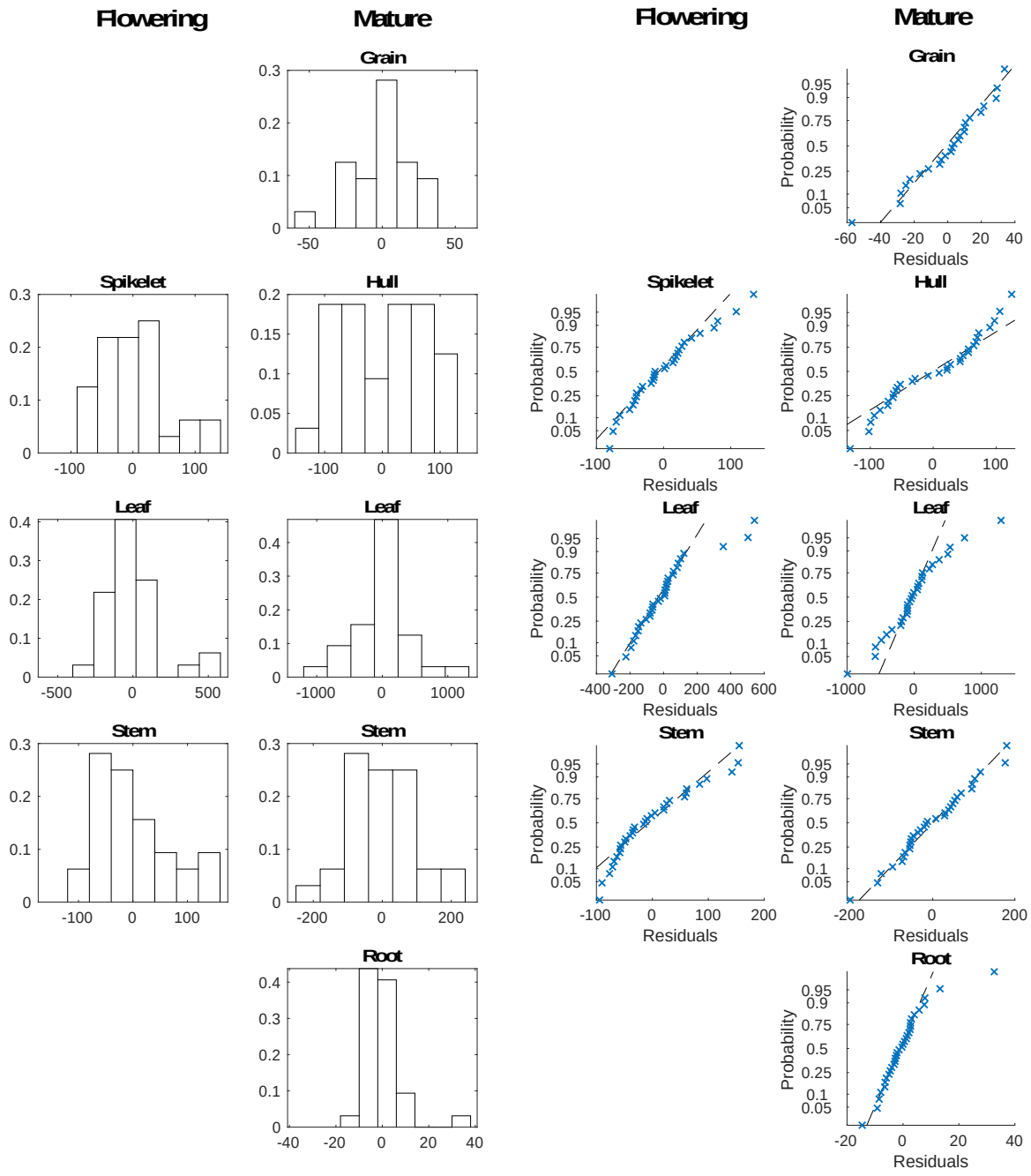

Figure A1.1. *Residuals of linear regression between tissue concentration of arsenic and average daytime air temperature (Figure 2.2). Histograms demonstrate residual frequency, where the idealized shape is a bell curve indicating variance in normally distributed. Q-Q plots depicts residuals and their statistical probability in a normal distribution. Based on these plots, we concluded that grain arsenic and stems at maturity had a normal and linear relationship with temperature. We used a non-parametric Spearman rank correlation to describe trends in other tissues.*

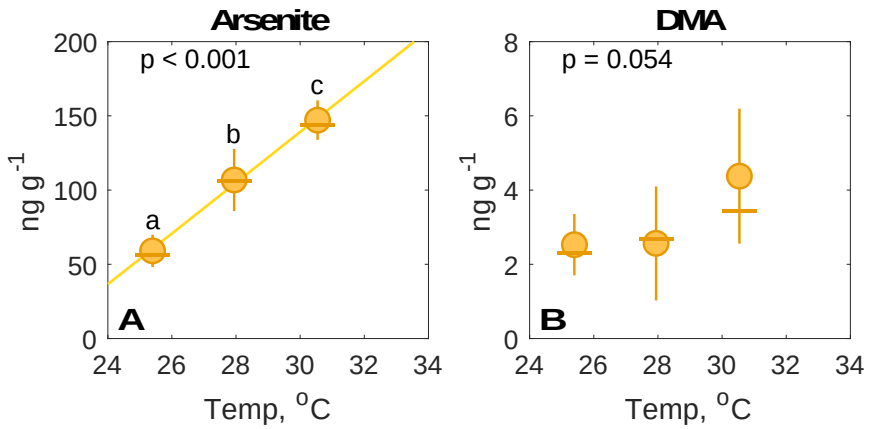

Figure A1.2. *Arsenic speciation in rice grains analyzed by 2% HNO_3 extraction and quantified using HPLC-ICP-MS. Mean (circle, •) and median (dash, –) concentrations of arsenic species with associated interquartile ranges (error bars) as a function of average daytime growing temperature during the experiment. No grain samples were collected from highest temperature treatment (HT) due to severe heat stress which prevented seed set. Statistical differences were determined by ANOVA (α = 0.05) on log_{10} transformed values followed by Tukey-Kramer post hoc.*

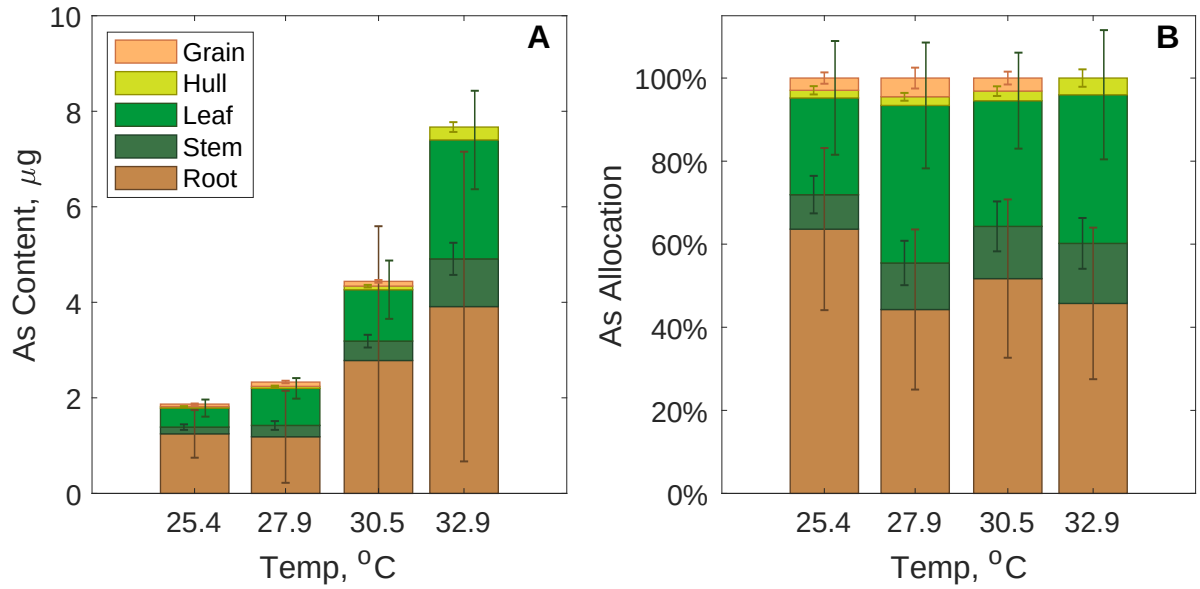

Figure A1.3. *Whole plant arsenic accumulation and allocation. (A) Average total arsenic content in each tissue type in different temperature treatments, calculated as tissue concentration of arsenic multiplied by tissue mass. Error bars show standard deviation from mean. (B) Percentage of total arsenic content present in each tissue compartment.*

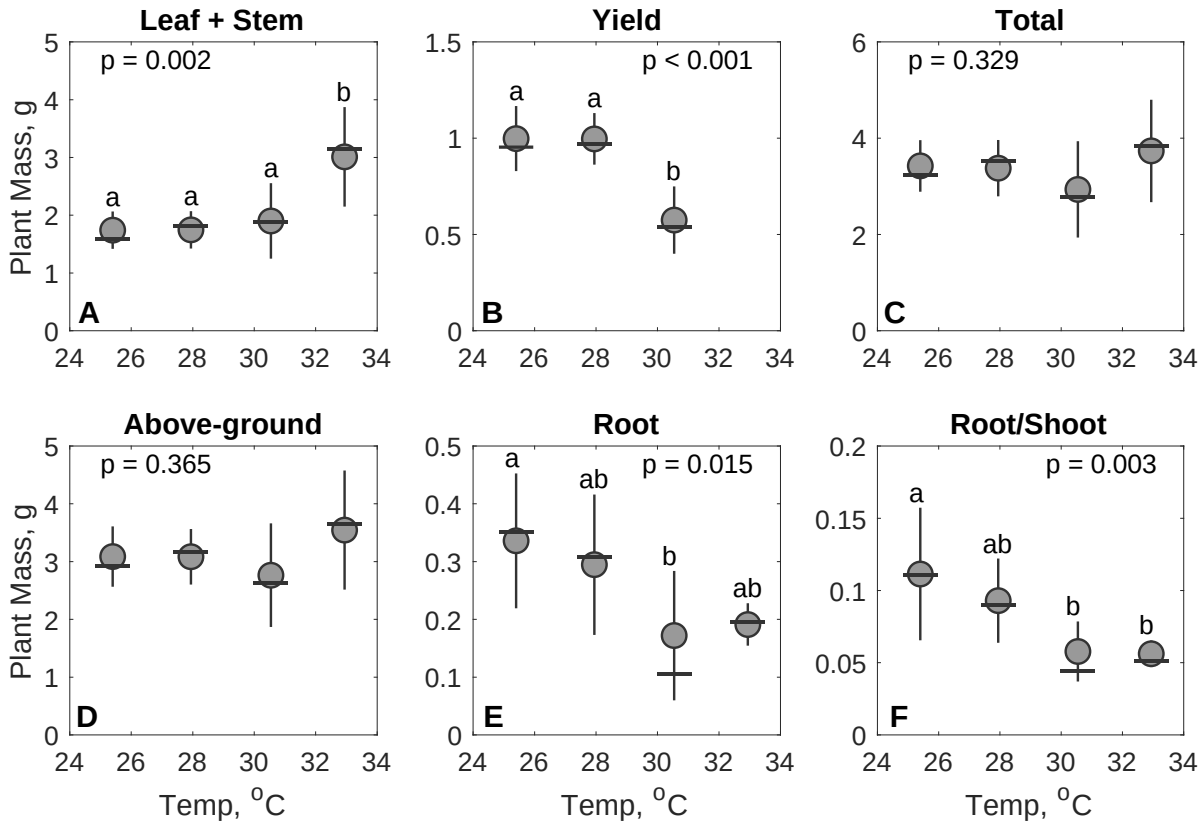

Figure A1.4. *Biomass of plant samples at maturity on a per plant basis. During the final harvest, two plants were removed, dried, and aggregated into a single pot sample. The total combined biomass was divided by two to give the pot average biomass on a per plant basis. Statistical differences were determined by ANOVA ($\alpha = 0.05$) on log_{10} transformed values followed by Tukey-Kramer post hoc. There was a statistically significant increasing trend in straw tissue (leaf + stem weight) and statistically significant decreasing trend in panicle weight, root weight, and root to shoot ratio. Yield is mass of brown rice per plant, but there was no grain produced in the highest temperature condition – resulting in the strong decreasing trend. There was no statistical trend in total above-ground biomass (straw + panicle weight).*

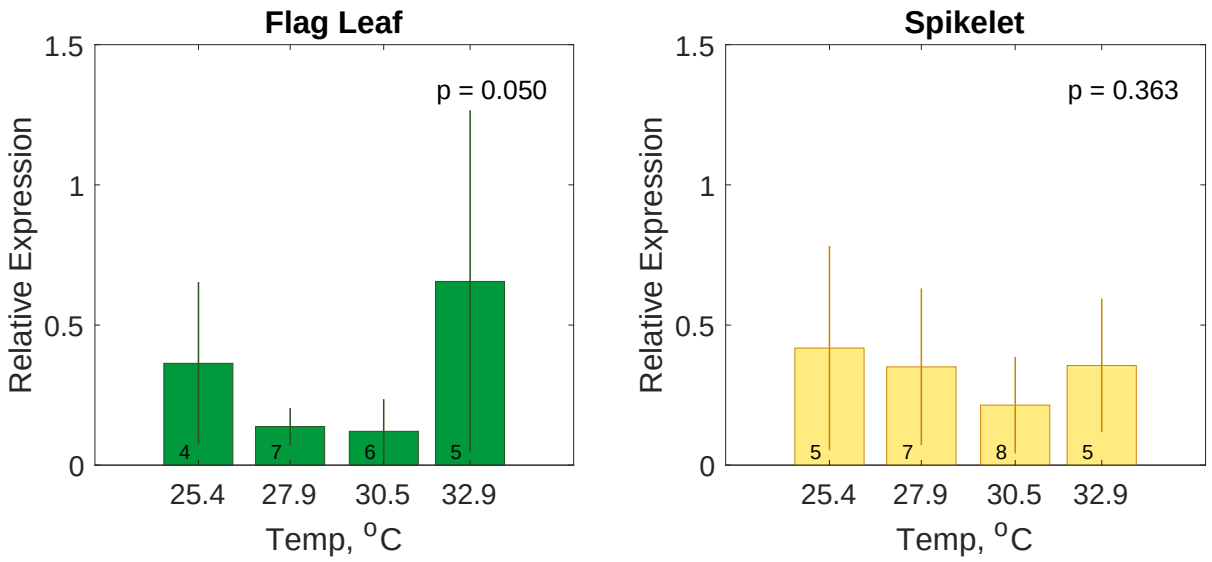

Figure A1.5. *Relative expression of OsABCC1 normalized with HisH3 expression measured by quantitative reverse transcription PCR (RT-qPCR). Numbers above each bar indicated the respective number of biological replicates within each treatment. Statistical differences were determined by ANOVA ($\alpha = 0.05$) on log_{10} transformed values followed by Tukey-Kramer post hoc. We found no clear statistical trend and quite high variance, possibly due to low expression in our low arsenic system.*

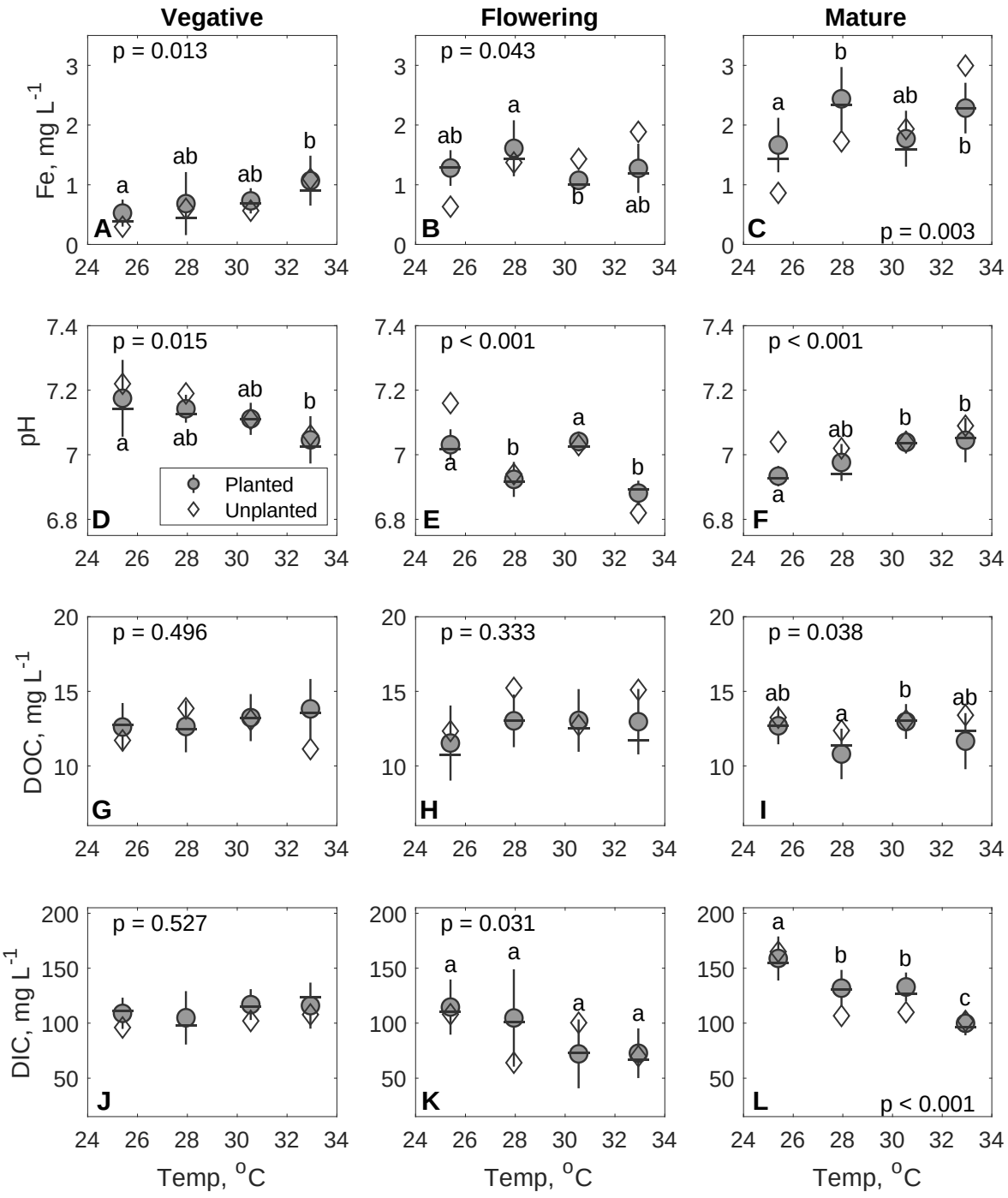

Figure A1.6. *Additional porewater measurements: pH, dissolved organic carbon (DOC), and dissolved inorganic carbon (DIC). Planted pot mean (circle, •) and median (dash, –) values are provided with associated interquartile ranges (error bars). Diamond (◊) depicts unplanted pot value. DOC/DIC analysis preformed with front end HPLC (Dionex UltiMate 3000) connected to Sievers TOC 900 (General Electric). Statistical differences were determined by ANOVA ($\alpha = 0.05$) on log_{10} transformed values followed by Tukey-Kramer post hoc.*

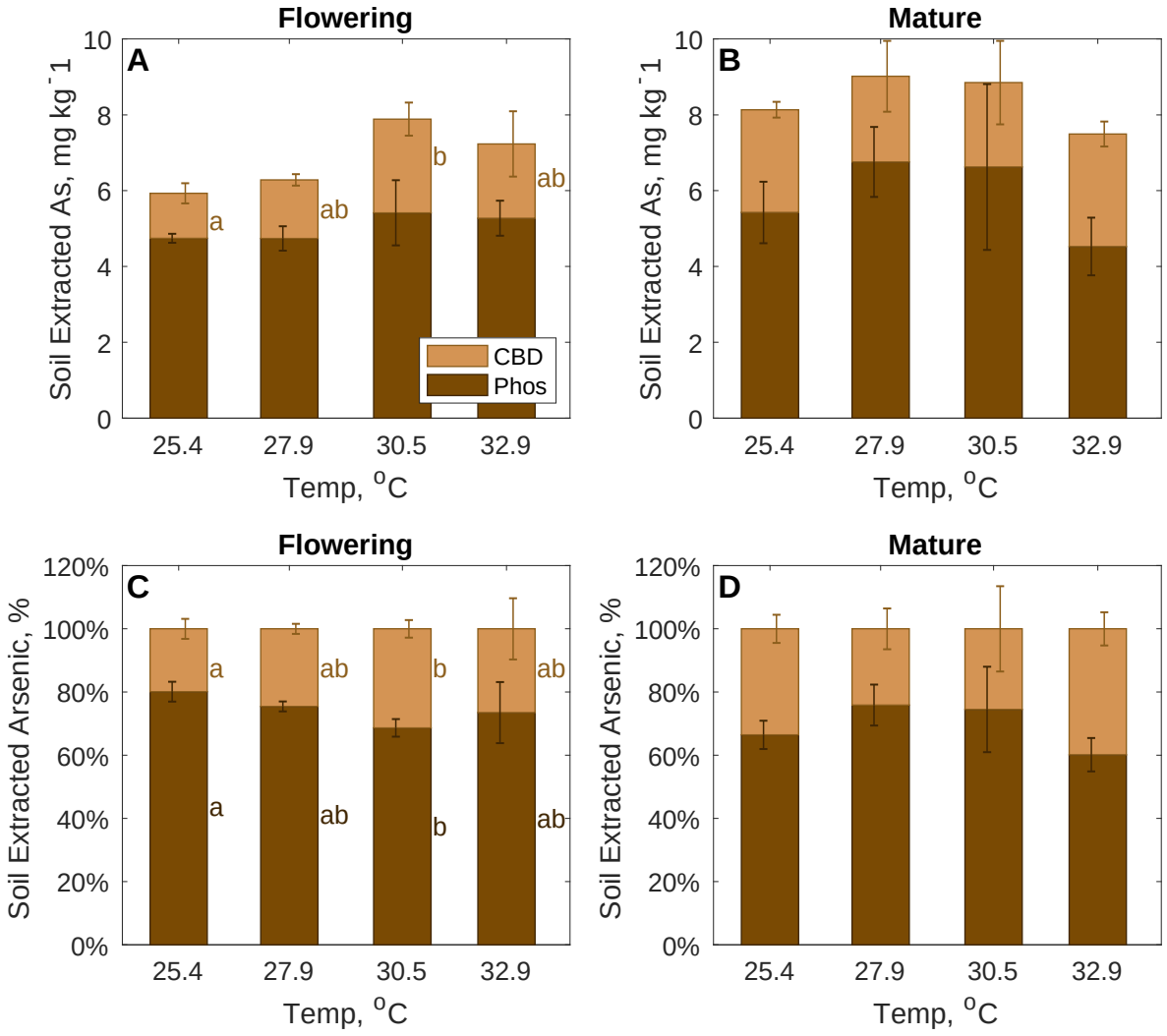

Figure A1.7. *Sequential extraction of soil collected from experimental pots at flowering and maturity time points. Ion-exchangeable arsenic (As) was determined by phosphate (Phos) extraction. Arsenic associated with iron reducible minerals was removed using a dithionite-citrate-bicarbonate (CBD) extraction. Statistical differences were determined by ANOVA ($\alpha = 0.05$) on log_{10} transformed values followed by Tukey-Kramer post hoc. A and B show the concentrations of arsenic removed in both extraction steps. C and D show the percent of extracted arsenic (Phos + CBD) removed in each step.*

A2. Appendix 2: Chapter 3 Supplement

A2.1. Supplemental Tables

Table A2.1. *Growing conditions of each treatment during the experiment. Averages reported with associated standard deviation in parenthesis. Air temperature and relative humidity were measured using Onset's Smart Sensors, placed at the leaf level. PAR was measured using PAR Smart Sensors, Onset, also placed at leaf level.*

Measurement	**NH**	**VH**	**RH**	**CH**
Day Temp, °C	25.8 (1.3)	25.9 (1.4)	26.0 (1.3)	30.1 (1.2)
Night Temp, °C	22.1 (1.0)	22.0 (1.2)	23.1 (1.1)	27.2 (1.9)
PAR, µmol m^{-2} s^{-1}	224 (46)	240 (62)	234 (59)	244 (47)
Relative Humidity, %	87.2 (4.1)	83.7 (6.3)	84.1 (5.6)	82.5 (5.3)
Heat Spike: Day Temp, °C	-	28.8 (1.6)	30.2 (0.7)	-
Heat Spike: Night Temp, °C	-	25.9 (1.8)	26.3 (1.0)	-

Table A2.2. *Key setup and analysis dates throughout the experiment.*

Event	**NH**	**VH**	**RH**	**CH**
Set-up:				
Germinating	12/16/17	12/16/17	12/16/17	12/16/17
Transplanting	1/4/18	1/4/18	1/4/18	1/4/18
Water + Plant No.	1/22/18	1/22/18	1/22/18	1/22/18
Porewater Sampling:				
Early Veg.	2/8/18	2/8/18	2/8/18	2/8/18
Late Veg.	2/24/18	2/26/18	2/24/18	2/15/18
Early Ripen.	4/11/18	4/11/18	4/9/18	3/28/18
Late Ripen.			5/1/18	4/23/18
Mature	5/17/18	5/17/18	5/14/18	5/14/18
Harvests:				
Harvest 1 (Late Veg.)	2/25/18	3/1/18	2/25/18	2/17/18
Harvest 2 (Early Ripen.)	4/12/18	4/12/18	4/10/18	3/29/18
Harvest 3 (Mature)	5/19/18	5/18/18	5/16/18	5/15/18
Heat Spikes:				
Heat Spike Start		2/9/18	4/11/18	
Heat Spike End		3/1/18	5/1/18	

A2.2. Supplemental Figures

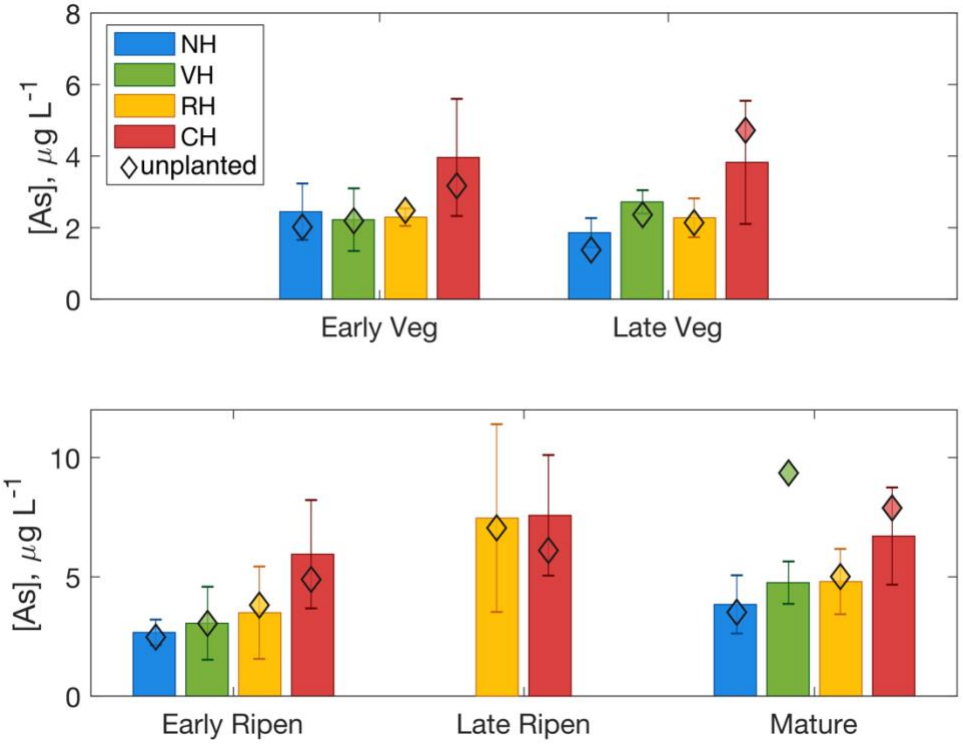

Figure A2.1. *Mean porewater in planted pots and unplanted pots in each treatment. Error bars are the standard deviation of planted pots. Each treatment only contained one unplanted pot. Porewater samples were collected based on observed plant phenology and not necessarily on the same day. See* ***Table A2.2*** *for date of collection for each treatment.*

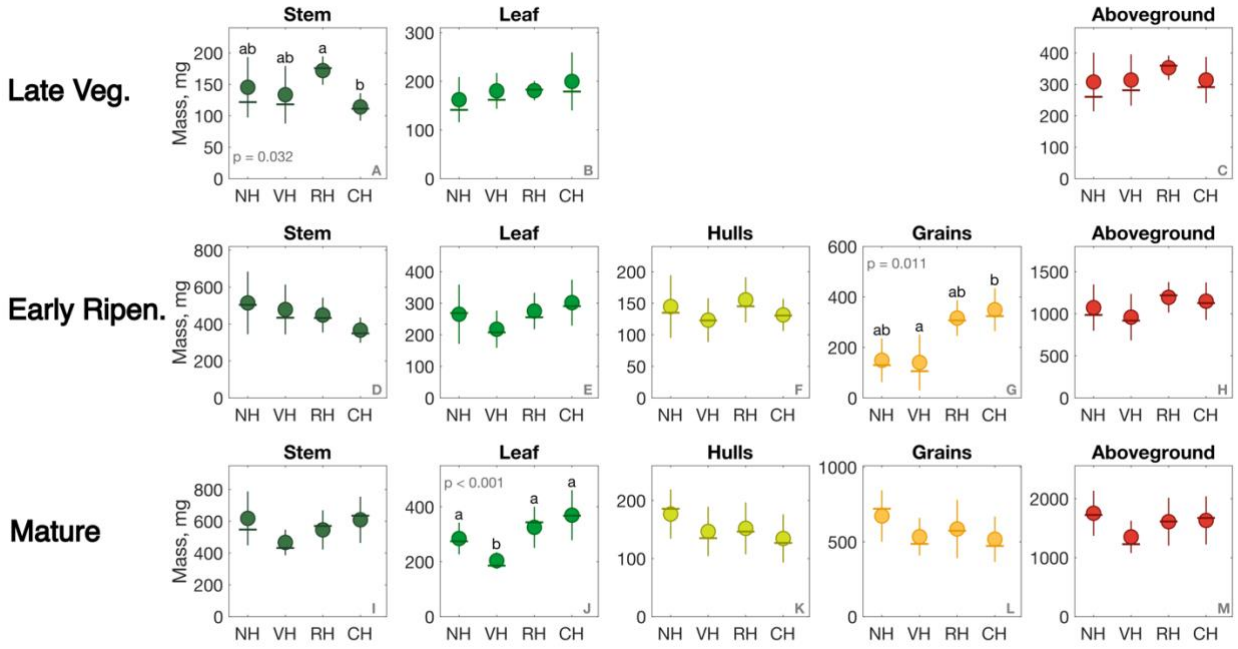

Figure A2.2. *Aboveground biomass of rice plants at different developmental stages. Row 1 shows plants at (late) vegetative stage, row 2 shows plants at early ripening stage, and row 3 shows plants at maturity. Statistical analyses were preformed using log_{10} transformed data for improved normality. At each time point and tissue type we performed an ANOVA followed by a Tukey post-hoc. ANOVA p-values are only provided when less than 0.05.*

A3. Appendix 3: Chapter 4 Supplement

A3.1. Supplemental Figures

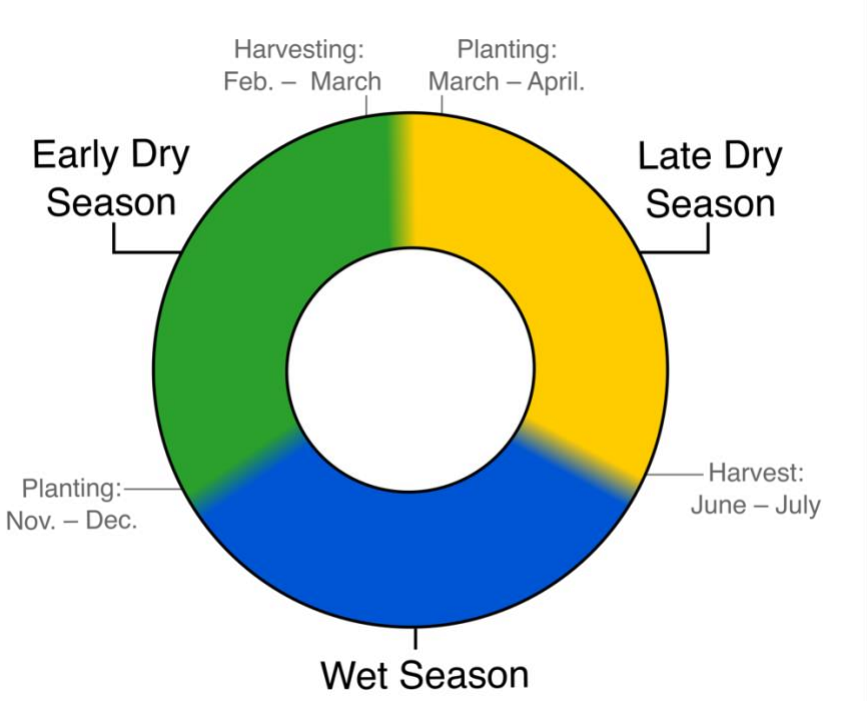

Figure A3.1. *Pictural depiction of dry season planting and harvesting times. Information is based on 2018 surveys of 12 farmers in Steung Saen Municipality. Fragments of the circle are conceptual and are not mathematically accurate.*

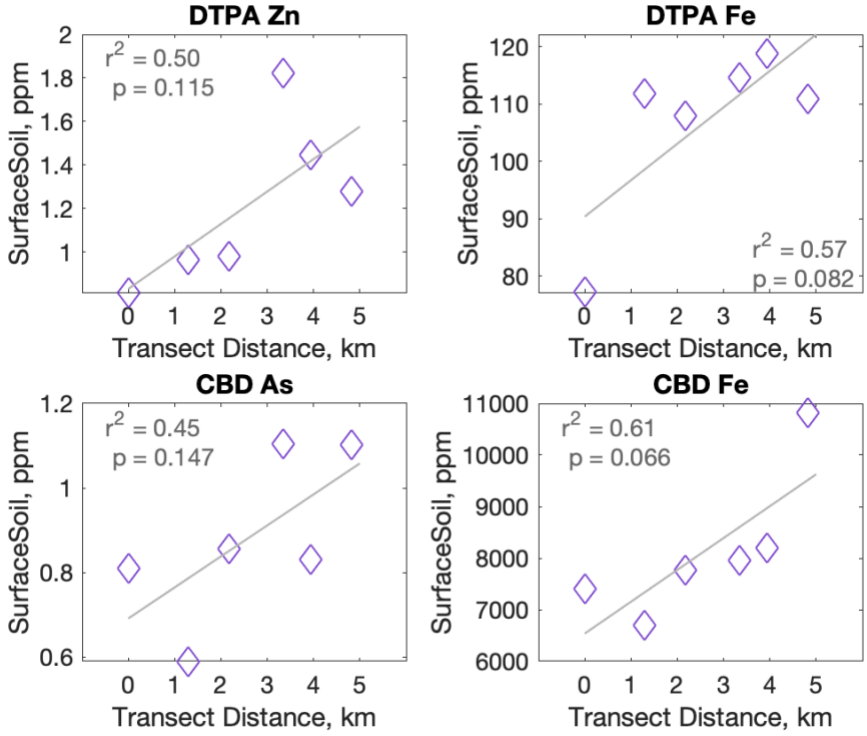

Figure A3.2. *Surface soil extracted metals against transect distance. DTPA extraction was used to analyze bioavailable zinc and CBD extractions analyzed reducible iron and arsenic. DTPA extractions were also run for iron, however this is an uncommon analysis in the literature and was not included in the main text of this chapter. Correlation coefficient (r^2) and p-value from regression are provided.*

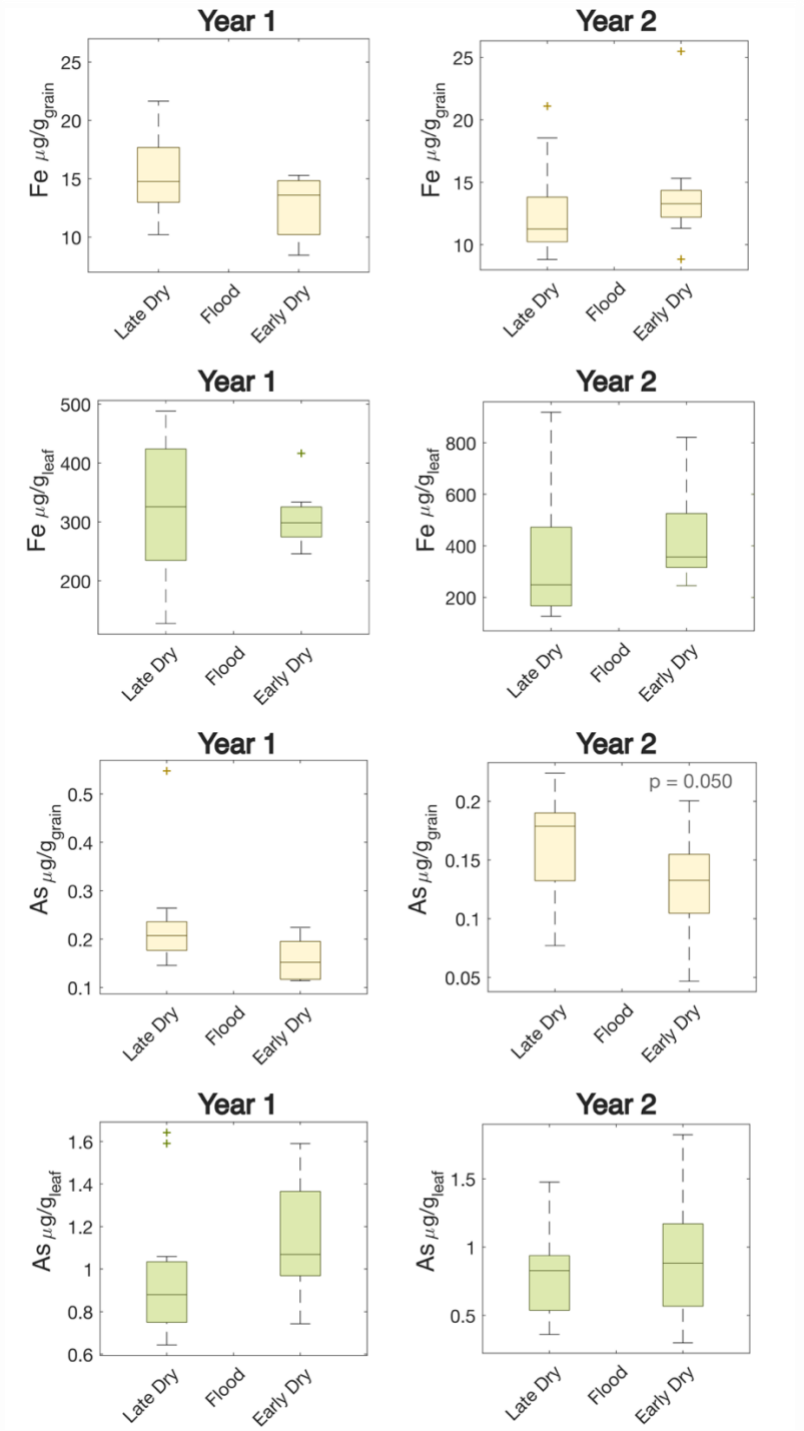

Figure A3.3. *Concentration of iron and arsenic in leaf and grain tissue, pre- and post-flood. Year 1 includes the late dry season of 2018 and the early dry season of 2019. Year 2 includes the late dry season of 2019 and the early dry season of 2020. A two-sample t-test was used to compare tissue types before and after the flood and p-values are reported for when significantly different at* $\alpha = 0.05$.

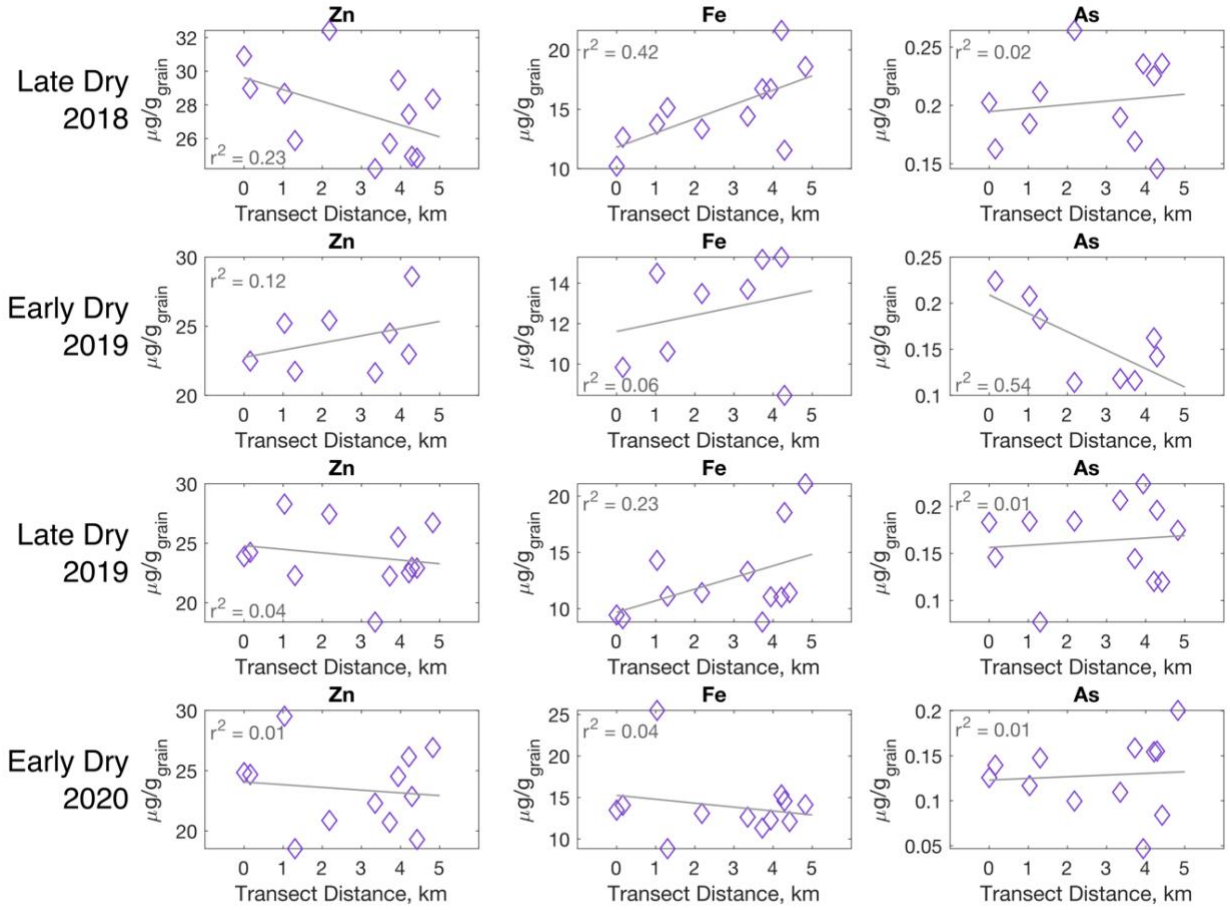

Figure A3.4. *Concentration of zinc, iron, and arsenic in rice grains over transect. Correlation coefficient (r^2) is provided. No comparison met threshold for statistical significance ($\alpha = 0.05$).*

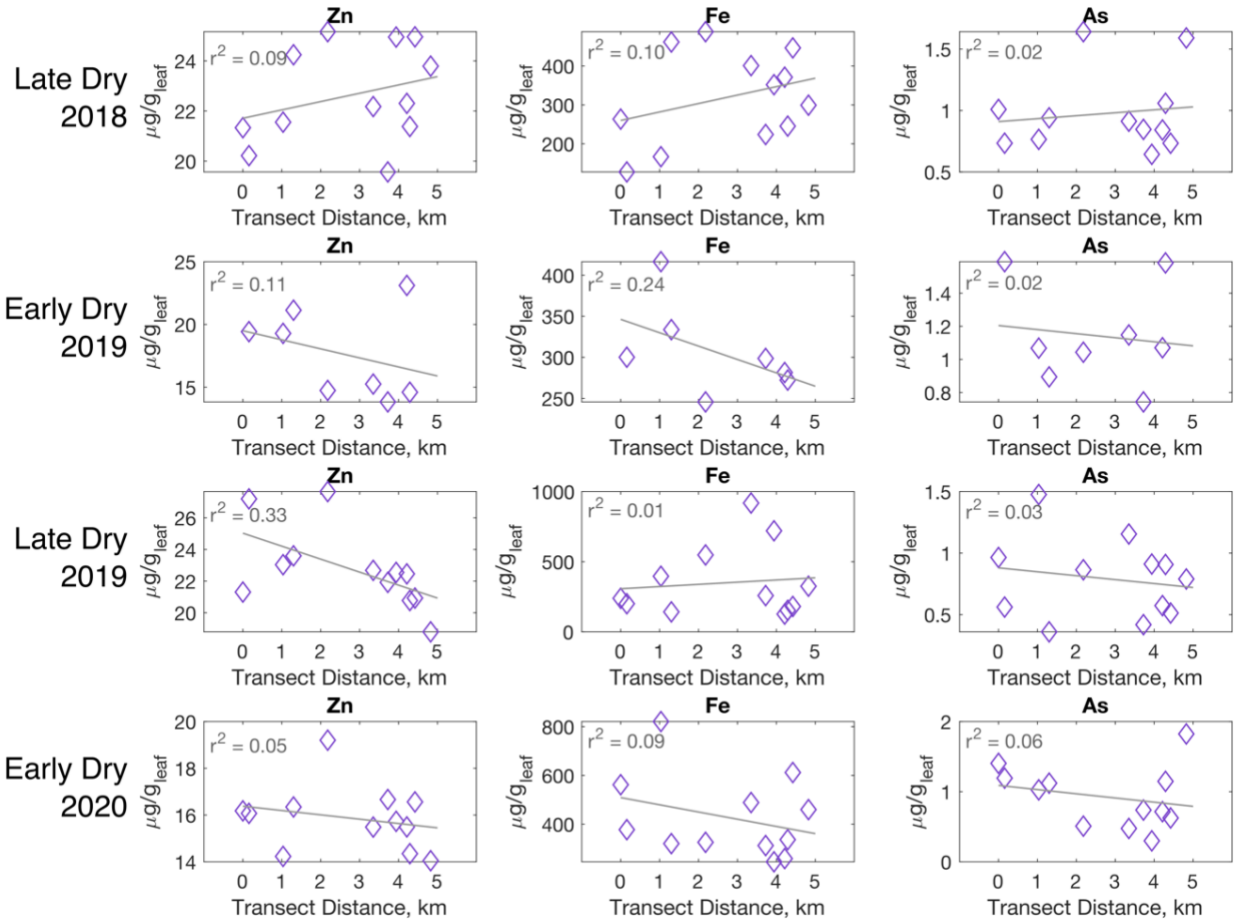

Figure A3.5. *Concentration of zinc, iron, and arsenic in mature leaves over transect. Correlation coefficient (r^2) is provided. No comparison met threshold for statistical significance ($\alpha = 0.05$).*

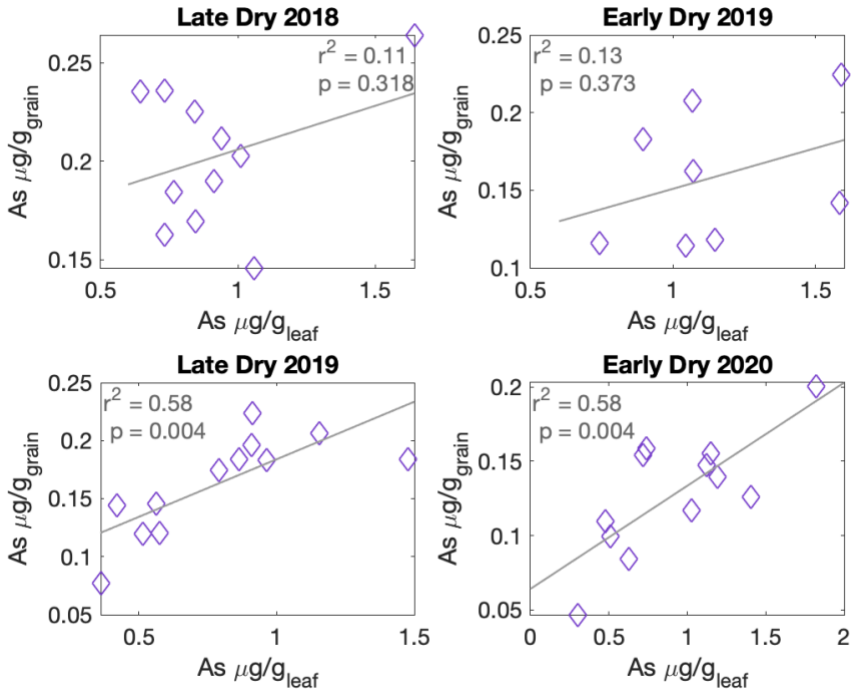

Figure A3.6. *Correlation between leaf and grain arsenic concentrations in each season. Correlation coefficient (r^2) and p-value from regression are provided.*

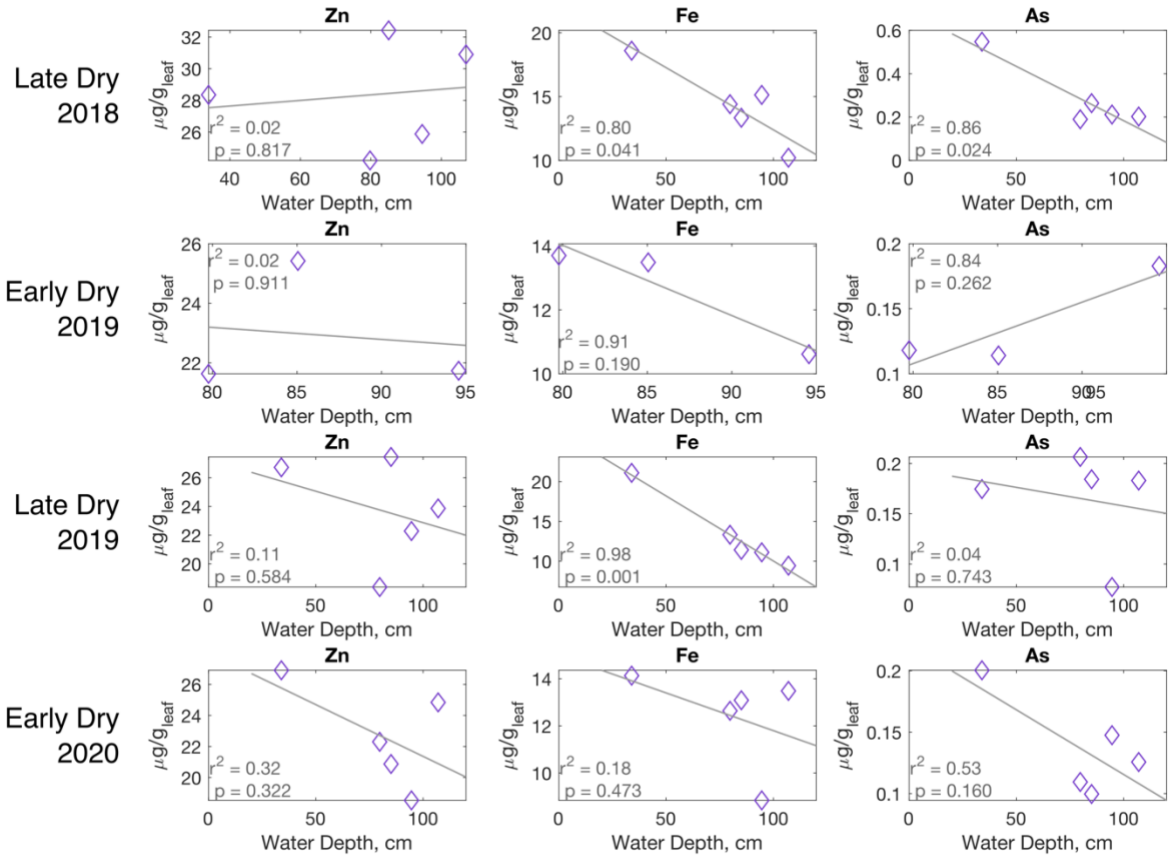

Figure A3.7. *Correlation between grain metal concentration and maximum flooding depth. Correlation coefficient (r^2) and p-value of regression are provided.*